

CERN-PH-EP-2013-032

Submitted to: Physical Review D

A search for $t\bar{t}$ resonances in the lepton plus jets final state with ATLAS using 4.7 fb^{-1} of pp collisions at $\sqrt{s} = 7 \text{ TeV}$

The ATLAS Collaboration

Abstract

A search for new particles that decay into top quark pairs ($t\bar{t}$) is performed with the ATLAS experiment at the LHC using an integrated luminosity of 4.7 fb^{-1} of proton–proton (pp) collision data collected at a center-of-mass energy $\sqrt{s} = 7 \text{ TeV}$. In the $t\bar{t} \rightarrow WbWb$ decay, the lepton plus jets final state is used, where one W boson decays leptonically and the other hadronically. The $t\bar{t}$ system is reconstructed using both small-radius and large-radius jets, the latter being supplemented by a jet substructure analysis. A search for local excesses in the number of data events compared to the Standard Model expectation in the $t\bar{t}$ invariant mass spectrum is performed. No evidence for a $t\bar{t}$ resonance is found and 95% credibility-level limits on the production rate are determined for massive states predicted in two benchmark models. The upper limits on the cross section times branching ratio of a narrow Z' resonance range from 5.1 pb for a boson mass of 0.5 TeV to 0.03 pb for a mass of 3 TeV. A narrow leptophobic topcolor Z' resonance with a mass below 1.74 TeV is excluded. Limits are also derived for a broad color-octet resonance with $\Gamma/m = 15.3\%$. A Kaluza–Klein excitation of the gluon in a Randall–Sundrum model is excluded for masses below 2.07 TeV.

A search for $t\bar{t}$ resonances in the lepton plus jets final state with ATLAS using 4.7 fb^{-1} of pp collisions at $\sqrt{s} = 7\text{ TeV}$

The ATLAS Collaboration
(Dated: June 19, 2013)

A search for new particles that decay into top quark pairs ($t\bar{t}$) is performed with the ATLAS experiment at the LHC using an integrated luminosity of 4.7 fb^{-1} of proton–proton (pp) collision data collected at a center-of-mass energy $\sqrt{s} = 7\text{ TeV}$. In the $t\bar{t} \rightarrow WbWb$ decay, the lepton plus jets final state is used, where one W boson decays leptonically and the other hadronically. The $t\bar{t}$ system is reconstructed using both small-radius and large-radius jets, the latter being supplemented by a jet substructure analysis. A search for local excesses in the number of data events compared to the Standard Model expectation in the $t\bar{t}$ invariant mass spectrum is performed. No evidence for a $t\bar{t}$ resonance is found and 95% credibility-level limits on the production rate are determined for massive states predicted in two benchmark models. The upper limits on the cross section times branching ratio of a narrow Z' resonance range from 5.1 pb for a boson mass of 0.5 TeV to 0.03 pb for a mass of 3 TeV. A narrow leptophobic topcolor Z' resonance with a mass below 1.74 TeV is excluded. Limits are also derived for a broad color-octet resonance with $\Gamma/m = 15.3\%$. A Kaluza–Klein excitation of the gluon in a Randall–Sundrum model is excluded for masses below 2.07 TeV.

I. INTRODUCTION

Despite its many successes, the Standard Model (SM) of particle physics is believed to be an effective field theory valid only for energies up to the TeV scale. Due to its large mass, the top quark is of particular interest for the electroweak symmetry breaking mechanism and could potentially be connected with new phenomena. Several proposed extensions to the SM predict the existence of heavy particles that decay primarily to top quark pairs.

This paper presents the results of a search for production of new particles decaying to top quark pairs using a dataset corresponding to an integrated luminosity of 4.7 fb^{-1} of 7 TeV center-of-mass energy proton–proton (pp) collisions collected by the ATLAS experiment in 2011. The search is carried out using the lepton plus jets decay channel where the W boson from one top quark decays leptonically (to an electron or a muon, and a neutrino) and the other top quark decays hadronically. This search uses a combination of *resolved* and *boosted* reconstruction schemes, defined by the cases when the top-quark decay products are well-separated or merged in the detector, respectively. In the resolved reconstruction scheme, the hadronically decaying top quark is identified by two or three distinct small-radius jets, while in the boosted reconstruction scheme one large-radius jet with substructure consistent with jets from a W boson and a b -quark is used. The boosted reconstruction scheme is more suitable for high-mass $t\bar{t}$ resonances as the top-quark decay products become more collimated.

Examples of hypothetical models that contain high-mass $t\bar{t}$ resonances are the topcolor assisted technicolor model (TC2) [1–3], which predicts a leptophobic Z' particle [4], and a Randall–Sundrum (RS) warped extra-dimension model, which predicts a bulk Kaluza–Klein (KK) gluon [5–9], a color-octet. Two specific benchmark models are chosen and are used throughout the rest of the paper. In the first model, a leptophobic topcolor

Z' particle of width $\Gamma_{Z'}/m_{Z'} = 1.2\%$ is considered as a resonance that is narrow with respect to the detector resolution of typically 10%. In the second model, a KK gluon (g_{KK}) of width $\Gamma_{g_{\text{KK}}}/m_{g_{\text{KK}}} = 15.3\%$ is considered as a resonance that is broad with respect to the detector resolution.

Previous searches for $t\bar{t}$ resonances were carried out by ATLAS in the lepton plus jets final state with 2 fb^{-1} of integrated luminosity at $\sqrt{s} = 7\text{ TeV}$ using resolved and boosted reconstruction techniques separately [10, 11]. With a resolved reconstruction technique, a Z' resonance is excluded for $0.50 < m_{Z'} < 0.88\text{ TeV}$ and a KK gluon is excluded for $0.50 < m_{g_{\text{KK}}} < 1.13\text{ TeV}$, both at 95% credibility level (CL). With a boosted reconstruction technique, a leptophobic Z' is excluded for $0.60 < m_{Z'} < 1.15\text{ TeV}$ and a KK gluon is ruled out for $0.60 < m_{g_{\text{KK}}} < 1.5\text{ TeV}$ at 95% CL. Using both resolved and boosted reconstruction techniques on an integrated luminosity of 5 fb^{-1} of lepton plus jets events at $\sqrt{s} = 7\text{ TeV}$, the CMS experiment excludes a narrow leptophobic topcolor Z' resonance in the mass range 0.50–1.49 TeV and a KK gluon in the mass range 1.00–1.82 TeV [12]. A CMS study conducted on the same dataset, but using dilepton plus jets final states, sets slightly less stringent limits on the narrow Z' resonance, $0.75 < m_{Z'} < 1.3\text{ TeV}$ [13]. The ATLAS and CMS experiments also performed searches where the top quark pair decays hadronically, using 4.7 fb^{-1} and 5.0 fb^{-1} of integrated luminosity respectively at $\sqrt{s} = 7\text{ TeV}$. ATLAS excludes a narrow Z' resonance in the mass ranges 0.70–1.00 TeV and 1.28–1.32 TeV [14] as well as a broad KK gluon with mass 0.7–1.62 TeV. The CMS collaboration excludes a narrow Z' particle in the mass range 1.3–1.5 TeV [15]. The reach of the LHC searches now extends to far higher resonance masses than the Tevatron results [16–19].

Using 4.7 fb^{-1} of integrated luminosity, this analysis improves the previous ATLAS lepton plus jets analyses in that it uses a large-radius $R = 1.0$ jet trigger, applies

b -tagging in the boosted selection, utilizes an optimized method for charged lepton isolation and combines the resolved and boosted reconstruction analyses.

II. THE ATLAS DETECTOR

The ATLAS detector [20] is designed to measure the properties of a wide range of TeV-scale physics processes that may occur in pp interactions. It has a cylindrical geometry and close to 4π solid-angle coverage.

ATLAS uses a right-handed coordinate system with its origin at the nominal interaction point (IP) in the center of the detector and the z -axis along the beam pipe. The x -axis points from the IP to the center of the LHC ring, and the y -axis points upward. Cylindrical coordinates (r, ϕ) are used in the transverse plane, ϕ being the azimuthal angle around the beam pipe, measured from the x -axis. The pseudorapidity is defined in terms of the polar angle θ as $\eta = -\ln \tan(\theta/2)$. Transverse momentum and energy are defined in the x - y -plane, as $p_T = p \cdot \sin(\theta)$ and $E_T = E \cdot \sin(\theta)$.

The inner detector (ID) covers the pseudorapidity range $|\eta| < 2.5$ and consists of multiple layers of silicon pixel and microstrip detectors as well as a straw-tube transition radiation tracker ($|\eta| < 2.0$), which also provides electron identification information. The ID is surrounded by a superconducting solenoid that provides a 2 T axial magnetic field.

The calorimeter system surrounds the ID and the solenoid and covers the pseudorapidity range $|\eta| < 4.9$. It consists of high-granularity lead/liquid-argon (LAr) electromagnetic calorimeters, a steel/scintillator-tile hadronic calorimeter within $|\eta| < 1.7$ and two copper/LAr hadronic endcap calorimeters covering $1.5 < |\eta| < 3.2$. The solid-angle coverage is completed out to $|\eta| = 4.9$ with forward copper/LAr and tungsten/LAr calorimeter modules.

The muon spectrometer (MS) surrounds the calorimeters, incorporating multiple layers of trigger and tracking chambers in an azimuthal magnetic field produced by an air-core toroid magnet, which enables an independent, precise measurement of muon track momentum for $|\eta| < 2.7$. The muon trigger covers the region $|\eta| < 2.4$.

A three-level trigger system [21] is employed for the ATLAS detector. The first-level trigger is implemented in hardware, using a subset of detector information to reduce the event rate to a design value of 75 kHz. This is followed by two software-based trigger levels, which together reduced the event rate to about 300 Hz in 2011.

III. DATA AND MONTE CARLO SAMPLES

The data used in this search were collected with the ATLAS detector at the LHC in 2011. The data are used only if they were recorded under stable beam conditions and with all relevant subdetector systems operational.

The data sample used for resolved reconstruction was collected with a single-muon trigger with a transverse momentum threshold of 18 GeV or a single-electron trigger with a transverse momentum threshold of 20 GeV, which was raised to 22 GeV later in the year. The data sample used for boosted reconstruction was collected with a single large-radius ($R = 1.0$) jet trigger with a transverse momentum threshold of 240 GeV. R is the radius parameter of the anti- k_t jet algorithm, which is discussed in Sec. IV. The jet trigger thresholds are measured at the electromagnetic (EM) energy scale, which, at threshold, is on average 80% of the true energy scale, increasing with p_T . The integrated luminosity for the data sample is $4.7 \pm 0.2 \text{ fb}^{-1}$.

Simulated samples are used to predict the contributions from various Standard Model processes to the expected background and to model possible $t\bar{t}$ resonance signals. After Monte Carlo event generation, all samples are passed through a GEANT4-based [22] simulation [23] of the ATLAS detector and reconstructed using the same software as for data. The effect of multiple pp interactions is included in the simulated samples, and the simulated events are weighted such that the distribution of the average number of pp interactions per bunch crossing agrees with data.

The primary irreducible background is Standard Model $t\bar{t}$ production, characterized by a smoothly falling invariant mass spectrum. It is modeled using the MC@NLO v4.01 [24–26] generator with HERWIG v6.520 [27, 28] for parton showering and hadronization and JIMMY [29] for modeling the multiple parton interactions. The CT10 [30] parton distribution functions (PDFs) are used and the top quark mass is set to 172.5 GeV. Only events in which at least one of the W bosons decays leptonically (including decays to τ leptons) are produced. This corresponds to an effective cross section times branching ratio at approximate NNLO (next-to-next-to-leading-order) of 90.5 pb [31, 32], obtained using the calculation described in Sec. VIII. Additional $t\bar{t}$ samples, generated with POWHEG [33] interfaced with PYTHIA or HERWIG, are used to evaluate the model uncertainty in the parton showering and fragmentation, as described in Sec. VIII.

Single top quark production is modeled using multiple generators. Production in the s -channel and production with an associated W boson (Wt) are modeled with MC@NLO/HERWIG/JIMMY [34, 35] as above. Production in the t -channel is modeled using the ACERMC v3.8 [36] generator and PYTHIA v6.421 [37] for parton showering and hadronization. For the s - and t -channels, events are generated in which the W boson is required to decay leptonically while for the Wt process there is no such requirement. The cross section times branching ratios used are based on approximate NNLO calculations: 20.9 pb (t -channel) [38], 15.7 pb (Wt process) [39] and 1.5 pb (s -channel) [40].

The Standard Model production of W and Z bosons that decay leptonically, accompanied by jets, is an im-

portant background. This includes decays to τ leptons. These samples are generated with ALPGEN v2.13 [41] with up to five extra partons in the matrix element. Modeling of parton showering, hadronization and the underlying event uses HERWIG and JIMMY as for the $t\bar{t}$ samples, and the matching of the matrix element to the parton shower is done using the MLM method [42]. The PDFs used are CTEQ6L1 [43]. Specific W boson plus heavy-flavor processes ($Wb\bar{b}$, $Wc\bar{c}$ and Wc) are generated separately with ALPGEN and double counting of the heavy-flavor contributions is removed from the W plus light-quark jets samples. The W +jets samples are normalized to the inclusive NNLO cross sections [44, 45] and then corrected using data as described in Sec. VII. The Z +jets production, modeled using ALPGEN, includes contributions from the interference between photon and Z boson exchanges, and events are required to have a dilepton invariant mass $40 < m_{\ell\ell} < 2000$ GeV. The $Zb\bar{b}$ process is generated separately with ALPGEN and heavy-flavor contribution overlap removal is done as in the W +jets case.

The diboson background is modeled using HERWIG and JIMMY with MRST2007LO* PDFs [46]. A filter at generator level requiring the presence of at least one lepton with $p_T > 10$ GeV and $|\eta| < 2.8$ is used. The NLO cross sections used for the samples before filtering are 17.0 pb for WW production, 5.5 pb for WZ production, and 1.3 pb for ZZ production, estimated with the MCFM [47] generator. The WZ and ZZ samples also include the off-shell photon contribution decaying to dilepton pairs [48].

Signal samples of Z' events are modeled using PYTHIA with CTEQ6L1 PDFs. This Monte Carlo sample, where the resonance width is 3%, is used to interpret the data in the topcolor Z' model (where the width is 1.2%) since in both cases the width is negligible compared to the detector resolution of 10%. The leptophobic topcolor Z' boson has a branching fraction to $t\bar{t}$ of 33% for masses above 700 GeV, approaching exactly 1/3 for very large masses. It is marginally smaller at lower masses with the smallest value being 31% at a mass of 500 GeV [2, 3]. A K -factor of 1.3 [49] is applied to account for NLO effects [50]. Signal samples of Randall–Sundrum KK gluons are generated via MADGRAPH [51] and then showered and hadronized using PYTHIA. The width of the KK gluon is 15.3% of its mass and its branching fraction to $t\bar{t}$ is 92.5% [5]. The production cross section times branching fractions for the two signals can be found in Table I.

IV. PHYSICS OBJECT SELECTION

The physics object selection criteria closely follow those in Ref. [52], the main exceptions being the treatment of charged lepton isolation and the use of large-radius jets.

Jets are reconstructed using the anti- k_t algorithm [53,

TABLE I. The production cross section times branching fraction (BR) for the resonant signal processes $pp \rightarrow Z' \rightarrow t\bar{t}$ in the topcolor model and $pp \rightarrow g_{\text{KK}} \rightarrow t\bar{t}$ for the KK gluon in a Randall–Sundrum model with warped extra dimensions. A K -factor of 1.3 has been applied to the Z' cross section to account for NLO effects.

Mass [GeV]	$Z' \rightarrow t\bar{t}$ $\sigma \times \text{BR} \times 1.3$ [pb]	$g_{\text{KK}} \rightarrow t\bar{t}$ $\sigma \times \text{BR}$ [pb]
500	19.6	81.3
1000	1.2	4.1
1500	0.13	0.50
2000	0.019	0.095
2500	0.0030	0.026
3000	0.00097	0.0097

54] applied to topological clusters [55] of calorimeter cells with significant energy above the noise threshold. Jets with radius parameters of $R = 0.4$ and $R = 1.0$ are used. For the small-radius $R = 0.4$ jets, topological clusters at the EM energy scale are used to form the jets [56], while for the large-radius $R = 1.0$ jets, locally calibrated topological clusters are used [56–58]. The usage of locally calibrated clusters ensures a more correct description of the energy distribution inside the large-radius jet, which is needed when using jet substructure variables, as described in Sec. V. Both the small-radius and large-radius jets have their final transverse momentum and pseudorapidity adjusted with energy- and η -dependent correction factors. These are derived from simulation [56, 59] and verified using data [56]. The small-radius jets are required to have $p_T > 25$ GeV and $|\eta| < 2.5$, while large-radius jets must have $p_T > 350$ GeV and $|\eta| < 2.0$. Above this jet p_T value, the large-radius jet trigger is more than 99% efficient. A $\Delta R = \sqrt{(\Delta\eta)^2 + (\Delta\phi)^2}$ separation requirement between small-radius and large-radius jets in the boosted event selection below ensures no double-counting of topological cluster energy.

Small-radius jets are tagged as b -jets using a neural-network-based b -tagging algorithm that uses as input the results of impact parameter, secondary vertex, and decay topology algorithms [60]. The operating point chosen for the resolved selection corresponds to an average b -tagging efficiency in simulated $t\bar{t}$ events of 70% and a light-quark rejection factor of 140 for $p_T > 20$ GeV. For events passing the boosted selection criteria, the b -tagging efficiency estimated from simulated $t\bar{t}$ events using small-radius jets with $p_T > 25$ GeV is 75% and the light-quark jet rejection factor is 85. The b -tag requirement for both the resolved and boosted event selections refers only to small-radius jets.

Electrons are identified by the shape of the shower in the EM calorimeter and must have a matching track in the inner detector [61]. The cluster in the EM calorimeter must satisfy $|\eta| < 2.47$ with the transition region $1.37 < |\eta| < 1.52$ between EM calorimeter sections excluded. Electrons are required to be isolated as described

below and their longitudinal impact distance ($|z_0|$) from the primary event vertex must be smaller than 2 mm. The primary event vertex is defined as the vertex with the highest sum of the squared p_T values of the associated tracks ($\sum p_{T,\text{track}}^2$) in the event. Electrons within a cone of $\Delta R = 0.4$ with respect to any small-radius jet are removed, which suppresses the background from multi-jet events with non-prompt electrons and removes events where the same calorimeter energy deposits would be counted within two physics objects. The electron transverse momentum, p_T , is calculated using the cluster energy and track direction, and must be greater than 25 GeV to ensure a fully efficient trigger.

Muon candidates are formed by matching reconstructed ID tracks with tracks reconstructed in the MS. Only muons with $|\eta| < 2.5$ are used. Muons are required to be isolated as described below and to have $|z_0| < 2$ mm. For the resolved reconstruction, muons are required to have a separation in ΔR of at least 0.1 from any small-radius jet. The muon momentum is calculated using both the MS and the ID tracks, taking the energy loss in the calorimeter into account. The transverse momentum of the muon must be greater than 25 GeV, well above the trigger threshold, chosen to reduce the multi-jet background without impacting the signal.

The isolation of charged leptons is typically defined using the transverse energy found in a fixed cone around the lepton [48]. Because the angle between the charged lepton and the b -quark decreases as the top quark is more boosted, a better measure of isolation, named *mini-isolation*, is used [62, 63]. The use of mini-isolation improves the lepton signal efficiency and background rejection with respect to the fixed-cone algorithm. For this analysis, mini-isolation is defined as

$$I_{\text{mini}}^\ell = \sum_{\text{tracks}} p_T^{\text{track}}, \quad \Delta R(\ell, \text{track}) < K_T/p_T^\ell, \quad (1)$$

where the scalar sum runs over all tracks (except the matched lepton track) that have $p_T^{\text{track}} > 1$ GeV, pass quality selection criteria, and fulfill the $\Delta R(\ell, \text{track})$ requirement shown in Eq. (1). Here p_T^ℓ is the lepton transverse momentum and K_T is an empirical scale parameter set to 10 GeV, chosen so that the size of the isolation cone is optimal both at high and low p_T . The requirement $I_{\text{mini}}^\ell/p_T^\ell < 0.05$ is used, corresponding to 95% (98%) efficiency for a muon (electron) in the p_T region used for this analysis. At low p_T , this mini-isolation criterion corresponds to a tighter isolation requirement than is used in other top quark analyses at ATLAS, and at high p_T it is looser.

The missing transverse momentum, E_T^{miss} , is calculated [64] from the vector sum of the transverse energy in calorimeter cells associated with topological clusters. The direction of the energy deposits is given by the line joining the cell to the interaction point. Calorimeter cells are first uniquely associated with a physics object (e.g. electron, jet or muon). The transverse energy of each cell is then calibrated according to the type of object to which

it belongs, and the vector sum of these is calculated. All muon transverse momenta are added and the associated calorimeter cell energies are subtracted. Finally, topological clusters not associated with any reconstructed object are calibrated at the EM energy scale and added to the transverse energy sum vector.

V. EVENT SELECTION

After passing a single-lepton trigger for the resolved reconstruction or a large-radius jet trigger for the boosted reconstruction, events are required to have exactly one isolated lepton with $p_T > 25$ GeV and $I_{\text{mini}}^\ell/p_T < 0.05$. The reconstructed primary event vertex is required to have at least five tracks with $p_T > 0.4$ GeV. In the electron channel, E_T^{miss} must be larger than 30 GeV and the transverse mass larger than 30 GeV. The transverse mass is defined as $m_T = \sqrt{2p_T E_T^{\text{miss}}(1 - \cos \Delta\phi)}$, where p_T is the transverse momentum of the charged lepton and $\Delta\phi$ is the azimuthal angle between the charged lepton and the missing transverse momentum, which is assumed to be due to the neutrino. In the muon channel, the selection is $E_T^{\text{miss}} > 20$ GeV and $E_T^{\text{miss}} + m_T > 60$ GeV. These selection criteria are chosen to suppress the multi-jet background.

The selection requirements for jets differ for the cases of resolved or boosted reconstruction. For the resolved reconstruction, events are required to have at least three small-radius jets with $p_T > 25$ GeV and $|\eta| < 2.5$. To reduce the effects of multiple pp interactions in the same bunch crossing, at least 75% of the scalar sum of the p_T of the tracks in each jet (called “jet vertex fraction”) is required to be associated with the primary vertex. If one of the jets has a mass [65] above 60 GeV, it is assumed to contain the two quarks from the hadronic W decay, or one of these quarks and the b -quark from the top-quark decay. If no jet has a mass above 60 GeV then at least four jets are required, one of which must be tagged as a b -jet.

For the boosted reconstruction, the three partons from the hadronic top-quark decay are expected to have merged into one large-radius jet. Thus, at least one large-radius jet with $p_T > 350$ GeV and a mass larger than 100 GeV is required. The constituents of the large-radius jets are then reclustered with the exclusive k_t algorithm [66, 67] using FASTJET [54] and $R = 1.0$. The last step in the reclustering of subjets within a jet has the splitting scale $\sqrt{d_{12}}$. Generally $d_{ij} = \min(p_{T,i}^2, p_{T,j}^2) \Delta R_{ij}^2 / R^2$, where i and j refer to the two last proto-jets to be merged, ΔR_{ij} is a measure of the angle between them and $R = 1.0$ is the fixed radius parameter [66, 67]. The value of $\sqrt{d_{12}}$ is expected to be larger for jets that contain a top-quark decay than for jets from the non-top-quark backgrounds. The splitting scale $\sqrt{d_{12}}$ is required to be larger than 40 GeV, a criterion that rejects about 40% of the non-top-quark background, but only 10% of the $t\bar{t}$ sample.

The jet formed by the b -quark from the semileptonically decaying top quark is selected as a small-radius jet that fulfills the same p_T , η and jet vertex fraction criteria as used in the resolved reconstruction and has a ΔR separation smaller than 1.5 from the lepton. If more than one jet fulfills these criteria, the one closest to the lepton is chosen. Two other requirements are applied to the event: the decay products from the two top quarks are required to be well separated through the criteria $\Delta\phi(\ell, j_{1.0}) > 2.3$ and $\Delta R(j_{0.4}, j_{1.0}) > 1.5$, where $j_{0.4}$ and $j_{1.0}$ denote the jets with $R = 0.4$ and $R = 1.0$, respectively. The $\Delta R(j_{0.4}, j_{1.0})$ requirement guarantees that there is no energy overlap between the two jets [11]. The highest- p_T large-radius jet passing these criteria is taken as the hadronically decaying top quark candidate.

Finally, in both selections at least one small-radius b -tagged jet is required. In the boosted analysis this requirement is independent of any large-radius jet in the event, i.e. the b -tagged jet may originate from the hadronic top-quark decay and overlap with the large-radius jet or it may originate from the leptonic top-quark decay and thus be near the lepton.

VI. EVENT RECONSTRUCTION

The $t\bar{t}$ candidate invariant mass, $m_{t\bar{t}}$, is computed from the four-momenta of the two reconstructed top quarks. For the semileptonically decaying top quark, in both the resolved and boosted selections, the longitudinal component of the neutrino momentum, p_z , is computed by imposing a W boson mass constraint on the lepton plus E_T^{miss} system [68, 69]. If only one real solution for p_z exists, this is used. If two real solutions exist, the solution with the smallest $|p_z|$ is chosen or both are tested, depending on the reconstruction algorithm. In events where no real solution is found, the E_T^{miss} vector is rescaled and rotated, applying the minimum variation necessary to find exactly one real solution. This procedure is justified since mismeasurement of the E_T^{miss} vector is the likeliest explanation for the lack of a solution to the p_z equation, assuming that the lepton indeed comes from a W boson decay.

For the resolved reconstruction, a χ^2 minimization algorithm is used to select the best assignment of jets to the hadronically and semileptonically decaying top quarks. The χ^2 minimization uses the reconstructed top quark and W boson masses as constraints:

$$\begin{aligned} \chi^2 = & \left[\frac{m_{jj} - m_W}{\sigma_W} \right]^2 \\ & + \left[\frac{m_{j\bar{j}b} - m_{jj} - m_{t_h - W}}{\sigma_{t_h - W}} \right]^2 + \left[\frac{m_{j\ell\nu} - m_{t_\ell}}{\sigma_{t_\ell}} \right]^2 \\ & + \left[\frac{(p_{T,j\bar{j}b} - p_{T,j\ell\nu}) - (p_{T,t_h} - p_{T,t_\ell})}{\sigma_{\text{diff}p_T}} \right]^2, \quad (2) \end{aligned}$$

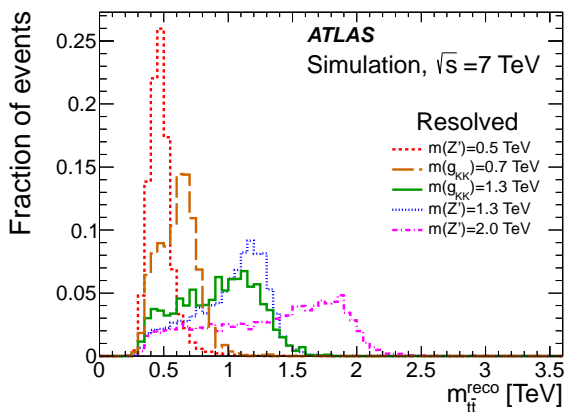
where t_h and t_ℓ denote the hadronically and semileptonically decaying top quarks respectively, and j and b denote

the jets originated by the light quarks and b -quarks. The first term constrains the hadronically decaying W boson. The second term corresponds to the invariant mass of the hadronically decaying top quark, but since the invariant mass of the jets from the W candidate (m_{jj}) is heavily correlated with the mass of the three jets from the hadronic top quark candidate ($m_{j\bar{j}b}$), the mass of the hadronically decaying W boson is subtracted to decouple this term from the first one. The third term represents the semileptonically decaying top quark, and the last term constrains the transverse momenta of the two top quarks to be similar, as expected for a resonance decay. The parameters of Eq. (2) (m_W , $m_{t_h - W}$, m_{t_ℓ} , σ_W , $\sigma_{t_h - W}$, σ_{t_ℓ} , $p_{T,t_h} - p_{T,t_\ell}$ and $\sigma_{\text{diff}p_T}$) are determined from Monte Carlo simulation studies comparing partons from the top-quark decay with reconstructed objects [70]. All small-radius jets satisfying the physics object selection requirements of Sec. IV and $p_T > 20$ GeV are tried and the permutation with the lowest χ^2 is used to calculate $m_{t\bar{t}}$. The correct assignment of the jets to the partons of the $t\bar{t}$ decay (q , q' , b , \bar{b}) is achieved in approximately 65% of the $t\bar{t}$ events for which all the decay products of the top quarks are in the acceptance of the detector and can be matched to reconstructed objects. If one of the jets has a mass larger than 60 GeV, the χ^2 is slightly modified to allow the heavy jet to contain either the two light quarks from the W boson decay or one quark from the W boson and the b -quark from the top-quark decay. The reconstructed $t\bar{t}$ invariant mass, $m_{t\bar{t}}^{\text{reco}}$, in simulated events is shown in Fig. 1(a) for a selection of Z' and g_{KK} mass values.

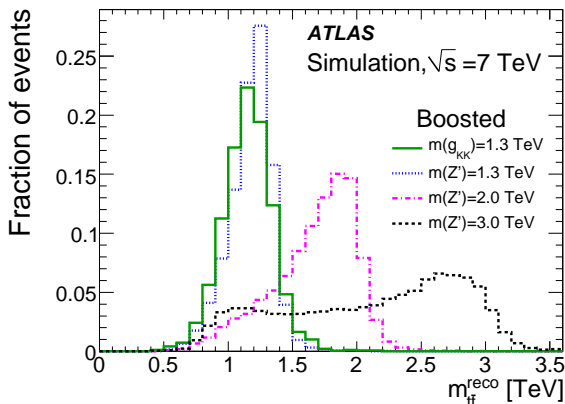
For the boosted reconstruction, the hadronically decaying top-quark four-momentum is taken to be that of the large-radius jet, while the semileptonically decaying top-quark four-momentum is formed from the neutrino solution from the W boson mass constraint, the high- p_T lepton and the nearest small-radius jet. In this case there is no ambiguity in the assignment of the objects to the original top quarks. The reconstructed $t\bar{t}$ invariant mass for a selection of simulated Z' and g_{KK} mass points is shown in Fig. 1(b).

The extended tails at low masses for high-mass resonances in Fig. 1 are caused mainly by the convolution of the Z' line shape and the steeply falling parton distribution functions. The χ^2 method sometimes also reconstructs a slightly lower $m_{t\bar{t}}$ value in the case of hard final-state radiation, since it tends to select the soft jets from the light quarks in the top-quark decay, rather than hard jets from final-state radiation.

Four independent $m_{t\bar{t}}$ invariant mass spectra are used to search for $t\bar{t}$ resonances. For each of the e +jets and μ +jets decay channels, two orthogonal data samples are created. The first sample contains all events that pass the boosted event selection. For these events, $m_{t\bar{t}}$ is estimated using the boosted reconstruction. This first sample includes events that also pass the resolved event selection. For these events the boosted reconstruction is used because of its better reconstructed mass resolution.



(a) Resolved reconstruction.



(b) Boosted reconstruction.

FIG. 1. The reconstructed $t\bar{t}$ invariant mass, $m_{t\bar{t}}^{\text{reco}}$, using the (a) resolved and (b) boosted selection, for a variety of simulated Z' masses ($m(Z')$). The broad Kaluza–Klein gluon resonance at masses 0.7 TeV and 1.3 TeV are also shown for comparison.

The second sample, referred to as the *resolved selection* in the remainder of the paper, contains all events that pass the resolved event selection but do not pass the boosted event selection.

The efficiency of the boosted event selection for selecting $Z' \rightarrow t\bar{t}$ events (including all possible $t\bar{t}$ decay channels) as a function of the true invariant mass of the $t\bar{t}$ system is shown in Fig. 2, together with the selection efficiency for all events passing either selection method. These efficiencies are given with respect to the full set of events within the fiducial acceptance and the fraction of those events that pass the criteria for reconstructed objects, as well as the branching fraction to the various final states. At masses below 1 TeV, the resolved selection is the most efficient, whereas the boosted selection gains in importance at high masses. The e +jets efficiency drops at high masses, due to the $\Delta R(j, e) > 0.4$ requirement, which removes highly collimated top-quark decays. The

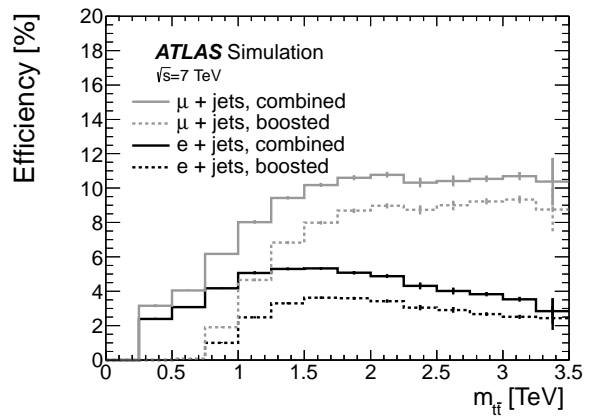


FIG. 2. The selection efficiency as a function of the true $m_{t\bar{t}}$ for simulated Z' resonances at various mass points. The μ +jets channel is shown with gray lines and the e +jets channel with black lines. Dashed lines show the boosted selection and solid lines the total selection efficiency.

overall selection efficiency is larger for the μ +jets channel because of an inherent larger selection efficiency of muons compared with electrons, and also because of the differences in the requirements on the missing transverse energy and transverse mass.

VII. BACKGROUNDS DETERMINED FROM DATA

The W +jets and multi-jet backgrounds and their uncertainties are largely determined from data. The expected shape of the $m_{t\bar{t}}^{\text{reco}}$ distribution of the W +jets background is estimated using ALPGEN simulation samples, but the overall normalization and flavor fractions are determined from data.

The total number of W +jets events passing selection criteria in the data, $N_{W^+} + N_{W^-}$, is estimated from the observed charge asymmetry in data [71, 72] and the predicted charge asymmetry in W +jets events from Monte Carlo simulation:

$$N_{W^+} + N_{W^-} = \left(\frac{r_{\text{MC}} + 1}{r_{\text{MC}} - 1} \right) (D_{\text{corr}^+} - D_{\text{corr}^-}), \quad (3)$$

where r_{MC} is the predicted ratio in Monte Carlo simulation of the W^+ to W^- boson cross sections after event selection criteria are applied (but without b -tagging) and $D_{\text{corr}^+(-)}$ is the number of observed events with a positively (negatively) charged lepton. Charge-symmetric contributions from $t\bar{t}$ and Z +jets processes cancel in the difference and the contributions from the remaining, slightly charge-asymmetric processes are accounted for by Monte Carlo simulation. To increase the sample size for the boosted selection, the jet mass and $\sqrt{d_{12}}$ requirements are not applied and the p_{T} requirement on the large-radius jet is relaxed to be > 300 GeV. From stability tests performed by varying the p_{T} requirement, it

is concluded that no additional uncertainty for the extrapolation to the signal region is needed. The resulting corrections for the W +jets yields from Monte Carlo simulation to agree with data are unity within their uncertainties (10%–20%) for both the boosted and resolved selections.

Data are also used to determine scale factors for the relative fraction of W +jets events with heavy-flavor jets. A system of three equations is solved to determine the fractions of events containing two b -quarks, two c -quarks, one c -quark or only light quarks, for each jet multiplicity i of the events. The ratio of events containing two b -quarks to events with two c -quarks is taken from Monte Carlo simulation. The sum of all flavor fractions is constrained to unity. By comparing the number of events with i jets before and after b -tagging (separately for positively and negatively charged leptons) between data and Monte Carlo simulation, correction factors for the flavor fractions for each jet bin i are determined [52, 72, 73].

The normalization and shape of the multi-jet backgrounds are determined directly from data using a matrix method [52] for both the resolved and boosted selections. The multi-jet backgrounds include all background sources from processes with non-prompt leptons or jets misreconstructed as leptons, including the fully hadronic decays of W and Z bosons and $t\bar{t}$ pairs (both from Standard Model production and from possible signal). The matrix method uses efficiencies, measured in data, associated with prompt leptons (from W and Z boson decays) and non-prompt leptons (from multi-jet events) passing the required isolation criterion. An alternative method, called the jet–electron method [69] is used to estimate the systematic uncertainty of the normalization and shape of the invariant mass spectrum associated with this background. Consistency checks comparing the matrix method with the jet–electron method show that the normalization uncertainty is 60%, for both the resolved and boosted selections, and that the impact of the shape uncertainty is negligible.

For both selection methods, the modeling of the multi-jet contribution is validated using a multi-jet-enriched control region with $E_T^{\text{miss}} < 50$ GeV and $m_T < 50$ GeV. For muons, both selection methods require a transverse impact parameter significance $|d_0|/\sigma(d_0) > 4$ to enhance the fraction of heavy-flavor jets in the sample, which is the dominant source of multi-jet events after b -tagging. For the boosted selection, at least one large-radius jet with $p_T > 150$ GeV is also required and the jet mass and k_t splitting scale requirements are inverted to $m_{\text{jet}} < 100$ GeV and $\sqrt{d_{12}} < 40$ GeV. The control region for the boosted selection is disjoint from the signal region, while 14% (6%) of events from the control region for the resolved selection also pass the signal region criteria for the e +jets (μ +jets) channel. Within the quoted systematic uncertainties, the modeling of the multi-jet background agrees with the data in the control regions, as shown in Fig. 3.

VIII. SYSTEMATIC UNCERTAINTIES

The final observables are the four $t\bar{t}$ invariant mass spectra (two selections and two decay channels). The uncertainties can be broadly divided into two categories: uncertainties that affect reconstructed physics objects (such as jets) and uncertainties that affect the modeling of certain backgrounds or signals. Some of the uncertainties affect both the shape and the normalization of the spectrum, while others affect the normalization only.

The dominant normalization uncertainty on the total background is the Standard Model $t\bar{t}$ cross-section uncertainty of 11%. The uncertainty has been calculated at approximate NNLO in QCD [31] with HATHOR 1.2 [32] using the MSTW2008 90% confidence-level NNLO PDF sets [74] and PDF+ α_S uncertainties according to the MSTW prescription [75]. These uncertainties are then added in quadrature to the normalization and factorization scale uncertainty and found to give results consistent with the NLO+NNLL calculation of Ref. [76] as implemented in Top++ 1.0 [77]. A cross section uncertainty from varying the top-quark mass by ± 1 GeV, added in quadrature to the scale and PDF+ α_S uncertainties, is also included.

The W +jets normalization is varied within the uncertainty, dominated by statistics, of the data-driven determination, corresponding to 12% (10%) for the resolved selection in the e +jets (μ +jets) channel and 19% (18%) for the boosted selection in the e +jets (μ +jets) channel. Four variations of the flavor composition are considered, including the statistical uncertainty on their data-driven determination, the uncertainty on the extrapolation to different jet multiplicities, and the correlations between different flavor fractions, giving a change in the W +jets event yield of about 10% per variation. The normalization uncertainty on the multi-jet background is 60%, coming from the difference between the matrix and jet–electron methods. The single top quark background uncertainty [38–40] is 7.7%. The normalization uncertainty of the Z +jets sample is 48%, estimated using Berends–Giele scaling [48]. The diboson normalization uncertainty is 34%, which is a combination of the PDF uncertainty and additional uncertainties from each extra selected jet.

The preliminary estimate of the 2011 luminosity uncertainty of 3.9% is used, based on the techniques explained in Ref. [78], and is applied to the signal samples and all backgrounds except multi-jets and W +jets, which are estimated from data.

The variation in the shape of the $t\bar{t}$ mass spectrum due to the next-to-leading-order scale variation is accounted for as a mass-dependent scaling, obtained by varying the renormalization and factorization scales up and down by a factor of two in MC@NLO, and normalizing to the nominal cross section (described in Sec. III). The resulting uncertainties range from 10% of the $t\bar{t}$ background at low $m_{t\bar{t}}$ to 20% at masses above 1 TeV. The PDF uncertainty on all Monte Carlo samples is estimated by taking the envelope of the MSTW2008NLO, NNPDF2.3 [79] and

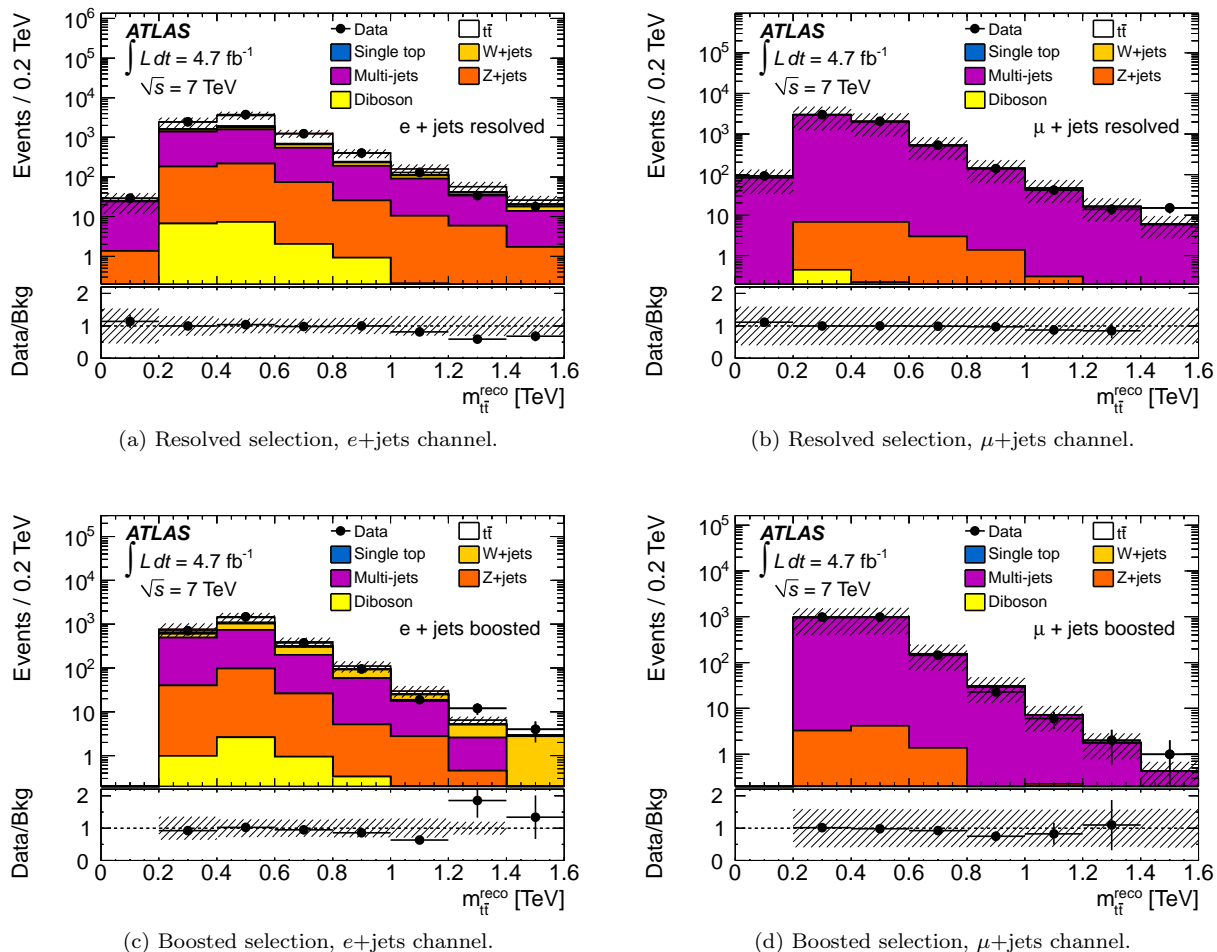
(a) Resolved selection, $e + \text{jets}$ channel.(b) Resolved selection, $\mu + \text{jets}$ channel.(c) Boosted selection, $e + \text{jets}$ channel.(d) Boosted selection, $\mu + \text{jets}$ channel.

FIG. 3. The reconstructed $t\bar{t}$ invariant mass, $m_{t\bar{t}}^{\text{reco}}$, in the multi-jet control regions for the resolved (a, b) and boosted (c, d) selections. The 60% uncertainty on the multi-jet contribution is indicated as the shaded area. The multi-jet fraction is significantly larger for the $\mu + \text{jets}$ channel than for the $e + \text{jets}$ channel because of the impact parameter requirement on the muons, which suppresses prompt muons.

CT10 PDF set uncertainties at 68% confidence-level [80] following the PDF4LHC recommendation [81] and normalizing to the nominal cross section. The PDF uncertainty has a much larger effect on the $t\bar{t}$ mass spectrum in the boosted sample than in the resolved sample, with variations in the number of $t\bar{t}$ events increasing from 5% at 1 TeV to over 50% above 2 TeV, due primarily to the larger relative PDF uncertainties in the higher-mass (higher partonic x) regime. The effect on the total background from the PDF variations is 4.7% (7.3%) after the resolved (boosted) selection.

One of the dominant uncertainties affecting reconstructed physics objects is the jet energy scale (JES) uncertainty, especially for large-radius jets [59, 65], which has an effect of 17% on the background yield in the boosted selection. This uncertainty also includes variations in the jet mass scale (JMS) and the k_t splitting scales within their uncertainties [59]. The uncertainty is

smaller for the resolved selection, since the large-radius jets are only used indirectly there, in the veto of events that pass the boosted selection. For small-radius jets, the uncertainties in the JES, the jet reconstruction efficiency and the jet energy resolution (JER) are considered [56]. The b -tagging uncertainty is modeled through simultaneous variations of the uncertainties on the efficiency and rejection scale factors [60, 82]. An additional b -tagging uncertainty is applied for high-momentum jets ($p_T > 200$ GeV) to account for uncertainties in the modeling of the track reconstruction in dense environments with high track multiplicities [83]. The effect of uncertainties associated with the jet vertex fraction is also considered.

The uncertainty on the Standard Model $t\bar{t}$ background due to uncertainties in the modeling of QCD initial- and final-state radiation (ISR/FSR) is estimated using ACERMC [36] plus PYTHIA Monte Carlo samples by vary-

ing the PYTHIA ISR and FSR parameters while retaining consistency with a previous ATLAS measurement of $t\bar{t}$ production with a veto on additional central jet activity [84]. The magnitude of the variations comes from a measurement of extra radiation in top quark events. Higher-order electroweak virtual corrections to the $t\bar{t}$ mass spectrum have been estimated in Ref. [85] and are used as an estimate of the systematic uncertainty of the $t\bar{t}$ Monte Carlo sample normalization. The parton showering and fragmentation uncertainty on the $t\bar{t}$ background is estimated by comparing the result from samples generated with POWHEG interfaced with PYTHIA or HERWIG for the parton showering and hadronization.

For the W +jets background, the uncertainty on the shape of the mass distribution is estimated by varying the parameterization of the renormalization and factorization scales [41].

The shape uncertainty of the multi-jet background is estimated by comparing the matrix method and the jet–electron method, and its impact on the expected upper cross-section limit of the signal models (discussed in Sec. X) is found to be negligible.

For the leptons, the uncertainties on the mini-isolation efficiency, the single-lepton trigger and the reconstruction efficiency are estimated using $Z \rightarrow ee$ and $Z \rightarrow \mu\mu$ events. The difference between Z boson and $t\bar{t}$ events is part of the mini-isolation uncertainty. Uncertainties on the E_T^{miss} reconstruction, as well as on the energy scale and energy resolution of the leptons are also considered, and generally have a smaller impact on the yield and the expected limits than the uncertainties mentioned above.

In Table II, an overview of the effects of the dominant systematic uncertainties on the background and signal yields is given. Only the impact on the overall normalization is shown in the table. Some of the systematic uncertainties also have a significant dependence on the reconstructed $t\bar{t}$ mass and this is fully taken into account in the analysis.

IX. COMPARISON OF DATA AND THE STANDARD MODEL PREDICTION

After all event selection criteria are applied, 61931 resolved and 1078 boosted events remain. A total of 701 events pass both sets of selection criteria, and in the analysis they are treated as boosted events. The event yields from data and from the expected backgrounds for 4.7 fb^{-1} are listed in Table III, along with the total systematic uncertainties, described in Sec. VIII.

Figures 4 and 5 show the transverse momentum of the leading (small-radius) jet after the resolved selection and the transverse momentum of the selected large-radius jet after the boosted selection, respectively. In Figs. 6 and 7, the reconstructed mass distributions of the semileptonically and hadronically decaying top quark candidates are shown, using the boosted event selection. Figure 8 shows the distribution of the first k_t splitting scale of the

TABLE II. Average uncertainty from the dominant systematic effects on the total background yield and on the estimated yield of a Z' with $m = 1.6$ TeV. The e +jets and μ +jets spectra are added. The shift is given in percent of the nominal value. The error on the yield from all systematic effects is estimated as the quadratic sum of all systematic uncertainties. Certain systematic effects are not relevant for the Z' samples, which is indicated with a bar (–) in the table.

Systematic effect	Resolved selection uncertainty [%]		Boosted selection uncertainty [%]	
	tot. bkg.	Z'	tot. bkg.	Z'
Luminosity	3.3	3.9	3.5	3.9
PDF	4.7	3.2	7.3	1.5
ISR/FSR	0.5	–	0.9	–
Parton shower and fragm.	0.1	–	7.4	–
$t\bar{t}$ normalization	8.2	–	9.0	–
$t\bar{t}$ EW virtual correction	1.9	–	4.2	–
$t\bar{t}$ NLO scale variation	1.2	–	8.9	–
W +jets $bb+cc+c$ vs. light	1.7	–	1.1	–
W +jets bb variation	1.3	–	1.1	–
W +jets c variation	0.8	–	0.1	–
W +jets normalization	1.3	–	1.5	–
Multi-jets norm, e +jets	1.7	–	0.4	–
Multi-jets norm, μ +jets	1.0	–	1.1	–
JES, small-radius jets	7.9	3.1	0.6	0.4
JES+JMS, large-radius jets	0.2	4.7	17.3	2.8
Jet energy resolution	1.3	0.7	0.5	0.2
Jet vertex fraction	1.4	1.8	1.9	1.9
b -tag efficiency	3.8	7.9	6.1	3.7
c -tag efficiency	1.2	0.6	0.1	2.6
Mistag rate	1.0	0.3	0.6	0.1
Electron efficiency	0.6	0.7	0.5	0.5
Muon efficiency	0.9	0.9	0.6	0.6
All systematic effects	14.1	11.2	25.4	7.1

TABLE III. Data and expected background event yields after the resolved and boosted selections. The total systematic uncertainty of the expected background yields is listed.

Type	Resolved selection	Boosted selection
$t\bar{t}$	44200 ± 7000	940 ± 260
Single top	3200 ± 500	50 ± 10
Multi-jets e	1600 ± 1000	8 ± 5
Multi-jets μ	1000 ± 600	19 ± 11
W +jets	7000 ± 2200	90 ± 30
Z +jets	800 ± 500	11 ± 6
Dibosons	120 ± 50	0.9 ± 0.6
Total	58000 ± 8000	1120 ± 280
Data	61931	1078

selected large-radius jet. In these figures, the diboson background is too small to be visible. Good agreement is observed between the data and the expected background.

The $t\bar{t}$ invariant mass spectra for the resolved and the boosted selections in the e +jets and μ +jets decay channels are shown in Fig. 9. Figure 10 shows the $t\bar{t}$ invariant mass spectrum for all channels added together. The data agree with the Standard Model prediction within the un-

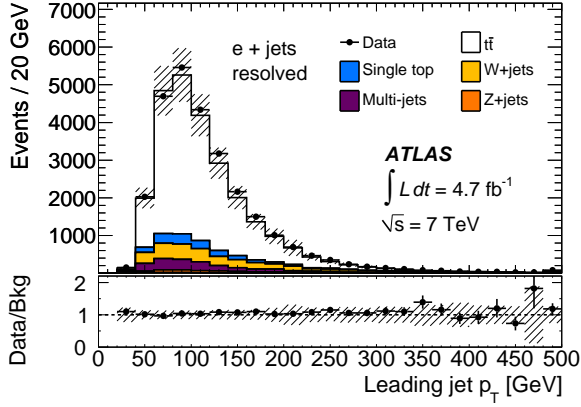
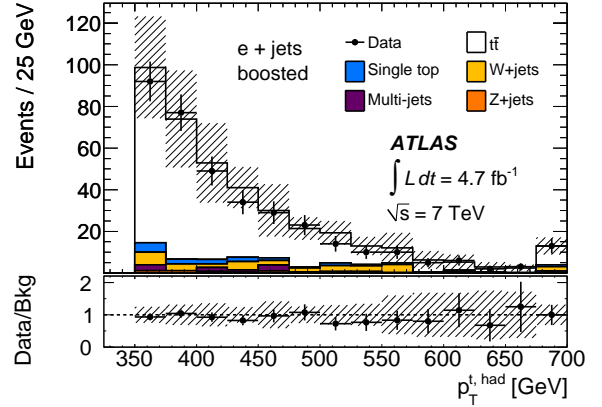
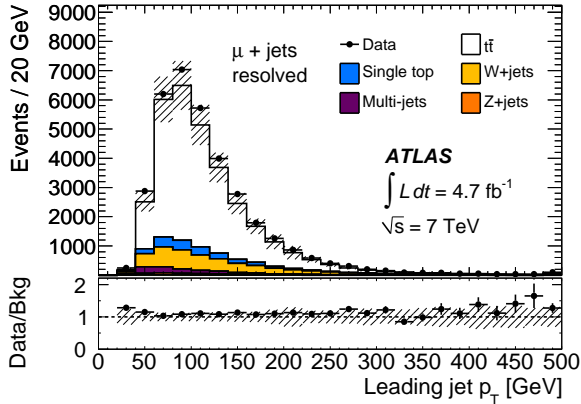
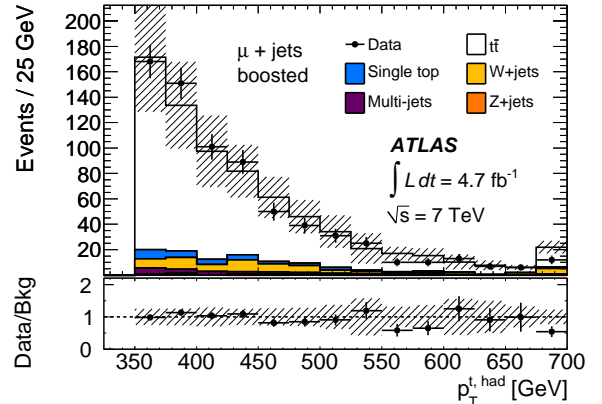
(a) e +jets channel.(a) e +jets channel.(b) μ +jets channel.(b) μ +jets channel.

FIG. 4. The transverse momentum of the leading jet in (a) the e +jets and (b) the μ +jets channels, after the resolved selection. The shaded area indicates the total systematic uncertainties.

certainties. The slight shape mismatch between data and the Standard Model prediction seen in Fig. 9, especially for the resolved selection, is fully covered by the uncertainties. Systematic uncertainties that tilt the shape in this way include the $t\bar{t}$ generator uncertainty, the small-radius jet energy scale and resolution uncertainties, and the ISR/FSR modeling.

X. RESULTS

After the reconstruction of the $t\bar{t}$ mass spectra, the data and expected background distributions are compared to search for hints of phenomena associated with new physics using BUMP HUNTER [86]. This is a hypothesis-testing tool that uses pseudo-experiments to search for local excesses or deficits in the data compared to the Standard Model prediction in binned histograms, taking the look-elsewhere effect into account over the full

FIG. 5. The transverse momentum of the hadronically decaying top quark candidate in (a) the e +jets and (b) the μ +jets channels, after the boosted selection. The shaded area indicates the total systematic uncertainties. The last bin contains histogram limit overflows.

mass spectrum. The Standard Model prediction is allowed to float within the systematic uncertainties. After accounting for the systematic uncertainties, no significant deviation from the expected background is found. Upper limits are set on the cross section times branching ratio of the Z' and KK gluon benchmark models using a Bayesian technique, implemented in a tool developed by the D0 collaboration [87]. The prior is taken to be constant in the signal cross section, which in this case is an excellent approximation of the reference prior that maximizes the amount of missing information [88], as given in Ref. [89]. The Bayesian limits are in good agreement with results obtained using the CL_s method [90, 91]. For each of the models investigated, 95% CL upper limits are set on the product of production cross section and branching ratio into $t\bar{t}$ pairs.

Figure 11 displays the upper limits on the cross section, with systematic and statistical uncertainties, ob-

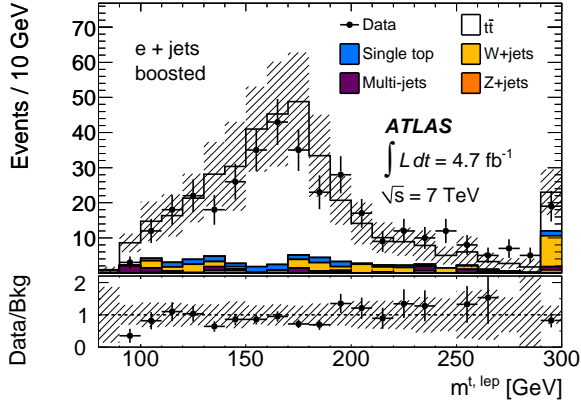
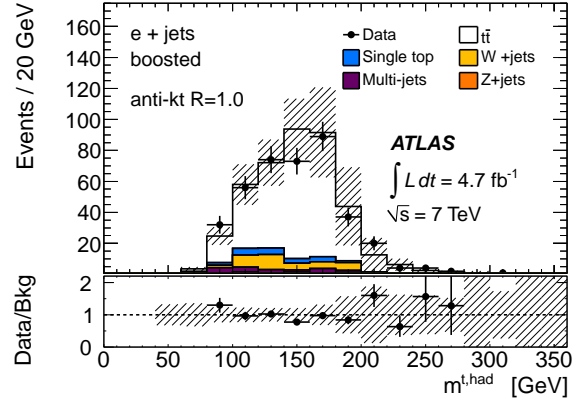
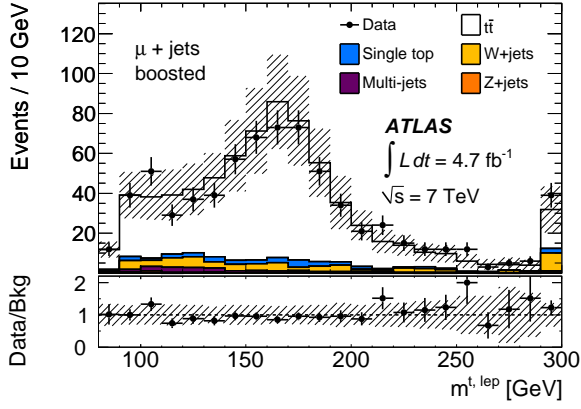
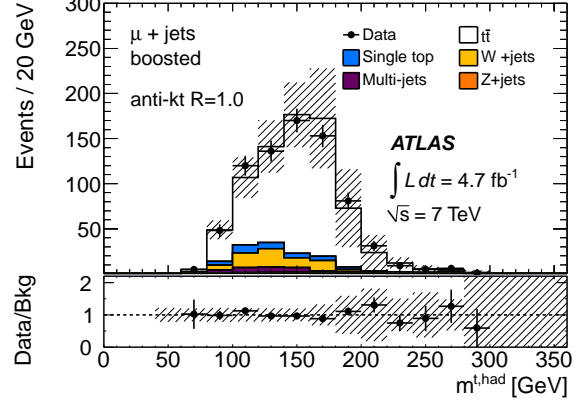
(a) e +jets channel.(a) e +jets channel.(b) μ +jets channel.(b) μ +jets channel.

FIG. 6. The invariant mass of the semileptonically decaying top quark candidate, $m^{t,\text{lep}}$, in (a) the e +jets and (b) the μ +jets channels, after the boosted selection. The mass has been reconstructed from the small-radius jet, the charged lepton and the missing transverse momentum, using a W mass constraint to obtain the longitudinal momentum of the neutrino. The shaded area indicates the total systematic uncertainties. The last bin contains histogram limit overflows.

tained from the combination of the two selections for each of the benchmark models. The numerical values of the upper limits on the cross section are given in Table IV (Z') and Table V (g_{KK}). The expected limits and uncertainty band are obtained using pseudo-experiments based on Poisson distributions for the number of entries in each bin. In the combination, the four disjoint spectra are used, corresponding to boosted and resolved selections, as well as e +jets and μ +jets decay channels. Due to the improvements in the analysis, the upper limits on the cross section for a Z' resonance at 1.6 TeV and a KK gluon resonance at 2.0 TeV are less than half the values that would be obtained by a simple rescaling of the previous best high-mass ATLAS limits [11] to account for the larger integrated luminosity. Using the combined upper

FIG. 7. The mass of the large-radius jet from the hadronically decaying top quark, $m^{t,\text{had}}$, in (a) the e +jets and (b) the μ +jets channels, after the boosted selection, except the requirement $m^{t,\text{had}} > 100$ GeV. The shaded area indicates the total systematic uncertainties.

limits on the cross section, a leptophobic topcolor Z' boson (KK gluon) with mass between 0.5 TeV and 1.74 TeV (0.7 TeV and 2.07 TeV) is excluded at 95% CL.

XI. SUMMARY

A search for $t\bar{t}$ resonances in the lepton plus jets decay channel has been carried out with the ATLAS experiment at the LHC. The search uses a data sample corresponding to an integrated luminosity of 4.7 fb^{-1} of proton–proton collisions at a center-of-mass energy of 7 TeV. The $t\bar{t}$ system is reconstructed in two different ways. For the resolved selection, the hadronic top-quark decay is reconstructed as two or three $R = 0.4$ jets, and for the boosted selection, it is reconstructed as one $R = 1.0$ jet. No excess of events beyond the Standard Model predictions is observed in the $t\bar{t}$ invariant mass spectrum. Up-

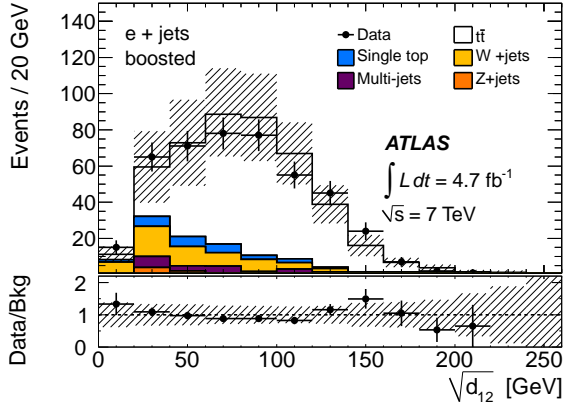
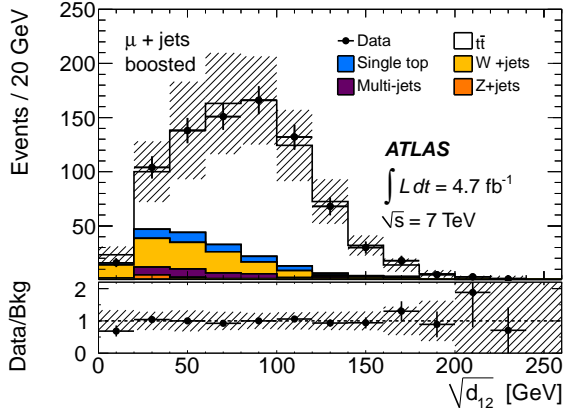
(a) e +jets channel.(b) μ +jets channel.

FIG. 8. The first k_t splitting scale, $\sqrt{d_{12}}$, of the large-radius jet from the hadronically decaying top quark in (a) the e +jets and (b) the μ +jets channels, after the boosted selection, except the requirement $\sqrt{d_{12}} > 40$ GeV. The shaded area indicates the total systematic uncertainties.

TABLE IV. Upper limits on the cross-section times branching ratio, at 95% CL, for a leptophobic topcolor Z' decaying to $t\bar{t}$, using the combination of all four samples. The observed and expected limits for each mass point are given, as well as the $\pm 1\sigma$ variation of the expected limit.

Mass [TeV]	Obs. [pb]	Exp. [pb]	Exp. -1σ [pb]	Exp. $+1\sigma$ [pb]
0.50	5.1	6.7	3.7	10.2
0.60	7.1	4.2	2.4	6.2
0.70	4.6	2.3	1.5	3.7
0.80	1.61	1.45	0.98	1.89
1.00	0.43	0.49	0.31	0.74
1.30	0.117	0.148	0.090	0.213
1.60	0.056	0.080	0.049	0.115
2.00	0.038	0.042	0.027	0.064
2.50	0.034	0.033	0.022	0.048
3.00	0.031	0.028	0.019	0.044

TABLE V. Upper limits on the cross-section times branching ratio, at 95% CL, for a Kaluza–Klein gluon decaying to $t\bar{t}$, using the combination of all four samples. The observed and expected limits for each mass point are given, as well as the $\pm 1\sigma$ variation of the expected limit.

Mass [TeV]	Obs. [pb]	Exp. [pb]	Exp. -1σ [pb]	Exp. $+1\sigma$ [pb]
0.70	5.0	3.5	2.2	5.5
0.80	2.6	1.86	1.29	3.1
1.00	0.66	0.76	0.51	1.14
1.15	0.29	0.38	0.24	0.58
1.30	0.20	0.24	0.15	0.37
1.60	0.106	0.140	0.082	0.198
1.80	0.072	0.105	0.066	0.159
2.00	0.077	0.089	0.056	0.129
2.25	0.075	0.084	0.054	0.126
2.50	0.077	0.078	0.050	0.119

per limits on the cross section times branching ratio are set for two benchmark models: a narrow Z' resonance from Ref. [1] and a broad Randall–Sundrum Kaluza–Klein gluon from Ref. [5]. The 95% credibility upper limits on the cross section times branching ratio for the narrow resonance range from 5.1 pb at a resonance mass of 0.5 TeV to 0.03 pb at 3 TeV. The upper limits on the cross section determined for the broad resonance are higher, 5.0 pb (0.08 pb) at 0.7 (2.0) TeV. Based on these results, the existence of a narrow leptophobic topcolor Z' boson with mass 0.5–1.74 TeV is excluded at 95% CL. A broad Kaluza–Klein gluon in the mass range 0.7–2.07 TeV is also excluded at 95% CL.

ACKNOWLEDGMENTS

We thank CERN for the very successful operation of the LHC, as well as the support staff from our institutions without whom ATLAS could not be operated efficiently.

We acknowledge the support of ANPCyT, Argentina; YerPhI, Armenia; ARC, Australia; BMWF and FWF, Austria; ANAS, Azerbaijan; SSTC, Belarus; CNPq and FAPESP, Brazil; NSERC, NRC and CFI, Canada; CERN; CONICYT, Chile; CAS, MOST and NSFC, China; COLCIENCIAS, Colombia; MSMT CR, MPO CR and VSC CR, Czech Republic; DNRF, DNSRC and Lundbeck Foundation, Denmark; EPLANET, ERC and NSRF, European Union; IN2P3-CNRS, CEA-DSM/IRFU, France; GNSF, Georgia; BMBF, DFG, HGF, MPG and AvH Foundation, Germany; GSRT and NSRF, Greece; ISF, MINERVA, GIF, DIP and Benoziyo Center, Israel; INFN, Italy; MEXT and JSPS, Japan; CNRST, Morocco; FOM and NWO, Netherlands; BRF and RCN, Norway; MNiSW, Poland; GRICES and FCT, Portugal; MERYS (MECTS), Romania; MES of Russia and ROSATOM, Russian Federation; JINR; MSTĐ, Serbia; MSSR, Slovakia; ARRS and MIZŠ, Slovenia;

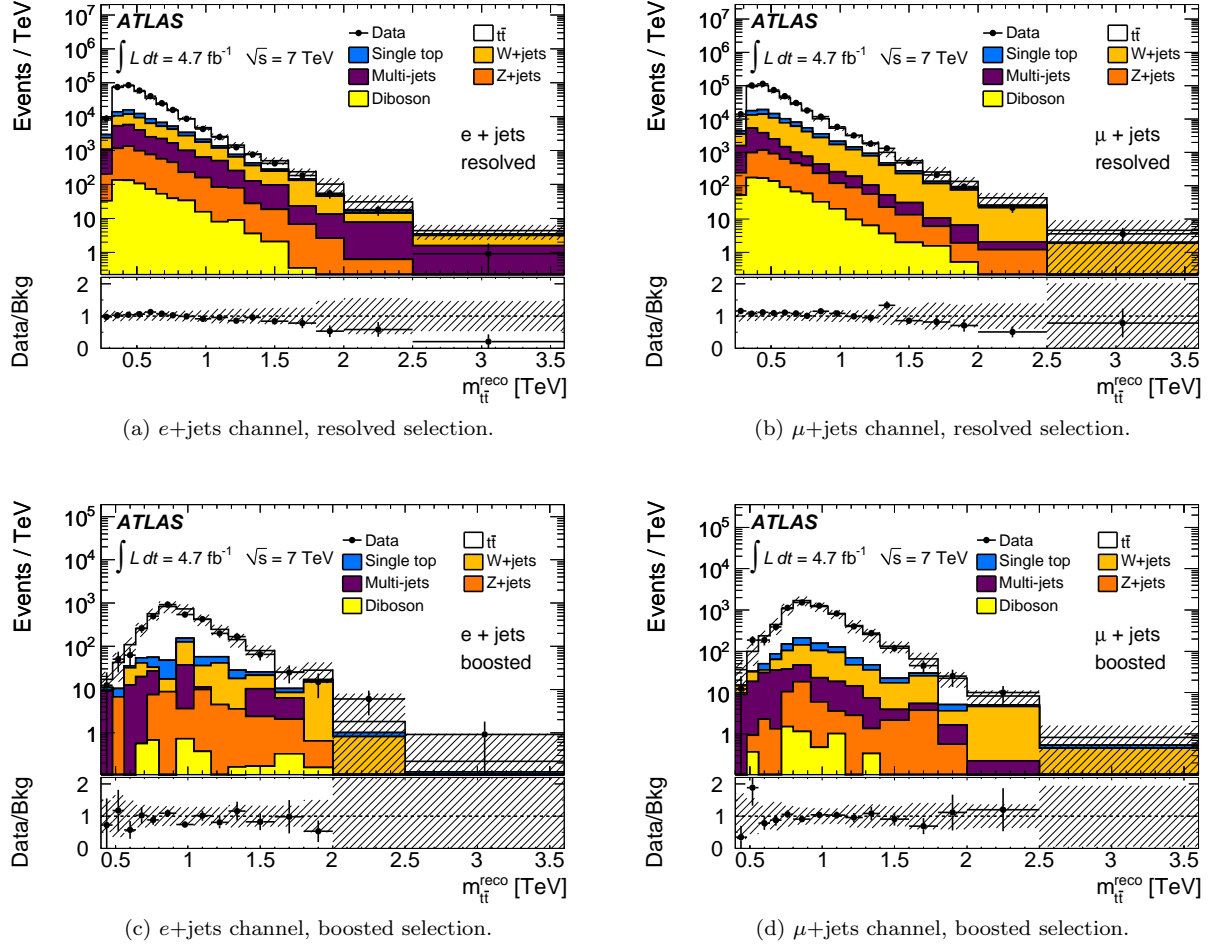


FIG. 9. The $t\bar{t}$ invariant mass spectra for the two channels and the two selection methods. The shaded area indicates the total systematic uncertainties.

DST/NRF, South Africa; MICINN, Spain; SRC and Wallenberg Foundation, Sweden; SER, SNSF and Cantons of Bern and Geneva, Switzerland; NSC, Taiwan; TAEK, Turkey; STFC, the Royal Society and Leverhulme Trust, United Kingdom; DOE and NSF, United States of America.

The crucial computing support from all WLCG partners is acknowledged gratefully, in particular from CERN and the ATLAS Tier-1 facilities at TRIUMF (Canada), NDGF (Denmark, Norway, Sweden), CC-IN2P3 (France), KIT/GridKA (Germany), INFN-CNAF (Italy), NL-T1 (Netherlands), PIC (Spain), ASGC (Taiwan), RAL (UK) and BNL (USA) and in the Tier-2 facilities worldwide.

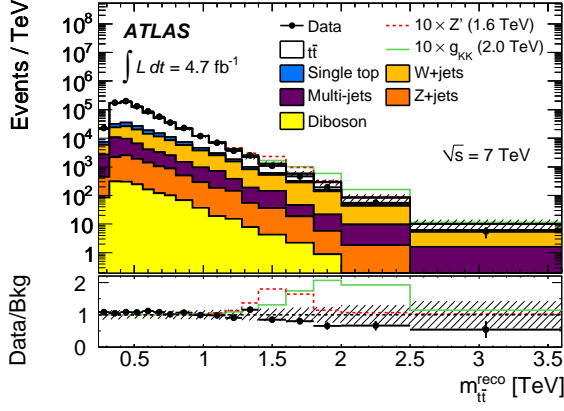
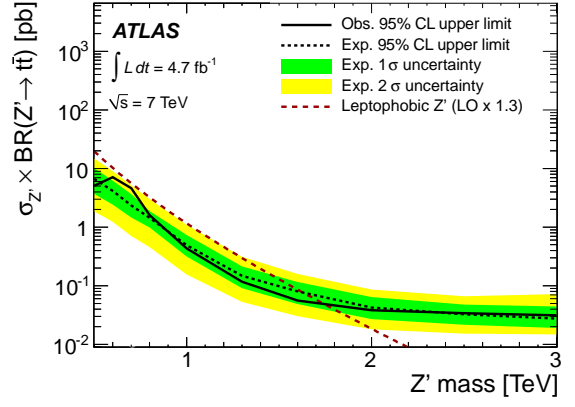
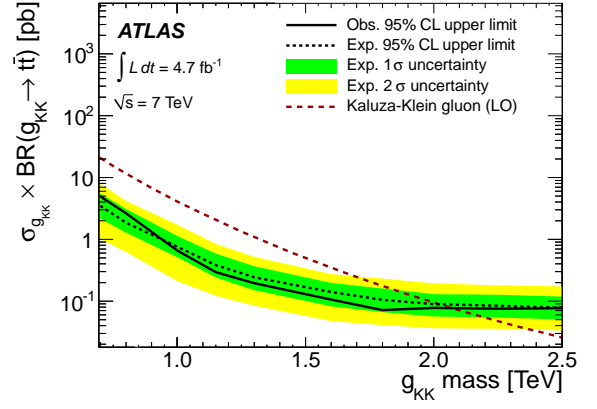


FIG. 10. The $t\bar{t}$ invariant mass spectrum, adding the spectra from the two channels and both selection methods. The shaded area indicates the total systematic uncertainties. Two benchmark signals are indicated on top of the background, a Z' resonance with $m = 1.6$ TeV and a KK gluon with $m = 2.0$ TeV. The assumed cross sections of the signals in this figure are ten times larger than the theoretical predictions in Table I.



(a) Z' upper cross-section limits.



(b) g_{KK} upper cross-section limits.

FIG. 11. Observed and expected upper cross-section limits times the $t\bar{t}$ branching ratio on (a) narrow Z' resonances and (b) Kaluza–Klein gluons. The resolved and the boosted selections have been combined in the estimation of the limits. Systematic and statistical uncertainties are included.

-
- [1] C. T. Hill, Phys. Lett. B **345**, 483 (1995), arXiv:hep-ph/9411426
- [2] R. M. Harris, C. T. Hill, and S. J. Parke, arXiv:hep-ph/9911288
- [3] R. M. Harris and S. Jain, Eur. Phys. J. C **72**, 2072 (2012), arXiv:1112.4928
- [4] In common with other experimental searches, the specific model used is the leptophobic scenario, model IV in Ref. [2] with $f_1 = 1$ and $f_2 = 0$. The corrections to the Lagrangian discussed in Ref. [3] are included.
- [5] B. Lillie, L. Randall, and L.-T. Wang, J. High Energy Phys. **0709**, 074 (2007), arXiv:hep-ph/0701166
- [6] B. Lillie, J. Shu, and T. M. P. Tait, Phys. Rev. D **76**, 115016 (2007), arXiv:0706.3960
- [7] K. Agashe *et al.*, Phys. Rev. D **77**, 015003 (2008), arXiv:hep-ph/0612015
- [8] A. Djouadi, G. Moreau, and R. K. Singh, Nucl. Phys. B **797**, 1 (2008), arXiv:0706.4191
- [9] K. Agashe, H. Davoudiasl, G. Perez, and A. Soni, Phys. Rev. D **76**, 036006 (2007), arXiv:hep-ph/0701186
- [10] ATLAS Collaboration, Eur. Phys. J. C **72**, 2083 (2012), arXiv:1205.5371
- [11] ATLAS Collaboration, J. High Energy Phys. **1209**, 041 (2012), arXiv:1207.2409
- [12] CMS Collaboration, J. High Energy Phys. **1212**, 015 (2012), arXiv:1209.4397
- [13] CMS Collaboration, Phys. Rev. D **87**, 072002 (2013), arXiv:1211.3338
- [14] ATLAS Collaboration, J. High Energy Phys. **1301**, 116 (2012), arXiv:1211.2202
- [15] CMS Collaboration, J. High Energy Phys. **1209**, 029 (2012), arXiv:1204.2488
- [16] CDF Collaboration, T. Aaltonen *et al.*, Phys. Rev. D **84**, 072004 (2011), arXiv:1107.5063
- [17] CDF Collaboration, T. Aaltonen *et al.*, Phys. Rev. D **84**, 072003 (2011), arXiv:1108.4755
- [18] D0 Collaboration, V. Abazov *et al.*, Phys. Rev. D **85**, 051101 (2012), arXiv:1111.1271
- [19] CDF Collaboration, T. Aaltonen *et al.* arXiv:1211.5363
- [20] ATLAS Collaboration, JINST **3**, S08003 (2008)
- [21] ATLAS Collaboration, Eur. Phys. J. C **72**, 1849 (2012), arXiv:1110.1530
- [22] S. Agostinelli *et al.* (GEANT4), Nucl. Instrum. Methods Phys. Res., Sect. A **506**, 250 (2003)
- [23] ATLAS Collaboration, Eur. Phys. J. C **70**, 823 (2010), arXiv:1005.4568
- [24] S. Frixione and B. R. Webber, J. High Energy Phys. **0206**, 029 (2002), arXiv:hep-ph/0204244
- [25] S. Frixione, P. Nason, and B. R. Webber, J. High Energy Phys. **0308**, 007 (2003), arXiv:hep-ph/0305252
- [26] S. Frixione, F. Stoeckli, P. Torrielli, B. R. Webber, and C. D. White(2010), arXiv:1010.0819
- [27] G. Corcella *et al.*, J. High Energy Phys. **0101**, 010 (2001), hep-ph/0011363
- [28] G. Corcella *et al.*, arXiv:hep-ph/0210213
- [29] J. M. Butterworth, J. R. Forshaw, and M. H. Seymour, Z. Phys. C **72**, 637 (1996), arXiv:hep-ph/9601371
- [30] H.-L. Lai *et al.*, Phys. Rev. D **82**, 074024 (2010), arXiv:1007.2241
- [31] M. Beneke *et al.*, Phys. Lett. B **690**, 483 (2010), arXiv:0911.5166
- [32] M. Aliev *et al.*, Comput. Phys. Commun. **182**, 1034 (2011), arXiv:1007.1327
- [33] S. Frixione, P. Nason, and C. Oleari, J. High Energy Phys. **0711**, 070 (2007), arXiv:0709.2092
- [34] S. Frixione, E. Laenen, P. Motylinski, and B. R. Webber, J. High Energy Phys. **0603**, 092 (2006), arXiv:hep-ph/0512250
- [35] S. Frixione *et al.*, J. High Energy Phys. **0807**, 029 (2008), arXiv:0805.3067
- [36] B. P. Kersevan and E. Richter-Was, arXiv:hep-ph/0405247
- [37] T. Sjöstrand, S. Mrenna, and P. Z. Skands, J. High Energy Phys. **0605**, 026 (2006), arXiv:hep-ph/0603175
- [38] N. Kidonakis, Phys. Rev. D **83**, 091503 (2011), arXiv:1103.2792
- [39] N. Kidonakis, Phys. Rev. D **82**, 054018 (2010), arXiv:1005.4451
- [40] N. Kidonakis, Phys. Rev. D **81**, 054028 (2010), arXiv:1001.5034
- [41] M. L. Mangano *et al.*, J. High Energy Phys. **0307**, 001 (2003), arXiv:hep-ph/0206293
- [42] J. Alwall *et al.*, Eur. Phys. J. C **53**, 473 (2008), arXiv:0706.2569
- [43] J. Pumplin *et al.*, J. High Energy Phys. **0207**, 012 (2002), arXiv:hep-ph/0201195
- [44] R. Hamberg, W. van Neerven, and T. Matsuura, Nucl. Phys. B **359**, 343 (1991)
- [45] R. Gavin, Y. Li, F. Petriello and S. Quackenbush, arXiv:1201.5896
- [46] A. Sherstnev and R. Thorne, Eur. Phys. J. C **55**, 553 (2008), arXiv:0711.2473
- [47] J. M. Campbell and R. K. Ellis, Phys. Rev. D **60**, 113006 (1999), arXiv:hep-ph/9905386
- [48] ATLAS Collaboration, Eur. Phys. J. C **71**, 1577 (2011), arXiv:1012.1792
- [49] J. Gao *et al.*, Phys. Rev. D **82**, 014020 (2010), arXiv:1004.0876
- [50] A recent full NLO calculation [92] gives smaller K -factors, which can partly be attributed to the use of different parameters than those in Ref. [49]. The parameters used for signal generation in this paper corresponds more closely to Ref. [49].
- [51] J. Alwall *et al.*, J. High Energy Phys. **0709**, 028 (2007), arXiv:0706.2334
- [52] ATLAS Collaboration, Phys. Lett. B **711**, 244 (2012), arXiv:1201.1889
- [53] M. Cacciari, G. P. Salam, and G. Soyez, J. High Energy Phys. **0804**, 063 (2008), arXiv:0802.1189
- [54] M. Cacciari, G. P. Salam, and G. Soyez, Eur. Phys. J. C **72**, 1896 (2012), arXiv:1111.6097
- [55] W. Lampl *et al.*, ATL-LARG-PUB-2008-002(2008), <https://cdsweb.cern.ch/record/1099735>
- [56] ATLAS Collaboration, Eur. Phys. J. C **73**, 2304 (2013), arXiv:1112.6426
- [57] Ç. İşsever, K. Borras, and D. Wegener, Nucl. Instrum. Methods Phys. Res., Sect. A **545**, 803 (2005), arXiv:physics/0408129
- [58] T. Barillari *et al.*, ATL-LARG-PUB-2009-001-2(2009), <https://cdsweb.cern.ch/record/1112035>
- [59] ATLAS Collaboration, ATLAS-CONF-2012-065 (2012), <https://cdsweb.cern.ch/record/1459530>

- [60] ATLAS Collaboration, ATLAS-CONF-2012-043 (2012), <https://cdsweb.cern.ch/record/1435197>
- [61] ATLAS Collaboration, Eur. Phys. J. C **72**, 1909 (2012), arXiv:1110.3174
- [62] K. Rehermann and B. Tweedie, J. High Energy Phys. **1103**, 059 (2011), arXiv:1007.2221
- [63] ATLAS Collaboration, ATLAS-PHYS-PUB-2010-008 (2010), <https://cdsweb.cern.ch/record/1278454>
- [64] ATLAS Collaboration, Eur. Phys. J. C **72**, 1844 (2012), arXiv:1108.5602
- [65] ATLAS Collaboration, J. High Energy Phys. **1205**, 128 (2012), arXiv:1203.4606
- [66] S. Catani, Y. L. Dokshitzer, M. H. Seymour, and B. R. Webber, Nucl. Phys. B **406**, 187 (1993)
- [67] S. D. Ellis and D. E. Soper, Phys. Rev. D **48**, 3160 (1993), arXiv:hep-ph/9305266
- [68] CDF Collaboration, T. Aaltonen *et al.*, Phys. Rev. D **82**, 112005 (2010), arXiv:1004.1181
- [69] ATLAS Collaboration, Phys. Lett. B **717**, 330 (2012), arXiv:1205.3130
- [70] The values used are $m_W = 83.2$ GeV, $m_{t_h-w} = 90.9$ GeV, $m_{t_\ell} = 167.6$ GeV, $\sigma_W = 10.7$ GeV, $\sigma_{t_h-w} = 12.8$ GeV, $\sigma_{t_\ell} = 20.5$ GeV, $p_{T,t_h} - p_{T,t_\ell} = -7.4$ GeV and $\sigma_{\text{diff}p_T} = 64.0$ GeV.
- [71] ATLAS Collaboration, Eur. Phys. J. C **72**, 2039 (2012), arXiv:1203.4211
- [72] ATLAS Collaboration, Eur. Phys. J. C **73**, 2261 (2013), arXiv:1207.5644
- [73] ATLAS Collaboration, Phys. Lett. B **707**, 418 (2012), arXiv:1109.1470
- [74] A. Martin, W. Stirling, R. Thorne, and G. Watt, Eur. Phys. J. C **63**, 189 (2009), arXiv:0901.0002
- [75] A. Martin, W. Stirling, R. Thorne, and G. Watt, Eur. Phys. J. C **64**, 653 (2009), arXiv:0905.3531
- [76] M. Cacciari *et al.*, Phys. Lett. B **710**, 612 (2012), arXiv:1111.5869
- [77] M. Czakon and A. Mitov, arXiv:1112.5675
- [78] ATLAS Collaboration. Submitted to Eur. Phys. J. C, arXiv:1302.4393
- [79] R. D. Ball *et al.*, Nucl. Phys. B **867**, 244 (2013), arXiv:1207.1303
- [80] The CT10 PDF uncertainties are scaled down by a factor 1.6645 to reach the 68% confidence-level.
- [81] M. Botje *et al.*, arXiv:1101.0538
- [82] ATLAS Collaboration, ATLAS-CONF-2012-040 (2012), <https://cdsweb.cern.ch/record/1435194>
- [83] The additional b -tagging uncertainty is an extrapolation of uncertainty from regions of lower p_T , and it is approximately 12% for b -jets and 17% for c -jets, added in quadrature with the jet efficiency correction factor for the 140–200 GeV region.
- [84] ATLAS Collaboration, Eur. Phys. J. C **72**, 2043 (2012), arXiv:1203.5015
- [85] A. V. Manohar and M. Trott, Phys. Lett. B **711**, 313 (2012), arXiv:1201.3926
- [86] G. Choudalakis, arXiv:1101.0390
- [87] I. Bertram *et al.*, FERMILAB-TM-2104, D0-NOTE-3476, D0-NOTE-2775-A(2000), FERMILAB-TM-2104
- [88] J. O. Berger, J. M. Bernardo, and D. Sun, Ann. Stat. **37**, 905 (2009), arXiv:0904.0156
- [89] D. Casadei, JINST **7**, P01012 (2012), arXiv:1108.4270
- [90] T. Junk, Nucl. Instrum. Methods Phys. Res., Sect. A **434**, 435 (1999), arXiv:hep-ex/9902006
- [91] A. L. Read, J. Phys. G **28**, 2693 (2002)
- [92] F. Caola, K. Melnikov, and M. Schulze, arXiv:1211.6387

The ATLAS Collaboration

G. Aad⁴⁸, T. Abajyan²¹, B. Abbott¹¹¹, J. Abdallah¹², S. Abdel Khalek¹¹⁵, A.A. Abdelalim⁴⁹, O. Abdinov¹¹, R. Aben¹⁰⁵, B. Abi¹¹², M. Abolins⁸⁸, O.S. AbouZeid¹⁵⁸, H. Abramowicz¹⁵³, H. Abreu¹³⁶, Y. Abulaiti^{146a,146b}, B.S. Acharya^{164a,164b,a}, L. Adamczyk³⁸, D.L. Adams²⁵, T.N. Addy⁵⁶, J. Adelman¹⁷⁶, S. Adomeit⁹⁸, P. Adragna⁷⁵, T. Adye¹²⁹, S. Aefsky²³, J.A. Aguilar-Saavedra^{124b,b}, M. Agustoni¹⁷, S.P. Ahlen²², F. Ahles⁴⁸, A. Ahmad¹⁴⁸, M. Ahsan⁴¹, G. Aielli^{133a,133b}, T.P.A. Åkesson⁷⁹, G. Akimoto¹⁵⁵, A.V. Akimov⁹⁴, M.A. Alam⁷⁶, J. Albert¹⁶⁹, S. Albrand⁵⁵, M. Aleksa³⁰, I.N. Aleksandrov⁶⁴, F. Alessandria^{89a}, C. Alexa^{26a}, G. Alexander¹⁵³, G. Alexandre⁴⁹, T. Alexopoulos¹⁰, M. Alhroob^{164a,164c}, M. Aliev¹⁶, G. Alimonti^{89a}, J. Alison¹²⁰, B.M.M. Allbrooke¹⁸, L.J. Allison⁷¹, P.P. Allport⁷³, S.E. Allwood-Spiers⁵³, J. Almond⁸², A. Aloisio^{102a,102b}, R. Alon¹⁷², A. Alonso³⁶, F. Alonso⁷⁰, A. Altheimer³⁵, B. Alvarez Gonzalez⁸⁸, M.G. Alviggi^{102a,102b}, K. Amako⁶⁵, C. Amelung²³, V.V. Ammosov^{128,*}, S.P. Amor Dos Santos^{124a}, A. Amorim^{124a,c}, S. Amoroso⁴⁸, N. Amram¹⁵³, C. Anastopoulos³⁰, L.S. Ancu¹⁷, N. Andari¹¹⁵, T. Andeen³⁵, C.F. Anders^{58b}, G. Anders^{58a}, K.J. Anderson³¹, A. Andreazza^{89a,89b}, V. Andrei^{58a}, X.S. Anduaga⁷⁰, S. Angelidakis⁹, P. Anger⁴⁴, A. Angerami³⁵, F. Anghinolfi³⁰, A. Anisenkov¹⁰⁷, N. Anjos^{124a}, A. Annovi⁴⁷, A. Antonaki⁹, M. Antonelli⁴⁷, A. Antonov⁹⁶, J. Antos^{144b}, F. Anulli^{132a}, M. Aoki¹⁰¹, L. Aperio Bella⁵, R. Apolle^{118,d}, G. Arabidze⁸⁸, I. Aracena¹⁴³, Y. Arai⁶⁵, A.T.H. Arce⁴⁵, S. Arfaoui¹⁴⁸, J-F. Arguin⁹³, S. Argyropoulos⁴², E. Arik^{19a,*}, M. Arik^{19a}, A.J. Armbruster⁸⁷, O. Arnaez⁸¹, V. Arnal⁸⁰, A. Artamonov⁹⁵, G. Artoni^{132a,132b}, D. Arutinov²¹, S. Asai¹⁵⁵, S. Ask²⁸, B. Åsman^{146a,146b}, L. Asquith⁶, K. Assamagan²⁵, R. Astalos^{144a}, A. Astbury¹⁶⁹, M. Atkinson¹⁶⁵, B. Auerbach⁶, E. Auge¹¹⁵, K. Augsten¹²⁶, M. Aurousseau^{145a}, G. Avolio³⁰, D. Axen¹⁶⁸, G. Azuelos^{93,e}, Y. Azuma¹⁵⁵, M.A. Baak³⁰, G. Baccagliani^{89a}, C. Bacci^{134a,134b}, A.M. Bach¹⁵, H. Bachacou¹³⁶, K. Bachas¹⁵⁴, M. Backes⁴⁹, M. Backhaus²¹, J. Backus Mayes¹⁴³, E. Badescu^{26a}, P. Bagnaia^{132a,132b}, Y. Bai^{33a}, D.C. Bailey¹⁵⁸, T. Bain³⁵, J.T. Baines¹²⁹, O.K. Baker¹⁷⁶, S. Baker⁷⁷, P. Balek¹²⁷, F. Balli¹³⁶, E. Banas³⁹, P. Banerjee⁹³, Sw. Banerjee¹⁷³, D. Banfi³⁰, A. Bangert¹⁵⁰, V. Bansal¹⁶⁹, H.S. Bansil¹⁸, L. Barak¹⁷², S.P. Baranov⁹⁴, T. Barber⁴⁸, E.L. Barberio⁸⁶, D. Barberis^{50a,50b}, M. Barbero⁸³, D.Y. Bardin⁶⁴, T. Barillari⁹⁹, M. Barisonzi¹⁷⁵, T. Barklow¹⁴³, N. Barlow²⁸, B.M. Barnett¹²⁹, R.M. Barnett¹⁵, A. Baroncelli^{134a}, G. Barone⁴⁹, A.J. Barr¹¹⁸, F. Barreiro⁸⁰, J. Barreiro Guimarães da Costa⁵⁷, R. Bartoldus¹⁴³, A.E. Barton⁷¹, V. Bartsch¹⁴⁹, A. Basye¹⁶⁵, R.L. Bates⁵³, L. Batkova^{144a}, J.R. Batley²⁸, A. Battaglia¹⁷, M. Battistin³⁰, F. Bauer¹³⁶, H.S. Bawa^{143,f}, S. Beale⁹⁸, T. Beau⁷⁸, P.H. Beauchemin¹⁶¹, R. Beccherle^{50a}, P. Bechtel²¹, H.P. Beck¹⁷, K. Becker¹⁷⁵, S. Becker⁹⁸, M. Beckingham¹³⁸, K.H. Becks¹⁷⁵, A.J. Beddall^{19c}, A. Beddall^{19c}, S. Bedikian¹⁷⁶, V.A. Bednyakov⁶⁴, C.P. Bee⁸³, L.J. Beamster¹⁰⁵, T.A. Beermann¹⁷⁵, M. Begel²⁵, S. Behar Harpaz¹⁵², C. Belanger-Champagne⁸⁵, P.J. Bell⁴⁹, W.H. Bell⁴⁹, G. Bella¹⁵³, L. Bellagamba^{20a}, M. Bellomo³⁰, A. Belloni⁵⁷, O. Beloborodova^{107,g}, K. Belotskiy⁹⁶, O. Beltramello³⁰, O. Benary¹⁵³, D. Bencheikroun^{135a}, K. Bendtz^{146a,146b}, N. Benekos¹⁶⁵, Y. Benhammou¹⁵³, E. Benhar Nocchioli⁴⁹, J.A. Benitez Garcia^{159b}, D.P. Benjamin⁴⁵, M. Benoit¹¹⁵, J.R. Bensinger²³, K. Benslama¹³⁰, S. Bentvelsen¹⁰⁵, D. Berge³⁰, E. Bergeas Kuutmann⁴², N. Berger⁵, F. Berghaus¹⁶⁹, E. Berglund¹⁰⁵, J. Beringer¹⁵, P. Bernat⁷⁷, R. Bernhard⁴⁸, C. Bernius²⁵, F.U. Bernlochner¹⁶⁹, T. Berry⁷⁶, C. Bertella⁸³, A. Bertin^{20a,20b}, F. Bertolucci^{122a,122b}, M.I. Besana^{89a,89b}, G.J. Besjes¹⁰⁴, N. Besson¹³⁶, S. Bethke⁹⁹, W. Bhimji⁴⁶, R.M. Bianchi³⁰, L. Bianchini²³, M. Bianco^{72a,72b}, O. Biebel⁹⁸, S.P. Bieniek⁷⁷, K. Bierwagen⁵⁴, J. Biesiada¹⁵, M. Biglietti^{134a}, H. Bilokon⁴⁷, M. Bindi^{20a,20b}, S. Binet¹¹⁵, A. Bingul^{19c}, C. Bini^{132a,132b}, C. Biscarat¹⁷⁸, B. Bittner⁹⁹, C.W. Black¹⁵⁰, J.E. Black¹⁴³, K.M. Black²², R.E. Blair⁶, J.-B. Blanchard¹³⁶, T. Blazek^{144a}, I. Bloch⁴², C. Blocker²³, J. Blocki³⁹, W. Blum⁸¹, U. Blumenschein⁵⁴, G.J. Bobbink¹⁰⁵, V.S. Bobrovnikov¹⁰⁷, S.S. Bocchetta⁷⁹, A. Bocci⁴⁵, C.R. Boddy¹¹⁸, M. Boehler⁴⁸, J. Boek¹⁷⁵, T.T. Boek¹⁷⁵, N. Boelaert³⁶, J.A. Bogaerts³⁰, A. Bogdanchikov¹⁰⁷, A. Bogouch^{90,*}, C. Bohm^{146a}, J. Bohm¹²⁵, V. Boisvert⁷⁶, T. Bold³⁸, V. Boldea^{26a}, N.M. Bolnet¹³⁶, M. Bomben⁷⁸, M. Bona⁷⁵, M. Boonekamp¹³⁶, S. Bordon⁷⁸, C. Borer¹⁷, A. Borisov¹²⁸, G. Borissov⁷¹, I. Borjanovic^{13a}, M. Borri⁸², S. Borroni⁴², J. Bortfeldt⁹⁸, V. Bortolotto^{134a,134b}, K. Bos¹⁰⁵, D. Boscherini^{20a}, M. Bosman¹², H. Boterenbrood¹⁰⁵, J. Bouchami⁹³, J. Boudreau¹²³, E.V. Bouhova-Thacker⁷¹, D. Boumediene³⁴, C. Bourdarios¹¹⁵, N. Bousson⁸³, S. Boutouil^{135d}, A. Boveia³¹, J. Boyd³⁰, I.R. Boyko⁶⁴, I. Bozovic-Jelisavcic^{13b}, J. Bracinik¹⁸, P. Branchini^{134a}, A. Brandt⁸, G. Brandt¹¹⁸, O. Brandt⁵⁴, U. Bratzler¹⁵⁶, B. Brau⁸⁴, J.E. Brau¹¹⁴, H.M. Braun^{175,*}, S.F. Brazzale^{164a,164c}, B. Brelier¹⁵⁸, J. Bremer³⁰, K. Brendlinger¹²⁰, R. Brenner¹⁶⁶, S. Bressler¹⁷², T.M. Bristow^{145b}, D. Britton⁵³, F.M. Brochu²⁸, I. Brock²¹, R. Brock⁸⁸, F. Broggi^{89a}, C. Bromberg⁸⁸, J. Bronner⁹⁹, G. Brooijmans³⁵, T. Brooks⁷⁶, W.K. Brooks^{32b}, G. Brown⁸², P.A. Bruckman de Renstrom³⁹, D. Bruncko^{144b}, R. Bruneliere⁴⁸, S. Brunet⁶⁰, A. Bruni^{20a}, G. Bruni^{20a}, M. Bruschi^{20a}, L. Bryngemark⁷⁹, T. Buanes¹⁴, Q. Buat⁵⁵, F. Bucci⁴⁹, J. Buchanan¹¹⁸, P. Buchholz¹⁴¹, R.M. Buckingham¹¹⁸, A.G. Buckley⁴⁶, S.I. Buda^{26a}, I.A. Budagov⁶⁴, B. Budick¹⁰⁸, L. Bugge¹¹⁷, O. Bulekov⁹⁶, A.C. Bundock⁷³, M. Bunse⁴³, T. Buran^{117,*}, H. Burckhart³⁰, S. Burdin⁷³, T. Burgess¹⁴, S. Burke¹²⁹, E. Busato³⁴, V. Büscher⁸¹, P. Bussey⁵³, C.P. Buszello¹⁶⁶, B. Butler¹⁴³, J.M. Butler²², C.M. Buttar⁵³, J.M. Butterworth⁷⁷, W. Buttinger²⁸, M. Byszewski³⁰, S. Cabrera Urbán¹⁶⁷, D. Caforio^{20a,20b}, O. Cakir^{4a}, P. Calafiura¹⁵, G. Calderini⁷⁸, P. Calfayan⁹⁸, R. Calkins¹⁰⁶, L.P. Caloba^{24a}, R. Caloi^{132a,132b}, D. Calvet³⁴, S. Calvet³⁴, R. Camacho Toro³⁴, P. Camarri^{133a,133b}, D. Cameron¹¹⁷, L.M. Caminada¹⁵, R. Caminal Armadans¹²,

S. Campana³⁰, M. Campanelli⁷⁷, V. Canale^{102a,102b}, F. Canelli³¹, A. Canepa^{159a}, J. Cantero⁸⁰, R. Cantrill⁷⁶, T. Cao⁴⁰, M.D.M. Capeans Garrido³⁰, I. Caprini^{26a}, M. Caprini^{26a}, D. Capriotti⁹⁹, M. Capua^{37a,37b}, R. Caputo⁸¹, R. Cardarelli^{133a}, T. Carli³⁰, G. Carlino^{102a}, L. Carminati^{89a,89b}, S. Caron¹⁰⁴, E. Carquin^{32b}, G.D. Carrillo-Montoya^{145b}, A.A. Carter⁷⁵, J.R. Carter²⁸, J. Carvalho^{124a,h}, D. Casadei¹⁰⁸, M.P. Casado¹², M. Cascella^{122a,122b}, C. Caso^{50a,50b,*}, E. Castaneda-Miranda¹⁷³, V. Castillo Gimenez¹⁶⁷, N.F. Castro^{124a}, G. Cataldi^{72a}, P. Catastini⁵⁷, A. Catinaccio³⁰, J.R. Catmore³⁰, A. Cattai³⁰, G. Cattani^{133a,133b}, S. Caughron⁸⁸, V. Cavaliere¹⁶⁵, P. Cavalleri⁷⁸, D. Cavalli^{89a}, M. Cavalli-Sforza¹², V. Cavasinni^{122a,122b}, F. Ceradini^{134a,134b}, A.S. Cerqueira^{24b}, A. Cerri¹⁵, L. Cerrito⁷⁵, F. Cerutti¹⁵, S.A. Cetin^{19b}, A. Chafaq^{135a}, D. Chakraborty¹⁰⁶, I. Chalupkova¹²⁷, K. Chan³, P. Chang¹⁶⁵, B. Chapleau⁸⁵, J.D. Chapman²⁸, J.W. Chapman⁸⁷, D.G. Charlton¹⁸, V. Chavda⁸², C.A. Chavez Barajas³⁰, S. Cheatham⁸⁵, S. Chekanov⁶, S.V. Chekulaev^{159a}, G.A. Chelkov⁶⁴, M.A. Chelstowska¹⁰⁴, C. Chen⁶³, H. Chen²⁵, S. Chen^{33c}, X. Chen¹⁷³, Y. Chen³⁵, Y. Cheng³¹, A. Cheplakov⁶⁴, R. Cherkaoui El Moursli^{135e}, V. Chernyatin²⁵, E. Cheu⁷, S.L. Cheung¹⁵⁸, L. Chevalier¹³⁶, G. Chiefari^{102a,102b}, L. Chikovani^{51a,*}, J.T. Childers³⁰, A. Chilingarov⁷¹, G. Chiodini^{72a}, A.S. Chisholm¹⁸, R.T. Chislett⁷⁷, A. Chitan^{26a}, M.V. Chizhov⁶⁴, G. Choudalakis³¹, S. Chouridou⁹, B.K.B. Chow⁹⁸, I.A. Christidi⁷⁷, A. Christov⁴⁸, D. Chromek-Burckhart³⁰, M.L. Chu¹⁵¹, J. Chudoba¹²⁵, G. Ciapetti^{132a,132b}, A.K. Ciftci^{4a}, R. Ciftci^{4a}, D. Cinca⁶², V. Cindro⁷⁴, A. Ciocio¹⁵, M. Cirilli⁸⁷, P. Cirkovic^{13b}, Z.H. Citron¹⁷², M. Citterio^{89a}, M. Ciubancan^{26a}, A. Clark⁴⁹, P.J. Clark⁴⁶, R.N. Clarke¹⁵, W. Cleland¹²³, J.C. Clemens⁸³, B. Clement⁵⁵, C. Clement^{146a,146b}, Y. Coadou⁸³, M. Cobal^{164a,164c}, A. Coccaro¹³⁸, J. Cochran⁶³, L. Coffey²³, J.G. Cogan¹⁴³, J. Coggeshall¹⁶⁵, J. Colas⁵, S. Cole¹⁰⁶, A.P. Colijn¹⁰⁵, N.J. Collins¹⁸, C. Collins-Tooth⁵³, J. Collot⁵⁵, T. Colombo^{119a,119b}, G. Colon⁸⁴, G. Compostella⁹⁹, P. Conde Muño^{124a}, E. Coniavitis¹⁶⁶, M.C. Conidi¹², S.M. Consonni^{89a,89b}, V. Consorti⁴⁸, S. Constantinescu^{26a}, C. Conta^{119a,119b}, G. Conti⁵⁷, F. Conventi^{102a,i}, M. Cooke¹⁵, B.D. Cooper⁷⁷, A.M. Cooper-Sarkar¹¹⁸, N.J. Cooper-Smith⁷⁶, K. Copic¹⁵, T. Cornelissen¹⁷⁵, M. Corradi^{20a}, F. Corriveau^{85,j}, A. Corso-Radu¹⁶³, A. Cortes-Gonzalez¹⁶⁵, G. Cortiana⁹⁹, G. Costa^{89a}, M.J. Costa¹⁶⁷, D. Costanzo¹³⁹, D. Côté³⁰, G. Cottin^{32a}, L. Courneyea¹⁶⁹, G. Cowan⁷⁶, B.E. Cox⁸², K. Cranmer¹⁰⁸, S. Crépe-Renaudin⁵⁵, F. Crescioli⁷⁸, M. Cristinziani²¹, G. Crosetti^{37a,37b}, C.-M. Cuciuc^{26a}, C. Cuenca Almenar¹⁷⁶, T. Cuhadar Donszelmann¹³⁹, J. Cummings¹⁷⁶, M. Curatolo⁴⁷, C.J. Curtis¹⁸, C. Cuthbert¹⁵⁰, P. Cwetanski⁶⁰, H. Czirr¹⁴¹, P. Czodrowski⁴⁴, Z. Czyczula¹⁷⁶, S. D'Auria⁵³, M. D'Onofrio⁷³, A. D'Orazio^{132a,132b}, M.J. Da Cunha Sargedas De Sousa^{124a}, C. Da Via⁸², W. Dabrowski³⁸, A. Dafinca¹¹⁸, T. Dai⁸⁷, F. Dallaire⁹³, C. Dallapiccola⁸⁴, M. Dam³⁶, D.S. Damiani¹³⁷, H.O. Danielsson³⁰, V. Dao¹⁰⁴, G. Darbo^{50a}, G.L. Darlea^{26b}, S. Darmora⁸, J.A. Dassoulas⁴², W. Davey²¹, T. Davidek¹²⁷, N. Davidson⁸⁶, R. Davidson⁷¹, E. Davies^{118,d}, M. Davies⁹³, O. Davignon⁷⁸, A.R. Davison⁷⁷, Y. Davygora^{58a}, E. Dawe¹⁴², I. Dawson¹³⁹, R.K. Daya-Ishmukhametova²³, K. De⁸, R. de Asmundis^{102a}, S. De Castro^{20a,20b}, S. De Cecco⁷⁸, J. de Graat⁹⁸, N. De Groot¹⁰⁴, P. de Jong¹⁰⁵, C. De La Taille¹¹⁵, H. De la Torre⁸⁰, F. De Lorenzi⁶³, L. De Nooij¹⁰⁵, D. De Pedis^{132a}, A. De Salvo^{132a}, U. De Sanctis^{164a,164c}, A. De Santo¹⁴⁹, J.B. De Vivie De Regie¹¹⁵, G. De Zorzi^{132a,132b}, W.J. Dearnaley⁷¹, R. Debbé²⁵, C. Debenedetti⁴⁶, B. Dechenaux⁵⁵, D.V. Dedovich⁶⁴, J. Degenhardt¹²⁰, J. Del Peso⁸⁰, T. Del Prete^{122a,122b}, T. Delemontex⁵⁵, M. Deliyergiyev⁷⁴, A. Dell'Acqua³⁰, L. Dell'Asta²², M. Della Pietra^{102a,i}, D. della Volpe^{102a,102b}, M. Delmastro⁵, P.A. Delsart⁵⁵, C. Deluca¹⁰⁵, S. Demers¹⁷⁶, M. Demichev⁶⁴, B. Demirköz^{12,k}, S.P. Denisov¹²⁸, D. Derendarz³⁹, J.E. Derkaoui^{135d}, F. Derue⁷⁸, P. Dervan⁷³, K. Desch²¹, P.O. Deviveiros¹⁰⁵, A. Dewhurst¹²⁹, B. DeWilde¹⁴⁸, S. Dhaliwal¹⁰⁵, R. Dhullipudi^{25,l}, A. Di Ciaccio^{133a,133b}, L. Di Ciaccio⁵, C. Di Donato^{102a,102b}, A. Di Girolamo³⁰, B. Di Girolamo³⁰, S. Di Luise^{134a,134b}, A. Di Mattia¹⁵², B. Di Micco³⁰, R. Di Nardo⁴⁷, A. Di Simone^{133a,133b}, R. Di Sipio^{20a,20b}, M.A. Diaz^{32a}, E.B. Diehl⁸⁷, J. Dietrich⁴², T.A. Dietzsch^{58a}, S. Diglio⁸⁶, K. Dindar Yagci⁴⁰, J. Dingfelder²¹, F. Dinut^{26a}, C. Dionisi^{132a,132b}, P. Dita^{26a}, S. Dita^{26a}, F. Dittus³⁰, F. Djama⁸³, T. Djobava^{51b}, M.A.B. do Vale^{24c}, A. Do Valle Wemans^{124a,m}, T.K.O. Doan⁵, M. Dobbs⁸⁵, D. Dobos³⁰, E. Dobson⁷⁷, J. Dodd³⁵, C. Doglioni⁴⁹, T. Doherty⁵³, T. Dohmae¹⁵⁵, Y. Doi^{65,*}, J. Dolejsi¹²⁷, Z. Dolezal¹²⁷, B.A. Dolgoshein^{96,*}, M. Donadelli^{24d}, J. Donini³⁴, J. Dopke³⁰, A. Doria^{102a}, A. Dos Anjos¹⁷³, A. Dotti^{122a,122b}, M.T. Dova⁷⁰, A.T. Doyle⁵³, N. Dressnandt¹²⁰, M. Dris¹⁰, J. Dubbert⁹⁹, S. Dube¹⁵, E. Dubreuil³⁴, E. Duchovni¹⁷², G. Duckeck⁹⁸, D. Duda¹⁷⁵, A. Dudarev³⁰, F. Dudziak⁶³, I.P. Duerdoth⁸², L. Dufloy¹¹⁵, M.-A. Dufour⁸⁵, L. Duguid⁷⁶, M. Dührssen³⁰, M. Dunford^{58a}, H. Duran Yildiz^{4a}, M. Düren⁵², R. Duxfield¹³⁹, M. Dwuznik³⁸, W.L. Ebenstein⁴⁵, J. Ebke⁹⁸, S. Eckweiler⁸¹, W. Edson², C.A. Edwards⁷⁶, N.C. Edwards⁵³, W. Ehrenfeld²¹, T. Eifert¹⁴³, G. Eigen¹⁴, K. Einsweiler¹⁵, E. Eisenhandler⁷⁵, T. Ekelof¹⁶⁶, M. El Kamimi^{135c}, M. Ellert¹⁶⁶, S. Elles⁵, F. Ellinghaus⁸¹, K. Ellis⁷⁵, N. Ellis³⁰, J. Elmsheuser⁹⁸, M. Elsing³⁰, D. Emeliyanov¹²⁹, Y. Enari¹⁵⁵, R. Engelmann¹⁴⁸, A. Engl⁹⁸, B. Epp⁶¹, J. Erdmann¹⁷⁶, A. Ereditato¹⁷, D. Eriksson^{146a}, J. Ernst², M. Ernst²⁵, J. Ernwein¹³⁶, D. Errede¹⁶⁵, S. Errede¹⁶⁵, E. Ertel⁸¹, M. Escalier¹¹⁵, H. Esch⁴³, C. Escobar¹²³, X. Espinal Curull¹², B. Esposito⁴⁷, F. Etienne⁸³, A.I. Etievre¹³⁶, E. Etzion¹⁵³, D. Evangelakou⁵⁴, H. Evans⁶⁰, L. Fabbri^{20a,20b}, C. Fabre³⁰, G. Facini³⁰, R.M. Fakhruddinov¹²⁸, S. Falciano^{132a}, Y. Fang^{33a}, M. Fanti^{89a,89b}, A. Farbin⁸, A. Farilla^{134a}, J. Farley¹⁴⁸, T. Farooque¹⁵⁸, S. Farrell¹⁶³, S.M. Farrington¹⁷⁰, P. Farthouat³⁰, F. Fassi¹⁶⁷, P. Fassnacht³⁰, D. Fassouliotis⁹, B. Fatholahzadeh¹⁵⁸, A. Favareto^{89a,89b}, L. Fayard¹¹⁵, P. Federic^{144a}, O.L. Fedin¹²¹, W. Fedorko¹⁶⁸, M. Fehling-Kaschek⁴⁸, L. Felgioni⁸³, C. Feng^{33d}, E.J. Feng⁶, A.B. Fenyuk¹²⁸, J. Ferencei^{144b}, W. Fernando⁶,

S. Ferrag⁵³, J. Ferrando⁵³, V. Ferrara⁴², A. Ferrari¹⁶⁶, P. Ferrari¹⁰⁵, R. Ferrari^{119a}, D.E. Ferreira de Lima⁵³,
 A. Ferrer¹⁶⁷, D. Ferrere⁴⁹, C. Ferretti⁸⁷, A. Ferretto Parodi^{50a,50b}, M. Fiascaris³¹, F. Fiedler⁸¹, A. Filipčić⁷⁴,
 F. Filthaut¹⁰⁴, M. Fincke-Keeler¹⁶⁹, K.D. Finelli⁴⁵, M.C.N. Fiolhais^{124a,h}, L. Fiorini¹⁶⁷, A. Firan⁴⁰, J. Fischer¹⁷⁵,
 M.J. Fisher¹⁰⁹, E.A. Fitzgerald²³, M. Flechl⁴⁸, I. Fleck¹⁴¹, P. Fleischmann¹⁷⁴, S. Fleischmann¹⁷⁵, G.T. Fletcher¹³⁹,
 G. Fletcher⁷⁵, T. Flick¹⁷⁵, A. Floderus⁷⁹, L.R. Flores Castillo¹⁷³, A.C. Florez Bustos^{159b}, M.J. Flowerdew⁹⁹,
 P. Fonseca Martin¹⁷, A. Formica¹³⁶, A. Forti⁸², D. Fortin^{159a}, D. Fournier¹¹⁵, A.J. Fowler⁴⁵, H. Fox⁷¹,
 P. Francavilla¹², M. Franchini^{20a,20b}, S. Franchino³⁰, D. Francis³⁰, T. Frank¹⁷², M. Franklin⁵⁷, S. Franz³⁰,
 M. Fraternali^{119a,119b}, S. Fratina¹²⁰, S.T. French²⁸, C. Friedrich⁴², F. Friedrich⁴⁴, D. Froidevaux³⁰, J.A. Frost²⁸,
 C. Fukunaga¹⁵⁶, E. Fullana Torregrosa¹²⁷, B.G. Fulson¹⁴³, J. Fuster¹⁶⁷, C. Gabaldon³⁰, O. Gabizon¹⁷²,
 S. Gadatsch¹⁰⁵, T. Gadfort²⁵, S. Gadowski⁴⁹, G. Gagliardi^{50a,50b}, P. Gagnon⁶⁰, C. Galea⁹⁸, B. Galhardo^{124a},
 E.J. Gallas¹¹⁸, V. Gallo¹⁷, B.J. Gallop¹²⁹, P. Gallus¹²⁶, K.K. Gan¹⁰⁹, R.P. Gandrajula⁶², Y.S. Gao^{143,f},
 A. Gaponenko¹⁵, F.M. Garay Walls⁴⁶, F. Garberson¹⁷⁶, C. García¹⁶⁷, J.E. García Navarro¹⁶⁷, M. Garcia-Sciveres¹⁵,
 R.W. Gardner³¹, N. Garelli¹⁴³, V. Garonne³⁰, C. Gatti⁴⁷, G. Gaudio^{119a}, B. Gaur¹⁴¹, L. Gauthier⁹³,
 P. Gauzzi^{132a,132b}, I.L. Gavrilenko⁹⁴, C. Gay¹⁶⁸, G. Gaycken²¹, E.N. Gazis¹⁰, P. Ge^{33d,n}, Z. Gecse¹⁶⁸, C.N.P. Gee¹²⁹,
 D.A.A. Geerts¹⁰⁵, Ch. Geich-Gimbel²¹, K. Gellerstedt^{146a,146b}, C. Gemme^{50a}, A. Gemmel⁵³, M.H. Genest⁵⁵,
 S. Gentile^{132a,132b}, M. George⁵⁴, S. George⁷⁶, D. Gerbaudo¹², P. Gerlach¹⁷⁵, A. Gershon¹⁵³, C. Geweniger^{58a},
 H. Ghazlane^{135b}, N. Ghodbane³⁴, B. Giacobbe^{20a}, S. Giagu^{132a,132b}, V. Giangiobbe¹², F. Gianotti³⁰, B. Gibbard²⁵,
 A. Gibson¹⁵⁸, S.M. Gibson³⁰, M. Gilchriese¹⁵, T.P.S. Gillam²⁸, D. Gillberg³⁰, A.R. Gillman¹²⁹, D.M. Gingrich^{3,e},
 N. Giokaris⁹, M.P. Giordani^{164c}, R. Giordano^{102a,102b}, F.M. Giorgi¹⁶, P. Giovannini⁹⁹, P.F. Giraud¹³⁶, D. Giugni^{89a},
 M. Giunta⁹³, B.K. Gjølsten¹¹⁷, L.K. Gladilin⁹⁷, C. Glasman⁸⁰, J. Glatzer²¹, A. Glazov⁴², G.L. Glonti⁶⁴,
 J.R. Goddard⁷⁵, J. Godfrey¹⁴², J. Godlewski³⁰, M. Goebel⁴², C. Goeringer⁸¹, S. Goldfarb⁸⁷, T. Golling¹⁷⁶,
 D. Golubkov¹²⁸, A. Gomes^{124a,c}, L.S. Gomez Fajardo⁴², R. Gonçalo⁷⁶, J. Goncalves Pinto Firmino Da Costa⁴²,
 L. Gonella²¹, S. González de la Hoz¹⁶⁷, G. Gonzalez Parra¹², M.L. Gonzalez Silva²⁷, S. Gonzalez-Sevilla⁴⁹,
 J.J. Goodson¹⁴⁸, L. Goossens³⁰, T. Göpfert⁴⁴, P.A. Gorbounov⁹⁵, H.A. Gordon²⁵, I. Gorelov¹⁰³, G. Gorfine¹⁷⁵,
 B. Gorini³⁰, E. Gorini^{72a,72b}, A. Gorišek⁷⁴, E. Gornicki³⁹, A.T. Goshaw⁶, C. Gössling⁴³, M.I. Gostkin⁶⁴,
 I. Gough Eschrich¹⁶³, M. Goughri^{135a}, D. Goujdami^{135c}, M.P. Goulette⁴⁹, A.G. Goussiou¹³⁸, C. Goy⁵,
 S. Gozpinar²³, L. Graber⁵⁴, I. Grabowska-Bold³⁸, P. Grafström^{20a,20b}, K.-J. Grahn⁴², E. Gramstad¹¹⁷,
 F. Grancagnolo^{72a}, S. Grancagnolo¹⁶, V. Grassi¹⁴⁸, V. Gratchev¹²¹, H.M. Gray³⁰, J.A. Gray¹⁴⁸, E. Graziani^{134a},
 O.G. Grebenyuk¹²¹, T. Greenshaw⁷³, Z.D. Greenwood^{25,l}, K. Gregersen³⁶, I.M. Gregor⁴², P. Grenier¹⁴³,
 J. Griffiths⁸, N. Grigalashvili⁶⁴, A.A. Grillo¹³⁷, K. Grimm⁷¹, S. Grinstein¹², Ph. Gris³⁴, Y.V. Grishkevich⁹⁷,
 J.-F. Grivaz¹¹⁵, J.P. Grohs⁴⁴, A. Grohsjean⁴², E. Gross¹⁷², J. Grosse-Knetter⁵⁴, J. Groth-Jensen¹⁷², K. Grybel¹⁴¹,
 D. Guest¹⁷⁶, O. Gueta¹⁵³, C. Guicheney³⁴, E. Guido^{50a,50b}, T. Guillemin¹¹⁵, S. Guindon⁵⁴, U. Gul⁵³, J. Gunther¹²⁵,
 B. Guo¹⁵⁸, J. Guo³⁵, P. Gutierrez¹¹¹, N. Guttman¹⁵³, O. Gutzwiller¹⁷³, C. Guyot¹³⁶, C. Gwenlan¹¹⁸,
 C.B. Gwilliam⁷³, A. Haas¹⁰⁸, S. Haas³⁰, C. Haber¹⁵, H.K. Hadavand⁸, D.R. Hadley¹⁸, P. Haefner²¹, Z. Hajduk³⁹,
 H. Hakobyan¹⁷⁷, D. Hall¹¹⁸, G. Halladjian⁶², K. Hamacher¹⁷⁵, P. Hamal¹¹³, K. Hamano⁸⁶, M. Hamer⁵⁴,
 A. Hamilton^{145b,o}, S. Hamilton¹⁶¹, L. Han^{33b}, K. Hanagaki¹¹⁶, K. Hanawa¹⁶⁰, M. Hance¹⁵, C. Handel⁸¹,
 P. Hanke^{58a}, J.R. Hansen³⁶, J.B. Hansen³⁶, J.D. Hansen³⁶, P.H. Hansen³⁶, P. Hansson¹⁴³, K. Hara¹⁶⁰, A.S. Hard¹⁷³,
 T. Harenberg¹⁷⁵, S. Harkusha⁹⁰, D. Harper⁸⁷, R.D. Harrington⁴⁶, O.M. Harris¹³⁸, J. Hartert⁴⁸, F. Hartjes¹⁰⁵,
 T. Haruyama⁶⁵, A. Harvey⁵⁶, S. Hasegawa¹⁰¹, Y. Hasegawa¹⁴⁰, S. Hassani¹³⁶, S. Haug¹⁷, M. Hauschild³⁰,
 R. Hauser⁸⁸, M. Havranek²¹, C.M. Hawkes¹⁸, R.J. Hawkins³⁰, A.D. Hawkins⁷⁹, T. Hayakawa⁶⁶, T. Hayashi¹⁶⁰,
 D. Hayden⁷⁶, C.P. Hays¹¹⁸, H.S. Hayward⁷³, S.J. Haywood¹²⁹, S.J. Head¹⁸, T. Heck⁸¹, V. Hedberg⁷⁹, L. Heelan⁸,
 S. Heim¹²⁰, B. Heinemann¹⁵, S. Heisterkamp³⁶, L. Helary²², C. Heller⁹⁸, M. Heller³⁰, S. Hellman^{146a,146b},
 D. Hellmich²¹, C. Helsen¹², R.C.W. Henderson⁷¹, M. Henke^{58a}, A. Henrichs¹⁷⁶, A.M. Henriques Correia³⁰,
 S. Henrot-Versille¹¹⁵, C. Hensel⁵⁴, C.M. Hernandez⁸, Y. Hernández Jiménez¹⁶⁷, R. Herrberg¹⁶, G. Herten⁴⁸,
 R. Hertenberger⁹⁸, L. Hervas³⁰, G.G. Hesketh⁷⁷, N.P. Hesse¹⁰⁵, R. Hickling⁷⁵, E. Higón-Rodríguez¹⁶⁷, J.C. Hill²⁸,
 K.H. Hiller⁴², S. Hillert²¹, S.J. Hillier¹⁸, I. Hinchliffe¹⁵, E. Hines¹²⁰, M. Hirose¹¹⁶, F. Hirsch⁴³, D. Hirschbuehl¹⁷⁵,
 J. Hobbs¹⁴⁸, N. Hod¹⁰⁵, M.C. Hodgkinson¹³⁹, P. Hodgson¹³⁹, A. Hoecker³⁰, M.R. Hoferkamp¹⁰³, J. Hoffman⁴⁰,
 D. Hoffmann⁸³, M. Hohlfield⁸¹, S.O. Holmgren^{146a}, T. Holy¹²⁶, J.L. Holzbauer⁸⁸, T.M. Hong¹²⁰,
 L. Hooft van Huysduynen¹⁰⁸, J.-Y. Hostachy⁵⁵, S. Hou¹⁵¹, A. Hoummada^{135a}, J. Howard¹¹⁸, J. Howarth⁸²,
 M. Hrabovsky¹¹³, I. Hristova¹⁶, J. Hrivnac¹¹⁵, T. Hryn'ova⁵, P.J. Hsu⁸¹, S.-C. Hsu¹³⁸, D. Hu³⁵, Z. Hubacek³⁰,
 F. Hubaut⁸³, F. Huegging²¹, A. Huettmann⁴², T.B. Huffman¹¹⁸, E.W. Hughes³⁵, G. Hughes⁷¹, M. Huhtinen³⁰,
 T.A. Hülsing⁸¹, M. Hurwitz¹⁵, N. Huseynov^{64,p}, J. Huston⁸⁸, J. Huth⁵⁷, G. Iacobucci⁴⁹, G. Iakovidis¹⁰,
 M. Ibbotson⁸², I. Ibragimov¹⁴¹, L. Iconomidou-Fayard¹¹⁵, J. Idarraga¹¹⁵, P. Iengo^{102a}, O. Igonkina¹⁰⁵, Y. Ikegami⁶⁵,
 K. Ikematsu¹⁴¹, M. Ikeno⁶⁵, D. Iliadis¹⁵⁴, N. Ilic¹⁵⁸, T. Ince⁹⁹, P. Ioannou⁹, M. Iodice^{134a}, K. Iordanidou⁹,
 V. Ippolito^{132a,132b}, A. Irls Quiles¹⁶⁷, C. Isaksson¹⁶⁶, M. Ishino⁶⁷, M. Ishitsuka¹⁵⁷, R. Ishmukhametov¹⁰⁹,
 C. Issever¹¹⁸, S. Istin^{19a}, A.V. Ivashin¹²⁸, W. Iwanski³⁹, H. Iwasaki⁶⁵, J.M. Izen⁴¹, V. Izzo^{102a}, B. Jackson¹²⁰,
 J.N. Jackson⁷³, P. Jackson¹, M.R. Jaekel³⁰, V. Jain², K. Jakobs⁴⁸, S. Jakobsen³⁶, T. Jakoubek¹²⁵, J. Jakubek¹²⁶,
 D.O. Jamin¹⁵¹, D.K. Jana¹¹¹, E. Jansen⁷⁷, H. Jansen³⁰, J. Janssen²¹, A. Jantsch⁹⁹, M. Janus⁴⁸, R.C. Jared¹⁷³,

G. Jarlskog⁷⁹, L. Jeanty⁵⁷, G.-Y. Jeng¹⁵⁰, I. Jen-La Plante³¹, D. Jennens⁸⁶, P. Jenni³⁰, C. Jeske¹⁷⁰, P. Jez³⁶, S. Jézéquel⁵, M.K. Jha^{20a}, H. Ji¹⁷³, W. Ji⁸¹, J. Jia¹⁴⁸, Y. Jiang^{33b}, M. Jimenez Belenguer⁴², S. Jin^{33a}, O. Jinnouchi¹⁵⁷, M.D. Joergensen³⁶, D. Joffe⁴⁰, M. Johansen^{146a,146b}, K.E. Johansson^{146a}, P. Johansson¹³⁹, S. Johnert⁴², K.A. Johns⁷, K. Jon-And^{146a,146b}, G. Jones¹⁷⁰, R.W.L. Jones⁷¹, T.J. Jones⁷³, C. Joram³⁰, P.M. Jorge^{124a}, K.D. Joshi⁸², J. Jovicevic¹⁴⁷, T. Jovin^{13b}, X. Ju¹⁷³, C.A. Jung⁴³, R.M. Jungst³⁰, V. Juranek¹²⁵, P. Jussel⁶¹, A. Juste Rozas¹², S. Kabana¹⁷, M. Kaci¹⁶⁷, A. Kaczmarska³⁹, P. Kadlecik³⁶, M. Kado¹¹⁵, H. Kagan¹⁰⁹, M. Kagan⁵⁷, E. Kajomovitz¹⁵², S. Kalinin¹⁷⁵, S. Kama⁴⁰, N. Kanaya¹⁵⁵, M. Kaneda³⁰, S. Kaneti²⁸, T. Kanno¹⁵⁷, V.A. Kantserov⁹⁶, J. Kanzaki⁶⁵, B. Kaplan¹⁰⁸, A. Kapliy³¹, D. Kar⁵³, M. Karagounis²¹, K. Karakostas¹⁰, M. Karnevskiy⁸¹, V. Kartvelishvili⁷¹, A.N. Karyukhin¹²⁸, L. Kashif¹⁷³, G. Kasieczka^{58b}, R.D. Kass¹⁰⁹, A. Kastanas¹⁴, Y. Kataoka¹⁵⁵, J. Katzy⁴², V. Kaushik⁷, K. Kawagoe⁶⁹, T. Kawamoto¹⁵⁵, G. Kawamura⁸¹, S. Kazama¹⁵⁵, V.F. Kazanin¹⁰⁷, M.Y. Kazarinov⁶⁴, R. Keeler¹⁶⁹, P.T. Keener¹²⁰, R. Kehoe⁴⁰, M. Keil⁵⁴, J.S. Keller¹³⁸, M. Kenyon⁵³, H. Keoshkerian⁵, O. Kepka¹²⁵, B.P. Kerševan⁷⁴, S. Kersten¹⁷⁵, K. Kessoku¹⁵⁵, J. Keung¹⁵⁸, F. Khalil-zada¹¹, H. Khandanyan^{146a,146b}, A. Khanov¹¹², D. Kharchenko⁶⁴, A. Khodinov⁹⁶, A. Khomich^{58a}, T.J. Khoo²⁸, G. Khoriauli²¹, A. Khoroshilov¹⁷⁵, V. Khovanskiy⁹⁵, E. Khramov⁶⁴, J. Khubua^{51b}, H. Kim^{146a,146b}, S.H. Kim¹⁶⁰, N. Kimura¹⁷¹, O. Kind¹⁶, B.T. King⁷³, M. King⁶⁶, R.S.B. King¹¹⁸, J. Kirk¹²⁹, A.E. Kiryunin⁹⁹, T. Kishimoto⁶⁶, D. Kisielewska³⁸, T. Kitamura⁶⁶, T. Kittelmann¹²³, K. Kiuchi¹⁶⁰, E. Kladiva^{144b}, M. Klein⁷³, U. Klein⁷³, K. Kleinknecht⁸¹, M. Klemetti⁸⁵, A. Klier¹⁷², P. Klimek^{146a,146b}, A. Klimentov²⁵, R. Klingenberg⁴³, J.A. Klinger⁸², E.B. Klinkby³⁶, T. Klioutchnikova³⁰, P.F. Klok¹⁰⁴, S. Klous¹⁰⁵, E.-E. Kluge^{58a}, T. Kluge⁷³, P. Kluit¹⁰⁵, S. Kluth⁹⁹, E. Kneringer⁶¹, E.B.F.G. Knoop⁸³, A. Knue⁵⁴, B.R. Ko⁴⁵, T. Kobayashi¹⁵⁵, M. Kobel⁴⁴, M. Kocian¹⁴³, P. Kodys¹²⁷, S. Koenig⁸¹, F. Koetsveld¹⁰⁴, P. Koesvarki²¹, T. Koffas²⁹, E. Koffeman¹⁰⁵, L.A. Kogan¹¹⁸, S. Kohlmann¹⁷⁵, F. Kohn⁵⁴, Z. Kohout¹²⁶, T. Kohriki⁶⁵, T. Koi¹⁴³, H. Kolanoski¹⁶, I. Koletsou^{89a}, J. Koll⁸⁸, A.A. Komar⁹⁴, Y. Komori¹⁵⁵, T. Kondo⁶⁵, K. Köneke³⁰, A.C. König¹⁰⁴, T. Kono^{42,q}, A.I. Kononov⁴⁸, R. Konoplich^{108,r}, N. Konstantinidis⁷⁷, R. Kopeliansky¹⁵², S. Koperny³⁸, L. Köpke⁸¹, A.K. Kopp⁴⁸, K. Korcyl³⁹, K. Kordas¹⁵⁴, A. Korn⁴⁶, A. Korol¹⁰⁷, I. Korolkov¹², E.V. Korolkova¹³⁹, V.A. Korotkov¹²⁸, O. Kortner⁹⁹, S. Kortner⁹⁹, V.V. Kostyukhin²¹, S. Kotov⁹⁹, V.M. Kotov⁶⁴, A. Kotwal⁴⁵, C. Kourkoumelis⁹, V. Kouskoura¹⁵⁴, A. Koutsman^{159a}, R. Kowalewski¹⁶⁹, T.Z. Kowalski³⁸, W. Kozanecki¹³⁶, A.S. Kozhin¹²⁸, V. Kral¹²⁶, V.A. Kramarenko⁹⁷, G. Kramberger⁷⁴, M.W. Krasny⁷⁸, A. Krasznahorkay¹⁰⁸, J.K. Kraus²¹, A. Kravchenko²⁵, S. Kreiss¹⁰⁸, F. Krejci¹²⁶, J. Kretzschmar⁷³, K. Kreutzfeldt⁵², N. Krieger¹⁵⁸, K. Kroeninger⁵⁴, H. Kroha⁹⁹, J. Kroll¹²⁰, J. Kroseberg²¹, J. Krstic^{13a}, U. Kruchonak⁶⁴, H. Krüger²¹, T. Kruker¹⁷, N. Krumnack⁶³, Z.V. Krumsteyn⁶⁴, M.K. Kruse⁴⁵, T. Kubota⁸⁶, S. Kuday^{4a}, S. Kuehn⁴⁸, A. Kugel^{58c}, T. Kuhl⁴², V. Kukhtin⁶⁴, Y. Kulchitsky⁹⁰, S. Kuleshov^{32b}, M. Kuna⁷⁸, J. Kunkle¹²⁰, A. Kupco¹²⁵, H. Kurashige⁶⁶, M. Kurata¹⁶⁰, Y.A. Kurochkin⁹⁰, V. Kus¹²⁵, E.S. Kuwertz¹⁴⁷, M. Kuze¹⁵⁷, J. Kvita¹⁴², R. Kwee¹⁶, A. La Rosa⁴⁹, L. La Rotonda^{37a,37b}, L. Labarga⁸⁰, S. Lablak^{135a}, C. Lacasta¹⁶⁷, F. Lacava^{132a,132b}, J. Lacey²⁹, H. Lacker¹⁶, D. Lacour⁷⁸, V.R. Lacuesta¹⁶⁷, E. Ladygin⁶⁴, R. Lafaye⁵, B. Laforge⁷⁸, T. Lagouri¹⁷⁶, S. Lai⁴⁸, E. Laisne⁵⁵, L. Lambourne⁷⁷, C.L. Lampen⁷, W. Lampl⁷, E. Lançon¹³⁶, U. Landgraf⁴⁸, M.P.J. Landon⁷⁵, V.S. Lang^{58a}, C. Lange⁴², A.J. Lankford¹⁶³, F. Lanni²⁵, K. Lantzsch³⁰, A. Lanza^{119a}, S. Laplace⁷⁸, C. Lapoire²¹, J.F. Laporte¹³⁶, T. Lari^{89a}, A. Larner¹¹⁸, M. Lassnig³⁰, P. Laurelli⁴⁷, V. Lavorini^{37a,37b}, W. Lavrijsen¹⁵, P. Laycock⁷³, O. Le Dortz⁷⁸, E. Le Guirrec⁸³, E. Le Menedeu¹², T. LeCompte⁶, F. Ledroit-Guillon⁵⁵, H. Lee¹⁰⁵, J.S.H. Lee¹¹⁶, S.C. Lee¹⁵¹, L. Lee¹⁷⁶, M. Lefebvre¹⁶⁹, M. Legendre¹³⁶, F. Legger⁹⁸, C. Leggett¹⁵, M. Lehmacher²¹, G. Lehmann Miotto³⁰, A.G. Leister¹⁷⁶, M.A.L. Leite^{24d}, R. Leitner¹²⁷, D. Lellouch¹⁷², B. Lemmer⁵⁴, V. Lendermann^{58a}, K.J.C. Leney^{145b}, T. Lenz¹⁰⁵, G. Lenzen¹⁷⁵, B. Lenzi³⁰, K. Leonhardt⁴⁴, S. Leontsinis¹⁰, F. Lepold^{58a}, C. Leroy⁹³, J-R. Lessard¹⁶⁹, C.G. Lester²⁸, C.M. Lester¹²⁰, J. Levêque⁵, D. Levin⁸⁷, L.J. Levinson¹⁷², A. Lewis¹¹⁸, G.H. Lewis¹⁰⁸, A.M. Leyko²¹, M. Leyton¹⁶, B. Li^{33b}, B. Li⁸³, H. Li¹⁴⁸, H.L. Li³¹, S. Li^{33b,s}, X. Li⁸⁷, Z. Liang^{118,t}, H. Liao³⁴, B. Liberti^{133a}, P. Lichard³⁰, K. Lie¹⁶⁵, J. Liebal²¹, W. Liebig¹⁴, C. Limbach²¹, A. Limosani⁸⁶, M. Limper⁶², S.C. Lin^{151,u}, F. Linde¹⁰⁵, J.T. Linnemann⁸⁸, E. Lipeles¹²⁰, A. Lipniacka¹⁴, M. Lisovyi⁴², T.M. Liss¹⁶⁵, D. Lissauer²⁵, A. Lister¹⁶⁸, A.M. Litke¹³⁷, D. Liu¹⁵¹, J.B. Liu^{33b}, L. Liu⁸⁷, M. Liu^{33b}, Y. Liu^{33b}, M. Livan^{119a,119b}, S.S.A. Livermore¹¹⁸, A. Lleres⁵⁵, J. Llorente Merino⁸⁰, S.L. Lloyd⁷⁵, F. Lo Sterzo^{132a,132b}, E. Lobodzinska⁴², P. Loch⁷, W.S. Lockman¹³⁷, T. Lodenkoetter²¹, F.K. Loebinger⁸², A.E. Loevschall-Jensen³⁶, A. Loginov¹⁷⁶, C.W. Loh¹⁶⁸, T. Lohse¹⁶, K. Lohwasser⁴⁸, M. Lokajicek¹²⁵, V.P. Lombardo⁵, R.E. Long⁷¹, L. Lopes^{124a}, D. Lopez Mateos⁵⁷, J. Lorenz⁹⁸, N. Lorenzo Martinez¹¹⁵, M. Losada¹⁶², P. Loscutoff¹⁵, M.J. Losty^{159a,*}, X. Lou⁴¹, A. Lounis¹¹⁵, K.F. Loureiro¹⁶², J. Love⁶, P.A. Love⁷¹, A.J. Lowe^{143,f}, F. Lu^{33a}, H.J. Lubatti¹³⁸, C. Luci^{132a,132b}, A. Lucotte⁵⁵, D. Ludwig⁴², I. Ludwig⁴⁸, J. Ludwig⁴⁸, F. Luehring⁶⁰, W. Lukas⁶¹, L. Luminari^{132a}, E. Lund¹¹⁷, B. Lundberg⁷⁹, J. Lundberg^{146a,146b}, O. Lundberg^{146a,146b}, B. Lund-Jensen¹⁴⁷, J. Lundquist³⁶, M. Lungwitz⁸¹, D. Lynn²⁵, R. Lysak¹²⁵, E. Lytken⁷⁹, H. Ma²⁵, L.L. Ma¹⁷³, G. Maccarrone⁴⁷, A. Macchiolo⁹⁹, B. Maček⁷⁴, J. Machado Miguens^{124a}, D. Macina³⁰, R. Mackeprang³⁶, R. Madar⁴⁸, R.J. Madaras¹⁵, H.J. Maddocks⁷¹, W.F. Mader⁴⁴, A. Madsen¹⁶⁶, M. Maeno⁵, T. Maeno²⁵, L. Magnoni¹⁶³, E. Magradze⁵⁴, K. Mahboubi⁴⁸, J. Mahlstedt¹⁰⁵, S. Mahmoud⁷³, G. Mahout¹⁸, C. Maiani¹³⁶, C. Maidantchik^{24a}, A. Maio^{124a,c}, S. Majewski²⁵, Y. Makida⁶⁵, N. Makovec¹¹⁵, P. Mal^{136,v}, B. Malaescu⁷⁸, Pa. Malecki³⁹, P. Malecki³⁹, V.P. Maleev¹²¹, F. Malek⁵⁵,

U. Mallik⁶², D. Malon⁶, C. Malone¹⁴³, S. Maltezos¹⁰, V. Malyshev¹⁰⁷, S. Malyukov³⁰, J. Mamuzic^{13b}, L. Mandelli^{89a}, I. Mandić⁷⁴, R. Mandrysch⁶², J. Maneira^{124a}, A. Manfredini⁹⁹, L. Manhaes de Andrade Filho^{24b}, J.A. Manjarres Ramos¹³⁶, A. Mann⁹⁸, P.M. Manning¹³⁷, A. Manousakis-Katsikakis⁹, B. Mansoulie¹³⁶, R. Mantifel³⁰, A. Mapelli³⁰, L. Mapelli³⁰, L. March¹⁶⁷, J.F. Marchand²⁹, F. Marchese^{133a,133b}, G. Marchiori⁷⁸, M. Marcisovsky¹²⁵, C.P. Marino¹⁶⁹, F. Marroquim^{24a}, Z. Marshall³⁰, L.F. Marti¹⁷, S. Marti-Garcia¹⁶⁷, B. Martin³⁰, B. Martin⁸⁸, J.P. Martin⁹³, T.A. Martin¹⁸, V.J. Martin⁴⁶, B. Martin dit Latour⁴⁹, H. Martinez¹³⁶, M. Martinez¹², V. Martinez Outschoorn⁵⁷, S. Martin-Haugh¹⁴⁹, A.C. Martyniuk¹⁶⁹, M. Marx⁸², F. Marzano^{132a}, A. Marzin¹¹¹, L. Masetti⁸¹, T. Mashimo¹⁵⁵, R. Mashinistov⁹⁴, J. Masik⁸², A.L. Maslennikov¹⁰⁷, I. Massa^{20a,20b}, N. Massol⁵, P. Mastrandrea¹⁴⁸, A. Mastroberardino^{37a,37b}, T. Masubuchi¹⁵⁵, H. Matsunaga¹⁵⁵, T. Matsushita⁶⁶, P. Mättig¹⁷⁵, S. Mättig⁴², C. Mattraversi^{118,d}, J. Maurer⁸³, S.J. Maxfield⁷³, D.A. Maximov^{107,g}, R. Mazini¹⁵¹, M. Mazur²¹, L. Mazzaferro^{133a,133b}, M. Mazzanti^{89a}, J. Mc Donald⁸⁵, S.P. Mc Kee⁸⁷, A. McCarn¹⁶⁵, R.L. McCarthy¹⁴⁸, T.G. McCarthy²⁹, N.A. McCubbin¹²⁹, K.W. McFarlane^{56,*}, J.A. Mcfayden¹³⁹, G. Mchedlidze^{51b}, T. McLaughlan¹⁸, S.J. McMahon¹²⁹, R.A. McPherson^{169,j}, A. Meade⁸⁴, J. Mechnich¹⁰⁵, M. Mechtel¹⁷⁵, M. Medinnis⁴², S. Meehan³¹, R. Meera-Lebbai¹¹¹, T. Meguro¹¹⁶, S. Mehlhase³⁶, A. Mehta⁷³, K. Meier^{58a}, C. Meineck⁹⁸, B. Meirose⁷⁹, C. Melachrinou³¹, B.R. Mellado Garcia¹⁷³, F. Meloni^{89a,89b}, L. Mendoza Navas¹⁶², Z. Meng^{151,w}, A. Mengarelli^{20a,20b}, S. Menke⁹⁹, E. Meoni¹⁶¹, K.M. Mercurio⁵⁷, N. Meric⁷⁸, P. Mermod⁴⁹, L. Merola^{102a,102b}, C. Meroni^{89a}, F.S. Merritt³¹, H. Merritt¹⁰⁹, A. Messina^{30,x}, J. Metcalfe²⁵, A.S. Mete¹⁶³, C. Meyer⁸¹, C. Meyer³¹, J-P. Meyer¹³⁶, J. Meyer³⁰, J. Meyer⁵⁴, S. Michal³⁰, R.P. Middleton¹²⁹, S. Migas⁷³, L. Mijović¹³⁶, G. Mikenberg¹⁷², M. Mikestikova¹²⁵, M. Mikuz⁷⁴, D.W. Miller³¹, R.J. Miller⁸⁸, W.J. Mills¹⁶⁸, C. Mills⁵⁷, A. Milov¹⁷², D.A. Milstead^{146a,146b}, D. Milstein¹⁷², A.A. Minaenko¹²⁸, M. Miñano Moya¹⁶⁷, I.A. Minashvili⁶⁴, A.I. Mincer¹⁰⁸, B. Mindur³⁸, M. Mineev⁶⁴, Y. Ming¹⁷³, L.M. Mir¹², G. Mirabelli^{132a}, J. Mitrevski¹³⁷, V.A. Mitsou¹⁶⁷, S. Mitsui⁶⁵, P.S. Miyagawa¹³⁹, J.U. Mjörnmark⁷⁹, T. Moa^{146a,146b}, V. Moeller²⁸, S. Mohapatra¹⁴⁸, W. Mohr⁴⁸, R. Moles-Valls¹⁶⁷, A. Molfetas³⁰, K. Mönig⁴², C. Monini⁵⁵, J. Monk³⁶, E. Monnier⁸³, J. Montejo Berlingen¹², F. Monticelli⁷⁰, S. Monzani^{20a,20b}, R.W. Moore³, C. Mora Herrera⁴⁹, A. Moraes⁵³, N. Morange⁶², J. Morel⁵⁴, D. Moreno⁸¹, M. Moreno Llacer¹⁶⁷, P. Morettini^{50a}, M. Morgenstern⁴⁴, M. Morii⁵⁷, A.K. Morley³⁰, G. Mornacchi³⁰, J.D. Morris⁷⁵, L. Morvaj¹⁰¹, N. Möser²¹, H.G. Moser⁹⁹, M. Mosidze^{51b}, J. Moss¹⁰⁹, R. Mount¹⁴³, E. Mountricha^{10,y}, S.V. Mouraviev^{94,*}, E.J.W. Moyse⁸⁴, F. Mueller^{58a}, J. Mueller¹²³, K. Mueller²¹, T. Mueller⁸¹, D. Muenstermann³⁰, T.A. Müller⁹⁸, Y. Munwes¹⁵³, W.J. Murray¹²⁹, I. Mussche¹⁰⁵, E. Musto¹⁵², A.G. Myagkov¹²⁸, M. Myska¹²⁵, O. Nackenhorst⁵⁴, J. Nadal¹², K. Nagai¹⁶⁰, R. Nagai¹⁵⁷, Y. Nagai⁸³, K. Nagano⁶⁵, A. Nagarkar¹⁰⁹, Y. Nagasaka⁵⁹, M. Nagel⁹⁹, A.M. Nairz³⁰, Y. Nakahama³⁰, K. Nakamura⁶⁵, T. Nakamura¹⁵⁵, I. Nakano¹¹⁰, H. Namasivayam⁴¹, G. Nanava²¹, A. Napier¹⁶¹, R. Narayan^{58b}, M. Nash^{77,d}, T. Nattermann²¹, T. Naumann⁴², G. Navarro¹⁶², H.A. Neal⁸⁷, P.Yu. Nechaeva⁹⁴, T.J. Neepe⁸², A. Negri^{119a,119b}, G. Negri³⁰, M. Negrini^{20a}, S. Nektarijevic⁴⁹, A. Nelson¹⁶³, T.K. Nelson¹⁴³, S. Nemecek¹²⁵, P. Nemethy¹⁰⁸, A.A. Nepomuceno^{24a}, M. Nessi^{30,z}, M.S. Neubauer¹⁶⁵, M. Neumann¹⁷⁵, A. Neusiedl⁸¹, R.M. Neves¹⁰⁸, P. Nevski²⁵, F.M. Newcomer¹²⁰, P.R. Newman¹⁸, D.H. Nguyen⁶, V. Nguyen Thi Hong¹³⁶, R.B. Nickerson¹¹⁸, R. Nicolaidou¹³⁶, B. Nicquevert³⁰, F. Niedercorn¹¹⁵, J. Nielsen¹³⁷, N. Nikiforou³⁵, A. Nikiforov¹⁶, V. Nikolaenko¹²⁸, I. Nikolic-Audit⁷⁸, K. Nikolics⁴⁹, K. Nikolopoulos¹⁸, H. Nilsen⁴⁸, P. Nilsson⁸, Y. Ninomiya¹⁵⁵, A. Nisati^{132a}, R. Nisius⁹⁹, T. Nobe¹⁵⁷, L. Nodulman⁶, M. Nomachi¹¹⁶, I. Nomidis¹⁵⁴, S. Norberg¹¹¹, M. Nordberg³⁰, J. Novakova¹²⁷, M. Nozaki⁶⁵, L. Nozka¹¹³, A.-E. Nuncio-Quiroz²¹, G. Nunes Hanninger⁸⁶, T. Nunnemann⁹⁸, E. Nurse⁷⁷, B.J. O'Brien⁴⁶, D.C. O'Neil¹⁴², V. O'Shea⁵³, L.B. Oakes⁹⁸, F.G. Oakham^{29,e}, H. Oberlack⁹⁹, J. Ocariz⁷⁸, A. Ochi⁶⁶, M.I. Ochoa⁷⁷, S. Oda⁶⁹, S. Odaka⁶⁵, J. Odier⁸³, H. Ogren⁶⁰, A. Oh⁸², S.H. Oh⁴⁵, C.C. Ohm³⁰, T. Ohshima¹⁰¹, W. Okamura¹¹⁶, H. Okawa²⁵, Y. Okumura³¹, T. Okuyama¹⁵⁵, A. Olariu^{26a}, A.G. Olchevski⁶⁴, S.A. Olivares Pino⁴⁶, M. Oliveira^{124a,h}, D. Oliveira Damazio²⁵, E. Oliver Garcia¹⁶⁷, D. Olivito¹²⁰, A. Olszewski³⁹, J. Olszowska³⁹, A. Onofre^{124a,aa}, P.U.E. Onyisi^{31,ab}, C.J. Oram^{159a}, M.J. Oreglia³¹, Y. Oren¹⁵³, D. Orestano^{134a,134b}, N. Orlando^{72a,72b}, C. Oropeza Barrera⁵³, R.S. Orr¹⁵⁸, B. Osculati^{50a,50b}, R. Ospanov¹²⁰, C. Osuna¹², G. Otero y Garzon²⁷, J.P. Ottersbach¹⁰⁵, M. Ouchrif^{135d}, E.A. Ouellette¹⁶⁹, F. Ould-Saada¹¹⁷, A. Ouraou¹³⁶, Q. Ouyang^{33a}, A. Ovcharova¹⁵, M. Owen⁸², S. Owen¹³⁹, V.E. Ozcan^{19a}, N. Ozturk⁸, A. Pacheco Pages¹², C. Padilla Aranda¹², S. Pagan Griso¹⁵, E. Paganis¹³⁹, C. Pahl⁹⁹, F. Paige²⁵, P. Pais⁸⁴, K. Pajchel¹¹⁷, G. Palacino^{159b}, C.P. Paleari⁷, S. Palestini³⁰, D. Pallin³⁴, A. Palma^{124a}, J.D. Palmer¹⁸, Y.B. Pan¹⁷³, E. Panagiotopoulou¹⁰, J.G. Panduro Vazquez⁷⁶, P. Pani¹⁰⁵, N. Panikashvili⁸⁷, S. Panitkin²⁵, D. Pantea^{26a}, A. Papadelis^{146a}, Th.D. Papadopolou¹⁰, A. Paramonov⁶, D. Paredes Hernandez³⁴, W. Park^{25,ac}, M.A. Parker²⁸, F. Parodi^{50a,50b}, J.A. Parsons³⁵, U. Parzefall⁴⁸, S. Pashapour⁵⁴, E. Pasqualucci^{132a}, S. Passaggio^{50a}, A. Passeri^{134a}, F. Pastore^{134a,134b,*}, Fr. Pastore⁷⁶, G. Pásztor^{49,ad}, S. Pataraja¹⁷⁵, N.D. Patel¹⁵⁰, J.R. Pater⁸², S. Patricelli^{102a,102b}, T. Pauly³⁰, J. Pearce¹⁶⁹, M. Pedersen¹¹⁷, S. Pedraza Lopez¹⁶⁷, M.I. Pedraza Morales¹⁷³, S.V. Peleganchuk¹⁰⁷, D. Pelikan¹⁶⁶, H. Peng^{33b}, B. Penning³¹, A. Penson³⁵, J. Penwell⁶⁰, T. Perez Cavalcanti⁴², E. Perez Codina^{159a}, M.T. Pérez García-Estanz¹⁶⁷, V. Perez Reale³⁵, L. Perini^{89a,89b}, H. Pernegger³⁰, R. Perrino^{72a}, P. Perrodo⁵, V.D. Peshekhonov⁶⁴, K. Peters³⁰, R.F.Y. Peters^{54,ae}, B.A. Petersen³⁰, J. Petersen³⁰, T.C. Petersen³⁶, E. Petit⁵, A. Petridis^{146a,146b}, C. Petridou¹⁵⁴, E. Petrolu^{132a}, F. Petrucci^{134a,134b}, D. Petschull⁴², M. Petteni¹⁴², R. Pezoa^{32b}, A. Phan⁸⁶, P.W. Phillips¹²⁹,

G. Piacquadio¹⁴³, E. Pianori¹⁷⁰, A. Picazio⁴⁹, E. Piccaro⁷⁵, M. Piccinini^{20a,20b}, S.M. Piec⁴², R. Piegai²⁷, D.T. Pignotti¹⁰⁹, J.E. Pilcher³¹, A.D. Pilkington⁸², J. Pina^{124a,c}, M. Pinamonti^{164a,164c,af}, A. Pinder¹¹⁸, J.L. Pinfeld³, A. Pingel³⁶, B. Pinto^{124a}, C. Pizio^{89a,89b}, M.-A. Pleier²⁵, V. Pleskot¹²⁷, E. Plotnikova⁶⁴, P. Plucinski^{146a,146b}, A. Poblaguev²⁵, S. Poddar^{58a}, F. Podlyski³⁴, R. Poettgen⁸¹, L. Poggioli¹¹⁵, D. Pohl²¹, M. Pohl⁴⁹, G. Polesello^{119a}, A. Policicchio^{37a,37b}, R. Polifka¹⁵⁸, A. Polini^{20a}, J. Poll⁷⁵, V. Polychronakos²⁵, D. Pomeroy²³, K. Pommès³⁰, L. Pontecorvo^{132a}, B.G. Pope⁸⁸, G.A. Popeneciu^{26a}, D.S. Popovic^{13a}, A. Poppleton³⁰, X. Portell Bueso³⁰, G.E. Pospelov⁹⁹, S. Pospisil¹²⁶, I.N. Potrap⁶⁴, C.J. Potter¹⁴⁹, C.T. Potter¹¹⁴, G. Poulard³⁰, J. Poveda⁶⁰, V. Pozdnyakov⁶⁴, R. Prabhu⁷⁷, P. Pralavorio⁸³, A. Pranko¹⁵, S. Prasad³⁰, R. Pravahan²⁵, S. Prell⁶³, K. Pretzl¹⁷, D. Price⁶⁰, J. Price⁷³, L.E. Price⁶, D. Prieur¹²³, M. Primavera^{72a}, M. Proissl⁴⁶, K. Prokofiev¹⁰⁸, F. Prokoshin^{32b}, E. Protopapadaki¹³⁶, S. Protopopescu²⁵, J. Proudfoot⁶, X. Prudent⁴⁴, M. Przybycien³⁸, H. Przysieznia⁵, S. Psoroulas²¹, E. Ptacek¹¹⁴, E. Pueschel⁸⁴, D. Puldon¹⁴⁸, M. Purohit^{25,ac}, P. Puzo¹¹⁵, Y. Pylypchenko⁶², J. Qian⁸⁷, A. Quadt⁵⁴, D.R. Quarrie¹⁵, W.B. Quayle¹⁷³, D. Quilty⁵³, M. Raas¹⁰⁴, V. Radeka²⁵, V. Radescu⁴², P. Radloff¹¹⁴, F. Ragusa^{89a,89b}, G. Rahal¹⁷⁸, A.M. Rahimi¹⁰⁹, S. Rajagopalan²⁵, M. Rammensee⁴⁸, M. Rammes¹⁴¹, A.S. Randle-Conde⁴⁰, K. Randrianarivony²⁹, C. Rangel-Smith⁷⁸, K. Rao¹⁶³, F. Rauscher⁹⁸, T.C. Rave⁴⁸, T. Ravenscroft⁵³, M. Raymond³⁰, A.L. Read¹¹⁷, D.M. Rebuffi^{119a,119b}, A. Redelbach¹⁷⁴, G. Redlinger²⁵, R. Reece¹²⁰, K. Reeves⁴¹, A. Reinsch¹¹⁴, I. Reisinger⁴³, M. Relich¹⁶³, C. Rembser³⁰, Z.L. Ren¹⁵¹, A. Renaud¹¹⁵, M. Rescigno^{132a}, S. Resconi^{89a}, B. Resende¹³⁶, P. Reznicek⁹⁸, R. Rezvani¹⁵⁸, R. Richter⁹⁹, E. Richter-Was⁵, M. Ridel⁷⁸, P. Rieck¹⁶, M. Rijssenbeek¹⁴⁸, A. Rimoldi^{119a,119b}, L. Rinaldi^{20a}, R.R. Rios⁴⁰, E. Ritsch⁶¹, I. Riu¹², G. Rivoltella^{89a,89b}, F. Rizatdinova¹¹², E. Rizvi⁷⁵, S.H. Robertson^{85,j}, A. Robichaud-Veronneau¹¹⁸, D. Robinson²⁸, J.E.M. Robinson⁸², A. Robson⁵³, J.G. Rocha de Lima¹⁰⁶, C. Roda^{122a,122b}, D. Roda Dos Santos³⁰, A. Roe⁵⁴, S. Roe³⁰, O. Røhne¹¹⁷, S. Rollin¹⁶¹, A. Romaniouk⁹⁶, M. Romano^{20a,20b}, G. Romeo²⁷, E. Romero Adam¹⁶⁷, N. Rompotis¹³⁸, L. Roos⁷⁸, E. Ros¹⁶⁷, S. Rosati^{132a}, K. Rosbach⁴⁹, A. Rose¹⁴⁹, M. Rose⁷⁶, G.A. Rosenbaum¹⁵⁸, P.L. Rosendahl¹⁴, O. Rosenthal¹⁴¹, L. Rosselet⁴⁹, V. Rossetti¹², E. Rossi^{132a,132b}, L.P. Rossi^{50a}, M. Rotaru^{26a}, I. Roth¹⁷², J. Rothberg¹³⁸, D. Rousseau¹¹⁵, C.R. Royon¹³⁶, A. Rozanov⁸³, Y. Rozen¹⁵², X. Ruan^{33a,ag}, F. Rubbo¹², I. Rubinskiy⁴², N. Ruckstuhl¹⁰⁵, V.I. Rud⁹⁷, C. Rudolph⁴⁴, M.S. Rudolph¹⁵⁸, F. Rühr⁷, A. Ruiz-Martinez⁶³, L. Rumyantsev⁶⁴, Z. Rurikova⁴⁸, N.A. Rusakovich⁶⁴, A. Ruschke⁹⁸, J.P. Rutherford⁷, N. Ruthmann⁴⁸, P. Ruzicka¹²⁵, Y.F. Ryabov¹²¹, M. Rybar¹²⁷, G. Rybkin¹¹⁵, N.C. Ryder¹¹⁸, A.F. Saavedra¹⁵⁰, I. Sadeh¹⁵³, H.F.-W. Sadrozinski¹³⁷, R. Sadykov⁶⁴, F. Safai Tehrani^{132a}, H. Sakamoto¹⁵⁵, G. Salamanna⁷⁵, A. Salamon^{133a}, M. Saleem¹¹¹, D. Salek³⁰, D. Salihagic⁹⁹, A. Salnikov¹⁴³, J. Salt¹⁶⁷, B.M. Salvachua Ferrando⁶, D. Salvatore^{37a,37b}, F. Salvatore¹⁴⁹, A. Salvucci¹⁰⁴, A. Salzburger³⁰, D. Sampsonidis¹⁵⁴, A. Sanchez^{102a,102b}, J. Sánchez¹⁶⁷, V. Sanchez Martinez¹⁶⁷, H. Sandaker¹⁴, H.G. Sander⁸¹, M.P. Sanders⁹⁸, M. Sandhoff¹⁷⁵, T. Sandoval²⁸, C. Sandoval¹⁶², R. Sandstroem⁹⁹, D.P.C. Sankey¹²⁹, A. Sansoni⁴⁷, C. Santoni³⁴, R. Santonico^{133a,133b}, H. Santos^{124a}, I. Santoyo Castillo¹⁴⁹, K. Sapp¹²³, J.G. Saraiva^{124a}, T. Sarangi¹⁷³, E. Sarkisyan-Grinbaum⁸, B. Sarrazin²¹, F. Sarri^{122a,122b}, G. Sartisohn¹⁷⁵, O. Sasaki⁶⁵, Y. Sasaki¹⁵⁵, N. Sasao⁶⁷, I. Satsounkevitch⁹⁰, G. Sauvage^{5,*}, E. Sauvan⁵, J.B. Sauvan¹¹⁵, P. Savard^{158,e}, V. Savinov¹²³, D.O. Savu³⁰, C. Sawyer¹¹⁸, L. Sawyer^{25,l}, D.H. Saxon⁵³, J. Saxon¹²⁰, C. Sbarra^{20a}, A. Sbrizzi³, D.A. Scannicchio¹⁶³, M. Scarcella¹⁵⁰, J. Schaarschmidt¹¹⁵, P. Schacht⁹⁹, D. Schaefer¹²⁰, A. Schaelicke⁴⁶, S. Schaepe²¹, S. Schaezel^{58b}, U. Schäfer⁸¹, A.C. Schaffer¹¹⁵, D. Schaile⁹⁸, R.D. Schamberger¹⁴⁸, V. Scharf^{58a}, V.A. Schegelsky¹²¹, D. Scheirich⁸⁷, M. Schernau¹⁶³, M.I. Scherzer³⁵, C. Schiavi^{50a,50b}, J. Schieck⁹⁸, C. Schillo⁴⁸, M. Schioppa^{37a,37b}, S. Schlenker³⁰, E. Schmidt⁴⁸, K. Schmieden²¹, C. Schmitt⁸¹, C. Schmitt⁹⁸, S. Schmitt^{58b}, B. Schneider¹⁷, Y.J. Schnellbach⁷³, U. Schnoor⁴⁴, L. Schoeffel¹³⁶, A. Schoening^{58b}, A.L.S. Schorlemmer⁵⁴, M. Schott⁸¹, D. Schouten^{159a}, J. Schovancova¹²⁵, M. Schram⁸⁵, C. Schroeder⁸¹, N. Schroer^{58c}, M.J. Schultens²¹, J. Schultes¹⁷⁵, H.-C. Schultz-Coulon^{58a}, H. Schulz¹⁶, M. Schumacher⁴⁸, B.A. Schumm¹³⁷, Ph. Schune¹³⁶, A. Schwartzman¹⁴³, Ph. Schwegler⁹⁹, Ph. Schwemling¹³⁶, R. Schwienhorst⁸⁸, J. Schwindling¹³⁶, T. Schwindt²¹, M. Schwoerer⁵, F.G. Sciacca¹⁷, E. Scifo¹¹⁵, G. Sciolla²³, W.G. Scott¹²⁹, J. Searcy⁸⁷, G. Sedov⁴², E. Sedykh¹²¹, S.C. Seidel¹⁰³, A. Seiden¹³⁷, F. Seifert⁴⁴, J.M. Seixas^{24a}, G. Sekhniaidze^{102a}, S.J. Sekula⁴⁰, K.E. Selbach⁴⁶, D.M. Seliverstov¹²¹, G. Sellers⁷³, M. Seman^{144b}, N. Semprini-Cesari^{20a,20b}, C. Serfon³⁰, L. Serin¹¹⁵, L. Serkin⁵⁴, T. Serre⁸³, R. Seuster^{159a}, H. Severini¹¹¹, A. Sfyrla³⁰, E. Shabalina⁵⁴, M. Shamim¹¹⁴, L.Y. Shan^{33a}, J.T. Shank²², Q.T. Shao⁸⁶, M. Shapiro¹⁵, P.B. Shatalov⁹⁵, K. Shaw^{164a,164c}, P. Sherwood⁷⁷, S. Shimizu¹⁰¹, M. Shimojima¹⁰⁰, T. Shin⁵⁶, M. Shiyakova⁶⁴, A. Shmeleva⁹⁴, M.J. Shochet³¹, D. Short¹¹⁸, S. Shrestha⁶³, E. Shulga⁹⁶, M.A. Shupe⁷, P. Sicho¹²⁵, A. Sidoti^{132a}, F. Siegert⁴⁸, Dj. Sijacki^{13a}, O. Silbert¹⁷², J. Silva^{124a}, Y. Silver¹⁵³, D. Silverstein¹⁴³, S.B. Silverstein^{146a}, V. Simak¹²⁶, O. Simard⁵, Lj. Simic^{13a}, S. Simion¹¹⁵, E. Simioni⁸¹, B. Simmons⁷⁷, R. Simoniello^{89a,89b}, M. Simonyan³⁶, P. Sinervo¹⁵⁸, N.B. Sinev¹¹⁴, V. Sipica¹⁴¹, G. Siragusa¹⁷⁴, A. Sircar²⁵, A.N. Sisakyan^{64,*}, S.Yu. Sivoklov⁹⁷, J. Sjölin^{146a,146b}, T.B. Sjurson¹⁴, L.A. Skinnari¹⁵, H.P. Skottowe⁵⁷, K. Skovpen¹⁰⁷, P. Skubic¹¹¹, M. Slater¹⁸, T. Slavicek¹²⁶, K. Sliwa¹⁶¹, V. Smakhtin¹⁷², B.H. Smart⁴⁶, L. Smestad¹¹⁷, S.Yu. Smirnov⁹⁶, Y. Smirnov⁹⁶, L.N. Smirnova^{97,ah}, O. Smirnova⁷⁹, B.C. Smith⁵⁷, K.M. Smith⁵³, M. Smizanska⁷¹, K. Smolek¹²⁶, A.A. Snesarev⁹⁴, G. Snidero⁷⁵, J. Snow¹¹¹, S. Snyder²⁵, R. Sobie^{169,j}, J. Sodomka¹²⁶, A. Soffer¹⁵³, D.A. Soh^{151,t}, C.A. Solans³⁰, M. Solar¹²⁶, J. Solc¹²⁶, E.Yu. Soldatov⁹⁶, U. Soldevila¹⁶⁷,

E. Solfaroli Camillocci^{132a,132b}, A.A. Solodkov¹²⁸, O.V. Solovyanov¹²⁸, V. Solovyev¹²¹, N. Soni¹, A. Sood¹⁵,
 V. Sopko¹²⁶, B. Sopko¹²⁶, M. Sosebee⁸, R. Soualah^{164a,164c}, P. Soueid⁹³, A. Soukharev¹⁰⁷, D. South⁴²,
 S. Spagnolo^{72a,72b}, F. Spano⁷⁶, R. Spighi^{20a}, G. Spigo³⁰, R. Spiwoaks³⁰, M. Spousta^{127,ai}, T. Spreitzer¹⁵⁸,
 B. Spurlock⁸, R.D. St. Denis⁵³, J. Stahlman¹²⁰, R. Stamen^{58a}, E. Stanecka³⁹, R.W. Stanek⁶, C. Stanescu^{134a},
 M. Stanescu-Bellu⁴², M.M. Stanitzki⁴², S. Stapnes¹¹⁷, E.A. Starchenko¹²⁸, J. Stark⁵⁵, P. Staroba¹²⁵,
 P. Starovoitov⁴², R. Staszewski³⁹, A. Staude⁹⁸, P. Stavina^{144a,*}, G. Steele⁵³, P. Steinbach⁴⁴, P. Steinberg²⁵,
 I. Stekl¹²⁶, B. Stelzer¹⁴², H.J. Stelzer⁸⁸, O. Stelzer-Chilton^{159a}, G. Stenzel⁵², S. Stern⁹⁹, G.A. Stewart³⁰,
 J.A. Stillings²¹, M.C. Stockton⁸⁵, M. Stoebe⁸⁵, K. Stoerig⁴⁸, H. Stoicea^{26a}, S. Stonjek⁹⁹, P. Strachota¹²⁷,
 A.R. Stradling⁸, A. Straessner⁴⁴, J. Strandberg¹⁴⁷, S. Strandberg^{146a,146b}, A. Strandlie¹¹⁷, M. Strang¹⁰⁹,
 E. Strauss¹⁴³, M. Strauss¹¹¹, P. Strizenec^{144b}, R. Ströhmer¹⁷⁴, D.M. Strom¹¹⁴, J.A. Strong^{76,*}, R. Stroynowski⁴⁰,
 B. Stugu¹⁴, I. Stumer^{25,*}, J. Stupak¹⁴⁸, P. Sturm¹⁷⁵, N.A. Styles⁴², D. Su¹⁴³, HS. Subramania³, R. Subramaniam²⁵,
 A. Succurro¹², Y. Sugaya¹¹⁶, C. Suhr¹⁰⁶, M. Suk¹²⁷, V.V. Sulin⁹⁴, S. Sultansoy^{4c}, T. Sumida⁶⁷, X. Sun⁵⁵,
 J.E. Sundermann⁴⁸, K. Suruliz¹³⁹, G. Susinno^{37a,37b}, M.R. Sutton¹⁴⁹, Y. Suzuki⁶⁵, Y. Suzuki⁶⁶, M. Svatos¹²⁵,
 S. Swedish¹⁶⁸, M. Swiatlowski¹⁴³, I. Sykora^{144a}, T. Sykora¹²⁷, D. Ta¹⁰⁵, K. Tackmann⁴², A. Taffard¹⁶³,
 R. Tafirout^{159a}, N. Taiblum¹⁵³, Y. Takahashi¹⁰¹, H. Takai²⁵, R. Takashima⁶⁸, H. Takeda⁶⁶, T. Takeshita¹⁴⁰,
 Y. Takubo⁶⁵, M. Talby⁸³, A. Talyshv^{107,g}, J.Y.C. Tam¹⁷⁴, M.C. Tamsett²⁵, K.G. Tan⁸⁶, J. Tanaka¹⁵⁵,
 R. Tanaka¹¹⁵, S. Tanaka¹³¹, S. Tanaka⁶⁵, A.J. Tanasijczuk¹⁴², K. Tani⁶⁶, N. Tannoury⁸³, S. Tapprogge⁸¹,
 D. Tardif¹⁵⁸, S. Tarem¹⁵², F. Tarrade²⁹, G.F. Tartarelli^{89a}, P. Tas¹²⁷, M. Tasevsky¹²⁵, E. Tassi^{37a,37b},
 Y. Tayalati^{135d}, C. Taylor⁷⁷, F.E. Taylor⁹², G.N. Taylor⁸⁶, W. Taylor^{159b}, M. Teinturier¹¹⁵, F.A. Teischinger³⁰,
 M. Teixeira Dias Castanheira⁷⁵, P. Teixeira-Dias⁷⁶, K.K. Temming⁴⁸, H. Ten Kate³⁰, P.K. Teng¹⁵¹, S. Terada⁶⁵,
 K. Terashi¹⁵⁵, J. Terron⁸⁰, M. Testa⁴⁷, R.J. Teuscher^{158,j}, J. Therhaag²¹, T. Theveneaux-Pelzer³⁴, S. Thoma⁴⁸,
 J.P. Thomas¹⁸, E.N. Thompson³⁵, P.D. Thompson¹⁸, P.D. Thompson¹⁵⁸, A.S. Thompson⁵³, L.A. Thomsen³⁶,
 E. Thomson¹²⁰, M. Thomson²⁸, W.M. Thong⁸⁶, R.P. Thun^{87,*}, F. Tian³⁵, M.J. Tibbetts¹⁵, T. Tic¹²⁵,
 V.O. Tikhomirov⁹⁴, Y.A. Tikhonov^{107,g}, S. Timoshenko⁹⁶, E. Tiouchichine⁸³, P. Tipton¹⁷⁶, S. Tisserant⁸³,
 T. Todorov⁵, S. Todorova-Nova¹⁶¹, B. Toggerson¹⁶³, J. Tojo⁶⁹, S. Tokár^{144a}, K. Tokushuku⁶⁵, K. Tollefson⁸⁸,
 L. Tomlinson⁸², M. Tomoto¹⁰¹, L. Tompkins³¹, K. Toms¹⁰³, A. Tonoyan¹⁴, C. Topfel¹⁷, N.D. Topilin⁶⁴,
 E. Torrence¹¹⁴, H. Torres⁷⁸, E. Torró Pastor¹⁶⁷, J. Toth^{83,ad}, F. Touchard⁸³, D.R. Tovey¹³⁹, H.L. Tran¹¹⁵,
 T. Trefzger¹⁷⁴, L. Tremblet³⁰, A. Tricoli³⁰, I.M. Trigger^{159a}, S. Trincaz-Duvoid⁷⁸, M.F. Tripiana⁷⁰, N. Triplett²⁵,
 W. Trischuk¹⁵⁸, B. Trocme⁵⁵, C. Troncon^{89a}, M. Trottier-McDonald¹⁴², M. Trovatelli^{134a,134b}, P. True⁸⁸,
 M. Trzebinski³⁹, A. Trzupek³⁹, C. Tsarouchas³⁰, J.C.-L. Tseng¹¹⁸, M. Tsiakiris¹⁰⁵, P.V. Tsiarehska⁹⁰, D. Tsiou¹³⁶,
 G. Tsipolitis¹⁰, S. Tsiskaridze¹², V. Tsiskaridze⁴⁸, E.G. Tskhadadze^{51a}, I.I. Tsukerman⁹⁵, V. Tsulaia¹⁵,
 J.-W. Tsung²¹, S. Tsuno⁶⁵, D. Tsybychev¹⁴⁸, A. Tua¹³⁹, A. Tudorache^{26a}, V. Tudorache^{26a}, J.M. Tuggle³¹,
 A.N. Tuna¹²⁰, M. Turala³⁹, D. Turecek¹²⁶, I. Turk Cakir^{4d}, R. Turra^{89a,89b}, P.M. Tuts³⁵, A. Tykhonov⁷⁴,
 M. Tylmad^{146a,146b}, M. Tyndel¹²⁹, G. Tzanakos⁹, K. Uchida²¹, I. Ueda¹⁵⁵, R. Ueno²⁹, M. Ughetto⁸³, M. Ugland¹⁴,
 M. Uhlenbrock²¹, F. Ukegawa¹⁶⁰, G. Unal³⁰, A. Undrus²⁵, G. Unel¹⁶³, F.C. Ungaro⁴⁸, Y. Unno⁶⁵, D. Urbaniec³⁵,
 P. Urquijo²¹, G. Usai⁸, L. Vacavant⁸³, V. Vacek¹²⁶, B. Vachon⁸⁵, S. Vahsen¹⁵, N. Valencic¹⁰⁵, S. Valentinetti^{20a,20b},
 A. Valero¹⁶⁷, L. Valery³⁴, S. Valkar¹²⁷, E. Valladolid Gallego¹⁶⁷, S. Vallecorsa¹⁵², J.A. Valls Ferrer¹⁶⁷,
 R. Van Berg¹²⁰, P.C. Van Der Deijl¹⁰⁵, R. van der Geer¹⁰⁵, H. van der Graaf¹⁰⁵, R. Van Der Leeuw¹⁰⁵,
 E. van der Poel¹⁰⁵, D. van der Ster³⁰, N. van Eldik³⁰, P. van Gemmeren⁶, J. Van Nieuwkoop¹⁴², I. van Vulpen¹⁰⁵,
 M. Vanadia⁹⁹, W. Vandelli³⁰, A. Vaniachine⁶, P. Vankov⁴², F. Vannucci⁷⁸, R. Vari^{132a}, E.W. Varnes⁷, T. Varol⁸⁴,
 D. Varouchas¹⁵, A. Vartapetian⁸, K.E. Varvell¹⁵⁰, V.I. Vassilakopoulos⁵⁶, F. Vazeille³⁴, T. Vazquez Schroeder⁵⁴,
 F. Veloso^{124a}, S. Veneziano^{132a}, A. Ventura^{72a,72b}, D. Ventura⁸⁴, M. Venturi⁴⁸, N. Venturi¹⁵⁸, V. Vercesi^{119a},
 M. Verducci¹³⁸, W. Verkerke¹⁰⁵, J.C. Vermeulen¹⁰⁵, A. Vest⁴⁴, M.C. Vetterli^{142,e}, I. Vichou¹⁶⁵, T. Vickey^{145b,aj},
 O.E. Vickey Boeriu^{145b}, G.H.A. Viehhauser¹¹⁸, S. Viel¹⁶⁸, M. Villa^{20a,20b}, M. Villaplana Perez¹⁶⁷, E. Vilucchi⁴⁷,
 M.G. Vincker²⁹, E. Vinek³⁰, V.B. Vinogradov⁶⁴, J. Virzi¹⁵, O. Vitells¹⁷², M. Viti⁴², I. Vivarelli⁴⁸, F. Vives Vaque³,
 S. Vlachos¹⁰, D. Vladouiu⁹⁸, M. Vlasak¹²⁶, A. Vogel²¹, P. Vokac¹²⁶, G. Volpi⁴⁷, M. Volpi⁸⁶, G. Volpini^{89a},
 H. von der Schmitt⁹⁹, H. von Radziewski⁴⁸, E. von Toerne²¹, V. Vorobel¹²⁷, V. Vorwerk¹², M. Vos¹⁶⁷, R. Voss³⁰,
 J.H. Vosseveld⁷³, N. Vranjes¹³⁶, M. Vranjes Milosavljevic¹⁰⁵, V. Vrba¹²⁵, M. Vreeswijk¹⁰⁵, T. Vu Anh⁴⁸,
 R. Vuillermet³⁰, I. Vukotic³¹, Z. Vykydal¹²⁶, W. Wagner¹⁷⁵, P. Wagner²¹, H. Wahlen¹⁷⁵, S. Wahrenmund⁴⁴,
 J. Wakabayashi¹⁰¹, S. Walch⁸⁷, J. Walder⁷¹, R. Walker⁹⁸, W. Walkowiak¹⁴¹, R. Wall¹⁷⁶, P. Waller⁷³, B. Walsh¹⁷⁶,
 C. Wang⁴⁵, H. Wang¹⁷³, H. Wang⁴⁰, J. Wang¹⁵¹, J. Wang^{33a}, K. Wang⁸⁵, R. Wang¹⁰³, S.M. Wang¹⁵¹, T. Wang²¹,
 X. Wang¹⁷⁶, A. Warburton⁸⁵, C.P. Ward²⁸, D.R. Wardrope⁷⁷, M. Warsinsky⁴⁸, A. Washbrook⁴⁶, C. Wasicki⁴²,
 I. Watanabe⁶⁶, P.M. Watkins¹⁸, A.T. Watson¹⁸, L.J. Watson¹⁵⁰, M.F. Watson¹⁸, G. Watts¹³⁸, S. Watts⁸²,
 A.T. Waugh¹⁵⁰, B.M. Waugh⁷⁷, M.S. Weber¹⁷, J.S. Webster³¹, A.R. Weidberg¹¹⁸, P. Weigell⁹⁹, J. Weingarten⁵⁴,
 C. Weiser⁴⁸, P.S. Wells³⁰, T. Wenaus²⁵, D. Wendland¹⁶, Z. Weng^{151,t}, T. Wengler³⁰, S. Wenig³⁰, N. Wermes²¹,
 M. Werner⁴⁸, P. Werner³⁰, M. Werth¹⁶³, M. Wessels^{58a}, J. Wetter¹⁶¹, C. Weydert⁵⁵, K. Whalen²⁹, A. White⁸,
 M.J. White⁸⁶, S. White^{122a,122b}, S.R. Whitehead¹¹⁸, D. Whiteson¹⁶³, D. Whittington⁶⁰, D. Wicke¹⁷⁵,
 F.J. Wickens¹²⁹, W. Wiedenmann¹⁷³, M. Wielers⁷⁹, P. Wienemann²¹, C. Wiglesworth⁷⁵, L.A.M. Wiik-Fuchs²¹,

P.A. Wijeratne⁷⁷, A. Wildauer⁹⁹, M.A. Wildt^{42,q}, I. Wilhelm¹²⁷, H.G. Wilkens³⁰, J.Z. Will⁹⁸, E. Williams³⁵, H.H. Williams¹²⁰, S. Williams²⁸, W. Willis^{35,*}, S. Willocq⁸⁴, J.A. Wilson¹⁸, M.G. Wilson¹⁴³, A. Wilson⁸⁷, I. Wingerter-Seez⁵, S. Winkelmann⁴⁸, F. Winklmeier³⁰, M. Wittgen¹⁴³, T. Wittig⁴³, J. Wittkowski⁹⁸, S.J. Wollstadt⁸¹, M.W. Wolter³⁹, H. Wolters^{124a,h}, W.C. Wong⁴¹, G. Wooden⁸⁷, B.K. Wosiek³⁹, J. Wotschack³⁰, M.J. Woudstra⁸², K.W. Wozniak³⁹, K. Wraight⁵³, M. Wright⁵³, B. Wrona⁷³, S.L. Wu¹⁷³, X. Wu⁴⁹, Y. Wu^{33b,ak}, E. Wulf³⁵, B.M. Wynne⁴⁶, S. Xella³⁶, M. Xiao¹³⁶, S. Xie⁴⁸, C. Xu^{33b,y}, D. Xu^{33a}, L. Xu^{33b}, B. Yabsley¹⁵⁰, S. Yacoob^{145a,al}, M. Yamada⁶⁵, H. Yamaguchi¹⁵⁵, Y. Yamaguchi¹⁵⁵, A. Yamamoto⁶⁵, K. Yamamoto⁶³, S. Yamamoto¹⁵⁵, T. Yamamura¹⁵⁵, T. Yamanaka¹⁵⁵, K. Yamauchi¹⁰¹, T. Yamazaki¹⁵⁵, Y. Yamazaki⁶⁶, Z. Yan²², H. Yang^{33e}, H. Yang¹⁷³, U.K. Yang⁸², Y. Yang¹⁰⁹, Z. Yang^{146a,146b}, S. Yanush⁹¹, L. Yao^{33a}, Y. Yasu⁶⁵, E. Yatsenko⁴², J. Ye⁴⁰, S. Ye²⁵, A.L. Yen⁵⁷, M. Yilmaz^{4b}, R. Yoosoofmiya¹²³, K. Yorita¹⁷¹, R. Yoshida⁶, K. Yoshihara¹⁵⁵, C. Young¹⁴³, C.J.S. Young¹¹⁸, S. Youssef²², D. Yu²⁵, D.R. Yu¹⁵, J. Yu⁸, J. Yu¹¹², L. Yuan⁶⁶, A. Yurkewicz¹⁰⁶, B. Zabinski³⁹, R. Zaidan⁶², A.M. Zaitsev¹²⁸, S. Zambito²³, L. Zanello^{132a,132b}, D. Zanzi⁹⁹, A. Zaytsev²⁵, C. Zeitnitz¹⁷⁵, M. Zeman¹²⁶, A. Zemla³⁹, O. Zenin¹²⁸, T. Ženis^{144a}, D. Zerwas¹¹⁵, G. Zevi della Porta⁵⁷, D. Zhang⁸⁷, H. Zhang⁸⁸, J. Zhang⁶, L. Zhang¹⁵¹, X. Zhang^{33d}, Z. Zhang¹¹⁵, L. Zhao¹⁰⁸, Z. Zhao^{33b}, A. Zhemchugov⁶⁴, J. Zhong¹¹⁸, B. Zhou⁸⁷, N. Zhou¹⁶³, Y. Zhou¹⁵¹, C.G. Zhu^{33d}, H. Zhu⁴², J. Zhu⁸⁷, Y. Zhu^{33b}, X. Zhuang^{33a}, V. Zhuravlov⁹⁹, A. Zibell⁹⁸, D. Zieminska⁶⁰, N.I. Zimin⁶⁴, R. Zimmermann²¹, S. Zimmermann²¹, S. Zimmermann⁴⁸, Z. Zinonos^{122a,122b}, M. Ziolkowski¹⁴¹, R. Zitoun⁵, L. Živković³⁵, V.V. Zmouchko^{128,*}, G. Zobernig¹⁷³, A. Zoccoli^{20a,20b}, M. zur Nedden¹⁶, V. Zutshi¹⁰⁶, L. Zwalinski³⁰.

¹ School of Chemistry and Physics, University of Adelaide, Adelaide, Australia

² Physics Department, SUNY Albany, Albany NY, United States of America

³ Department of Physics, University of Alberta, Edmonton AB, Canada

⁴ (a)Department of Physics, Ankara University, Ankara; (b)Department of Physics, Gazi University, Ankara;

(c)Division of Physics, TOBB University of Economics and Technology, Ankara; (d)Turkish Atomic Energy Authority, Ankara, Turkey

⁵ LAPP, CNRS/IN2P3 and Université de Savoie, Annecy-le-Vieux, France

⁶ High Energy Physics Division, Argonne National Laboratory, Argonne IL, United States of America

⁷ Department of Physics, University of Arizona, Tucson AZ, United States of America

⁸ Department of Physics, The University of Texas at Arlington, Arlington TX, United States of America

⁹ Physics Department, University of Athens, Athens, Greece

¹⁰ Physics Department, National Technical University of Athens, Zografou, Greece

¹¹ Institute of Physics, Azerbaijan Academy of Sciences, Baku, Azerbaijan

¹² Institut de Física d'Altes Energies and Departament de Física de la Universitat Autònoma de Barcelona and ICREA, Barcelona, Spain

¹³ (a)Institute of Physics, University of Belgrade, Belgrade; (b)Vinca Institute of Nuclear Sciences, University of Belgrade, Belgrade, Serbia

¹⁴ Department for Physics and Technology, University of Bergen, Bergen, Norway

¹⁵ Physics Division, Lawrence Berkeley National Laboratory and University of California, Berkeley CA, United States of America

¹⁶ Department of Physics, Humboldt University, Berlin, Germany

¹⁷ Albert Einstein Center for Fundamental Physics and Laboratory for High Energy Physics, University of Bern, Bern, Switzerland

¹⁸ School of Physics and Astronomy, University of Birmingham, Birmingham, United Kingdom

¹⁹ (a)Department of Physics, Bogazici University, Istanbul; (b)Division of Physics, Dogus University, Istanbul;

(c)Department of Physics Engineering, Gaziantep University, Gaziantep, Turkey

²⁰ (a)INFN Sezione di Bologna; (b)Dipartimento di Fisica, Università di Bologna, Bologna, Italy

²¹ Physikalisches Institut, University of Bonn, Bonn, Germany

²² Department of Physics, Boston University, Boston MA, United States of America

²³ Department of Physics, Brandeis University, Waltham MA, United States of America

²⁴ (a)Universidade Federal do Rio De Janeiro COPPE/EE/IF, Rio de Janeiro; (b)Federal University of Juiz de Fora (UFJF), Juiz de Fora; (c)Federal University of Sao Joao del Rei (UFSJ), Sao Joao del Rei; (d)Instituto de Fisica, Universidade de Sao Paulo, Sao Paulo, Brazil

²⁵ Physics Department, Brookhaven National Laboratory, Upton NY, United States of America

²⁶ (a)National Institute of Physics and Nuclear Engineering, Bucharest; (b)University Politehnica Bucharest, Bucharest; (c)West University in Timisoara, Timisoara, Romania

²⁷ Departamento de Física, Universidad de Buenos Aires, Buenos Aires, Argentina

²⁸ Cavendish Laboratory, University of Cambridge, Cambridge, United Kingdom

²⁹ Department of Physics, Carleton University, Ottawa ON, Canada

- ³⁰ CERN, Geneva, Switzerland
- ³¹ Enrico Fermi Institute, University of Chicago, Chicago IL, United States of America
- ³² ^(a)Departamento de Física, Pontificia Universidad Católica de Chile, Santiago; ^(b)Departamento de Física, Universidad Técnica Federico Santa María, Valparaíso, Chile
- ³³ ^(a)Institute of High Energy Physics, Chinese Academy of Sciences, Beijing; ^(b)Department of Modern Physics, University of Science and Technology of China, Anhui; ^(c)Department of Physics, Nanjing University, Jiangsu; ^(d)School of Physics, Shandong University, Shandong; ^(e)Physics Department, Shanghai Jiao Tong University, Shanghai, China
- ³⁴ Laboratoire de Physique Corpusculaire, Clermont Université and Université Blaise Pascal and CNRS/IN2P3, Clermont-Ferrand, France
- ³⁵ Nevis Laboratory, Columbia University, Irvington NY, United States of America
- ³⁶ Niels Bohr Institute, University of Copenhagen, Kobenhavn, Denmark
- ³⁷ ^(a)INFN Gruppo Collegato di Cosenza; ^(b)Dipartimento di Fisica, Università della Calabria, Rende, Italy
- ³⁸ AGH University of Science and Technology, Faculty of Physics and Applied Computer Science, Krakow, Poland
- ³⁹ The Henryk Niewodniczanski Institute of Nuclear Physics, Polish Academy of Sciences, Krakow, Poland
- ⁴⁰ Physics Department, Southern Methodist University, Dallas TX, United States of America
- ⁴¹ Physics Department, University of Texas at Dallas, Richardson TX, United States of America
- ⁴² DESY, Hamburg and Zeuthen, Germany
- ⁴³ Institut für Experimentelle Physik IV, Technische Universität Dortmund, Dortmund, Germany
- ⁴⁴ Institut für Kern-und Teilchenphysik, Technical University Dresden, Dresden, Germany
- ⁴⁵ Department of Physics, Duke University, Durham NC, United States of America
- ⁴⁶ SUPA - School of Physics and Astronomy, University of Edinburgh, Edinburgh, United Kingdom
- ⁴⁷ INFN Laboratori Nazionali di Frascati, Frascati, Italy
- ⁴⁸ Fakultät für Mathematik und Physik, Albert-Ludwigs-Universität, Freiburg, Germany
- ⁴⁹ Section de Physique, Université de Genève, Geneva, Switzerland
- ⁵⁰ ^(a)INFN Sezione di Genova; ^(b)Dipartimento di Fisica, Università di Genova, Genova, Italy
- ⁵¹ ^(a)E. Andronikashvili Institute of Physics, Iv. Javakhishvili Tbilisi State University, Tbilisi; ^(b)High Energy Physics Institute, Tbilisi State University, Tbilisi, Georgia
- ⁵² II Physikalisches Institut, Justus-Liebig-Universität Giessen, Giessen, Germany
- ⁵³ SUPA - School of Physics and Astronomy, University of Glasgow, Glasgow, United Kingdom
- ⁵⁴ II Physikalisches Institut, Georg-August-Universität, Göttingen, Germany
- ⁵⁵ Laboratoire de Physique Subatomique et de Cosmologie, Université Joseph Fourier and CNRS/IN2P3 and Institut National Polytechnique de Grenoble, Grenoble, France
- ⁵⁶ Department of Physics, Hampton University, Hampton VA, United States of America
- ⁵⁷ Laboratory for Particle Physics and Cosmology, Harvard University, Cambridge MA, United States of America
- ⁵⁸ ^(a)Kirchhoff-Institut für Physik, Ruprecht-Karls-Universität Heidelberg, Heidelberg; ^(b)Physikalisches Institut, Ruprecht-Karls-Universität Heidelberg, Heidelberg; ^(c)ZITI Institut für technische Informatik, Ruprecht-Karls-Universität Heidelberg, Mannheim, Germany
- ⁵⁹ Faculty of Applied Information Science, Hiroshima Institute of Technology, Hiroshima, Japan
- ⁶⁰ Department of Physics, Indiana University, Bloomington IN, United States of America
- ⁶¹ Institut für Astro-und Teilchenphysik, Leopold-Franzens-Universität, Innsbruck, Austria
- ⁶² University of Iowa, Iowa City IA, United States of America
- ⁶³ Department of Physics and Astronomy, Iowa State University, Ames IA, United States of America
- ⁶⁴ Joint Institute for Nuclear Research, JINR Dubna, Dubna, Russia
- ⁶⁵ KEK, High Energy Accelerator Research Organization, Tsukuba, Japan
- ⁶⁶ Graduate School of Science, Kobe University, Kobe, Japan
- ⁶⁷ Faculty of Science, Kyoto University, Kyoto, Japan
- ⁶⁸ Kyoto University of Education, Kyoto, Japan
- ⁶⁹ Department of Physics, Kyushu University, Fukuoka, Japan
- ⁷⁰ Instituto de Física La Plata, Universidad Nacional de La Plata and CONICET, La Plata, Argentina
- ⁷¹ Physics Department, Lancaster University, Lancaster, United Kingdom
- ⁷² ^(a)INFN Sezione di Lecce; ^(b)Dipartimento di Matematica e Fisica, Università del Salento, Lecce, Italy
- ⁷³ Oliver Lodge Laboratory, University of Liverpool, Liverpool, United Kingdom
- ⁷⁴ Department of Physics, Jožef Stefan Institute and University of Ljubljana, Ljubljana, Slovenia
- ⁷⁵ School of Physics and Astronomy, Queen Mary University of London, London, United Kingdom
- ⁷⁶ Department of Physics, Royal Holloway University of London, Surrey, United Kingdom
- ⁷⁷ Department of Physics and Astronomy, University College London, London, United Kingdom
- ⁷⁸ Laboratoire de Physique Nucléaire et de Hautes Energies, UPMC and Université Paris-Diderot and

CNRS/IN2P3, Paris, France

⁷⁹ Fysiska institutionen, Lunds universitet, Lund, Sweden

⁸⁰ Departamento de Fisica Teorica C-15, Universidad Autonoma de Madrid, Madrid, Spain

⁸¹ Institut für Physik, Universität Mainz, Mainz, Germany

⁸² School of Physics and Astronomy, University of Manchester, Manchester, United Kingdom

⁸³ CPPM, Aix-Marseille Université and CNRS/IN2P3, Marseille, France

⁸⁴ Department of Physics, University of Massachusetts, Amherst MA, United States of America

⁸⁵ Department of Physics, McGill University, Montreal QC, Canada

⁸⁶ School of Physics, University of Melbourne, Victoria, Australia

⁸⁷ Department of Physics, The University of Michigan, Ann Arbor MI, United States of America

⁸⁸ Department of Physics and Astronomy, Michigan State University, East Lansing MI, United States of America

⁸⁹ ^(a)INFN Sezione di Milano; ^(b)Dipartimento di Fisica, Università di Milano, Milano, Italy

⁹⁰ B.I. Stepanov Institute of Physics, National Academy of Sciences of Belarus, Minsk, Republic of Belarus

⁹¹ National Scientific and Educational Centre for Particle and High Energy Physics, Minsk, Republic of Belarus

⁹² Department of Physics, Massachusetts Institute of Technology, Cambridge MA, United States of America

⁹³ Group of Particle Physics, University of Montreal, Montreal QC, Canada

⁹⁴ P.N. Lebedev Institute of Physics, Academy of Sciences, Moscow, Russia

⁹⁵ Institute for Theoretical and Experimental Physics (ITEP), Moscow, Russia

⁹⁶ Moscow Engineering and Physics Institute (MEPhI), Moscow, Russia

⁹⁷ D.V.Skobeltzyn Institute of Nuclear Physics, M.V.Lomonosov Moscow State University, Moscow, Russia

⁹⁸ Fakultät für Physik, Ludwig-Maximilians-Universität München, München, Germany

⁹⁹ Max-Planck-Institut für Physik (Werner-Heisenberg-Institut), München, Germany

¹⁰⁰ Nagasaki Institute of Applied Science, Nagasaki, Japan

¹⁰¹ Graduate School of Science and Kobayashi-Maskawa Institute, Nagoya University, Nagoya, Japan

¹⁰² ^(a)INFN Sezione di Napoli; ^(b)Dipartimento di Scienze Fisiche, Università di Napoli, Napoli, Italy

¹⁰³ Department of Physics and Astronomy, University of New Mexico, Albuquerque NM, United States of America

¹⁰⁴ Institute for Mathematics, Astrophysics and Particle Physics, Radboud University Nijmegen/Nikhef, Nijmegen, Netherlands

¹⁰⁵ Nikhef National Institute for Subatomic Physics and University of Amsterdam, Amsterdam, Netherlands

¹⁰⁶ Department of Physics, Northern Illinois University, DeKalb IL, United States of America

¹⁰⁷ Budker Institute of Nuclear Physics, SB RAS, Novosibirsk, Russia

¹⁰⁸ Department of Physics, New York University, New York NY, United States of America

¹⁰⁹ Ohio State University, Columbus OH, United States of America

¹¹⁰ Faculty of Science, Okayama University, Okayama, Japan

¹¹¹ Homer L. Dodge Department of Physics and Astronomy, University of Oklahoma, Norman OK, United States of America

¹¹² Department of Physics, Oklahoma State University, Stillwater OK, United States of America

¹¹³ Palacký University, RCPTM, Olomouc, Czech Republic

¹¹⁴ Center for High Energy Physics, University of Oregon, Eugene OR, United States of America

¹¹⁵ LAL, Université Paris-Sud and CNRS/IN2P3, Orsay, France

¹¹⁶ Graduate School of Science, Osaka University, Osaka, Japan

¹¹⁷ Department of Physics, University of Oslo, Oslo, Norway

¹¹⁸ Department of Physics, Oxford University, Oxford, United Kingdom

¹¹⁹ ^(a)INFN Sezione di Pavia; ^(b)Dipartimento di Fisica, Università di Pavia, Pavia, Italy

¹²⁰ Department of Physics, University of Pennsylvania, Philadelphia PA, United States of America

¹²¹ Petersburg Nuclear Physics Institute, Gatchina, Russia

¹²² ^(a)INFN Sezione di Pisa; ^(b)Dipartimento di Fisica E. Fermi, Università di Pisa, Pisa, Italy

¹²³ Department of Physics and Astronomy, University of Pittsburgh, Pittsburgh PA, United States of America

¹²⁴ ^(a)Laboratorio de Instrumentacao e Fisica Experimental de Particulas - LIP, Lisboa, Portugal; ^(b)Departamento de Fisica Teorica y del Cosmos and CAFPE, Universidad de Granada, Granada, Spain

¹²⁵ Institute of Physics, Academy of Sciences of the Czech Republic, Praha, Czech Republic

¹²⁶ Czech Technical University in Prague, Praha, Czech Republic

¹²⁷ Faculty of Mathematics and Physics, Charles University in Prague, Praha, Czech Republic

¹²⁸ State Research Center Institute for High Energy Physics, Protvino, Russia

¹²⁹ Particle Physics Department, Rutherford Appleton Laboratory, Didcot, United Kingdom

¹³⁰ Physics Department, University of Regina, Regina SK, Canada

¹³¹ Ritsumeikan University, Kusatsu, Shiga, Japan

¹³² ^(a)INFN Sezione di Roma I; ^(b)Dipartimento di Fisica, Università La Sapienza, Roma, Italy

- 133 ^(a)INFN Sezione di Roma Tor Vergata; ^(b)Dipartimento di Fisica, Università di Roma Tor Vergata, Roma, Italy
- 134 ^(a)INFN Sezione di Roma Tre; ^(b)Dipartimento di Matematica e Fisica, Università Roma Tre, Roma, Italy
- 135 ^(a)Faculté des Sciences Ain Chock, Réseau Universitaire de Physique des Hautes Energies - Université Hassan II, Casablanca; ^(b)Centre National de l'Energie des Sciences Techniques Nucleaires, Rabat; ^(c)Faculté des Sciences Semlalia, Université Cadi Ayyad, LPHEA-Marrakech; ^(d)Faculté des Sciences, Université Mohamed Premier and LPTPM, Oujda; ^(e)Faculté des sciences, Université Mohammed V-Agdal, Rabat, Morocco
- 136 DSM/IRFU (Institut de Recherches sur les Lois Fondamentales de l'Univers), CEA Saclay (Commissariat à l'Energie Atomique et aux Energies Alternatives), Gif-sur-Yvette, France
- 137 Santa Cruz Institute for Particle Physics, University of California Santa Cruz, Santa Cruz CA, United States of America
- 138 Department of Physics, University of Washington, Seattle WA, United States of America
- 139 Department of Physics and Astronomy, University of Sheffield, Sheffield, United Kingdom
- 140 Department of Physics, Shinshu University, Nagano, Japan
- 141 Fachbereich Physik, Universität Siegen, Siegen, Germany
- 142 Department of Physics, Simon Fraser University, Burnaby BC, Canada
- 143 SLAC National Accelerator Laboratory, Stanford CA, United States of America
- 144 ^(a)Faculty of Mathematics, Physics & Informatics, Comenius University, Bratislava; ^(b)Department of Subnuclear Physics, Institute of Experimental Physics of the Slovak Academy of Sciences, Kosice, Slovak Republic
- 145 ^(a)Department of Physics, University of Johannesburg, Johannesburg; ^(b)School of Physics, University of the Witwatersrand, Johannesburg, South Africa
- 146 ^(a)Department of Physics, Stockholm University; ^(b)The Oskar Klein Centre, Stockholm, Sweden
- 147 Physics Department, Royal Institute of Technology, Stockholm, Sweden
- 148 Departments of Physics & Astronomy and Chemistry, Stony Brook University, Stony Brook NY, United States of America
- 149 Department of Physics and Astronomy, University of Sussex, Brighton, United Kingdom
- 150 School of Physics, University of Sydney, Sydney, Australia
- 151 Institute of Physics, Academia Sinica, Taipei, Taiwan
- 152 Department of Physics, Technion: Israel Institute of Technology, Haifa, Israel
- 153 Raymond and Beverly Sackler School of Physics and Astronomy, Tel Aviv University, Tel Aviv, Israel
- 154 Department of Physics, Aristotle University of Thessaloniki, Thessaloniki, Greece
- 155 International Center for Elementary Particle Physics and Department of Physics, The University of Tokyo, Tokyo, Japan
- 156 Graduate School of Science and Technology, Tokyo Metropolitan University, Tokyo, Japan
- 157 Department of Physics, Tokyo Institute of Technology, Tokyo, Japan
- 158 Department of Physics, University of Toronto, Toronto ON, Canada
- 159 ^(a)TRIUMF, Vancouver BC; ^(b)Department of Physics and Astronomy, York University, Toronto ON, Canada
- 160 Faculty of Pure and Applied Sciences, University of Tsukuba, Tsukuba, Japan
- 161 Department of Physics and Astronomy, Tufts University, Medford MA, United States of America
- 162 Centro de Investigaciones, Universidad Antonio Narino, Bogota, Colombia
- 163 Department of Physics and Astronomy, University of California Irvine, Irvine CA, United States of America
- 164 ^(a)INFN Gruppo Collegato di Udine; ^(b)ICTP, Trieste; ^(c)Dipartimento di Chimica, Fisica e Ambiente, Università di Udine, Udine, Italy
- 165 Department of Physics, University of Illinois, Urbana IL, United States of America
- 166 Department of Physics and Astronomy, University of Uppsala, Uppsala, Sweden
- 167 Instituto de Física Corpuscular (IFIC) and Departamento de Física Atómica, Molecular y Nuclear and Departamento de Ingeniería Electrónica and Instituto de Microelectrónica de Barcelona (IMB-CNM), University of Valencia and CSIC, Valencia, Spain
- 168 Department of Physics, University of British Columbia, Vancouver BC, Canada
- 169 Department of Physics and Astronomy, University of Victoria, Victoria BC, Canada
- 170 Department of Physics, University of Warwick, Coventry, United Kingdom
- 171 Waseda University, Tokyo, Japan
- 172 Department of Particle Physics, The Weizmann Institute of Science, Rehovot, Israel
- 173 Department of Physics, University of Wisconsin, Madison WI, United States of America
- 174 Fakultät für Physik und Astronomie, Julius-Maximilians-Universität, Würzburg, Germany
- 175 Fachbereich C Physik, Bergische Universität Wuppertal, Wuppertal, Germany
- 176 Department of Physics, Yale University, New Haven CT, United States of America
- 177 Yerevan Physics Institute, Yerevan, Armenia
- 178 Centre de Calcul de l'Institut National de Physique Nucléaire et de Physique des Particules (IN2P3),

Villeurbanne, France

^a Also at Department of Physics, King's College London, London, United Kingdom

^b Also at Laboratório de Instrumentação e Física Experimental de Partículas - LIP, Lisboa, Portugal

^c Also at Faculdade de Ciências and CFNUL, Universidade de Lisboa, Lisboa, Portugal

^d Also at Particle Physics Department, Rutherford Appleton Laboratory, Didcot, United Kingdom

^e Also at TRIUMF, Vancouver BC, Canada

^f Also at Department of Physics, California State University, Fresno CA, United States of America

^g Also at Novosibirsk State University, Novosibirsk, Russia

^h Also at Department of Physics, University of Coimbra, Coimbra, Portugal

ⁱ Also at Università di Napoli Parthenope, Napoli, Italy

^j Also at Institute of Particle Physics (IPP), Canada

^k Also at Department of Physics, Middle East Technical University, Ankara, Turkey

^l Also at Louisiana Tech University, Ruston LA, United States of America

^m Also at Dep Física and CEFITEC of Faculdade de Ciências e Tecnologia, Universidade Nova de Lisboa, Caparica, Portugal

ⁿ Also at Department of Physics and Astronomy, Michigan State University, East Lansing MI, United States of America

^o Also at Department of Physics, University of Cape Town, Cape Town, South Africa

^p Also at Institute of Physics, Azerbaijan Academy of Sciences, Baku, Azerbaijan

^q Also at Institut für Experimentalphysik, Universität Hamburg, Hamburg, Germany

^r Also at Manhattan College, New York NY, United States of America

^s Also at CPPM, Aix-Marseille Université and CNRS/IN2P3, Marseille, France

^t Also at School of Physics and Engineering, Sun Yat-sen University, Guanzhou, China

^u Also at Academia Sinica Grid Computing, Institute of Physics, Academia Sinica, Taipei, Taiwan

^v Also at School of Physical Sciences, National Institute of Science Education and Research, Bhubaneswar, India

^w Also at School of Physics, Shandong University, Shandong, China

^x Also at Dipartimento di Fisica, Università La Sapienza, Roma, Italy

^y Also at DSM/IRFU (Institut de Recherches sur les Lois Fondamentales de l'Univers), CEA Saclay (Commissariat à l'Energie Atomique et aux Energies Alternatives), Gif-sur-Yvette, France

^z Also at Section de Physique, Université de Genève, Geneva, Switzerland

^{aa} Also at Departamento de Física, Universidade de Minho, Braga, Portugal

^{ab} Also at Department of Physics, The University of Texas at Austin, Austin TX, United States of America

^{ac} Also at Department of Physics and Astronomy, University of South Carolina, Columbia SC, United States of America

^{ad} Also at Institute for Particle and Nuclear Physics, Wigner Research Centre for Physics, Budapest, Hungary

^{ae} Also at DESY, Hamburg and Zeuthen, Germany

^{af} Also at International School for Advanced Studies (SISSA), Trieste, Italy

^{ag} Also at LAL, Université Paris-Sud and CNRS/IN2P3, Orsay, France

^{ah} Also at Faculty of Physics, M.V.Lomonosov Moscow State University, Moscow, Russia

^{ai} Also at Nevis Laboratory, Columbia University, Irvington NY, United States of America

^{aj} Also at Department of Physics, Oxford University, Oxford, United Kingdom

^{ak} Also at Department of Physics, The University of Michigan, Ann Arbor MI, United States of America

^{al} Also at Discipline of Physics, University of KwaZulu-Natal, Durban, South Africa

* Deceased